Title
Mitochondria Lipid-Droplet Interaction in the Control of Cellular Lipid Metabolism

Author
Brownstein, alexandra Jeanette

Publication Date
2023

Peer reviewed|Thesis/dissertation

UNIVERSITY OF CALIFORNIA

Los Angeles

Mitochondria Lipid-Droplet Interaction in the Control of Cellular Lipid Metabolism

A dissertation submitted in partial satisfaction of the requirements for the degree

Doctor of Philosophy in Molecular, Cellular, and Integrative Physiology

by

Alexandra Brownstein

2023

ABSTRACT OF THE DISSERTATION

Mitochondria Lipid-Droplet Interaction in the Control of Cellular Lipid Metabolism

by

Alexandra Brownstein

Doctor of Philosophy in Molecular, Cellular, and Integrative Physiology

University of California, Los Angeles, 2023

Professor Orian Shirihai, Chair

An imbalance in energy homeostasis leads to increased lipid storage and obesity. Mechanisms that regulate cellular lipid storage or utilization are thought to play a key role in maintaining energy balance and overall metabolic health. However the mechanisms that regulate energy expenditure and fuel utilization are not well understood. Here we address these gaps in knowledge by first describing a novel mechanism to increase energy expenditure by regulating mitochondrial fuel utilization. We find that blocking pyruvate entry into the mitochondria increases energy expenditure by activating an ATP-demanding lipid cycle of LD breakdown and buildup that is fueled by lipid oxidation. Moreover, recent studies have demonstrated heterogeneity in mitochondrial function, and identified a unique population of BAT mitochondria that support lipid storage by anchoring themselves to LD and facilitating TG synthesis and LD expansion. However, it remains

unknown if these unique mitochondria are conserved in other tissues. Here, I describe the development of the first approach to isolate PDM from WAT. Using this approach I show that PDM in WAT have a unique function that is distinct from BAT. Future research understanding the mechanisms that control subpopulations of mitochondria and their roles in lipid homeostasis can provide novel methods of altering energy metabolism through mitochondria.

ATP-consuming futile cycles as energy dissipating mechanisms to counteract obesity

Obesity results from an imbalance in energy homeostasis, whereby excessive energy intake exceeds caloric expenditure. Energy can be dissipated out of an organism by producing heat (thermogenesis), explaining the long-standing interest in exploiting thermogenic processes to counteract obesity. Mitochondrial uncoupling is a process that expends energy by oxidizing nutrients to produce heat, instead of ATP synthesis. Energy can also be dissipated through mechanisms that do not involve mitochondrial uncoupling. Such mechanisms include futile cycles described as metabolic reactions that consume ATP to produce a product from a substrate but then converting the product back into the original substrate, releasing the energy as heat. Energy dissipation driven by cellular ATP demand can be regulated by adjusting the speed and number of futile cycles. Energy consuming futile cycles that are reviewed here are lipolysis/fatty acid re-esterification cycle, creatine/phosphocreatine cycle, and the SERCA-mediated calcium import and export cycle. Their reliance on ATP emphasizes that mitochondrial oxidative function coupled to ATP synthesis, and not just uncoupling, can play a role in thermogenic energy

dissipation. Here, we review ATP consuming futile cycles, the evidence for their function in humans, and their potential employment as a strategy to dissipate energy and counteract obesity.

Mitochondria isolated from lipid droplets in WAT reveal functional differences based on lipid droplet size

Recent studies in brown adipose tissue (BAT) described a unique subpopulation of mitochondria bound to lipid droplets (LDs), peridroplet mitochondria (PDM). PDMs can be isolated from BAT by simple differential centrifugation and salt washes. These protocols have so far not led to successful isolation of PDMs from WAT, which seem to show stronger binding to LD than in BAT. Here, we developed a method to isolate PDM from WAT with high yield and purity by an optimized proteolytic treatment that preserves the respiratory function of mitochondria intact. Using this approach, we show that, contrary to BAT, WAT PDM have lower respiratory and ATP synthesis capacity compared to WAT CM. Furthermore, by isolating PDM from fractions containing LDs of different sizes, we find a negative correlation between LD size and the respiratory capacity of their PDM in WAT. Thus, our new isolation method reveals tissue-specific characteristics of PDM and establishes the existence of heterogeneity in PDM function determined by LD size.

The dissertation of Alexandra Brownstein is approved.

Ajit S. Divakaruni

Linsey Stiles

Alexander M. van der Bliek

Ambre Marguerite Bertholet

Orian Shirihai, Committee Chair

University of California, Los Angeles

2023

DEDICATION

I would like to dedicate my graduate work to my amazing parents, Susan and Richard Brownstein who have been my biggest supporters throughout my life. I would not have been able to accomplish any of this without their love and belief in me. I would also like to dedicate this to my brother Ben Brownstein and my grandparents Rosylyn and Stanford (Woody) Kaiser and Beatrice and Mark Brownstein, who have supported me throughout my life. Last but not least, none of this would be possible without the unconditional love and companionship from Douglas and Daisy, my two best friends.

TABLE OF CONTENTS

LIST OF FIGURES AND TABLES

ACKNOWLEDGMENTS

I would like to thank my mentor Orian Shirihai and co-mentors Marc Liesa and Rebeca Acín-Pérez. When I first saw Orian give a talk and interact with his lab, I knew I wanted to be a part of his incredible group. I had a gut feeling when I first started that I was supposed to be in this lab, but my experience has been even more than I could have imagined. Orian is one of a kind mentor and scientist and I am so grateful to him for everything he has taught me. Orian brought the creativity and intrigue back into science and I learned to think outside the box and actually focus on what the science and data is telling us. I am so grateful for his mentorship and support, but most importantly for creating a collaborative and supportive lab family that allowed me to learn from my pears and be vulnerable. I am especially grateful for his emphasis on communication, and I have learned so much from his ability to communicate science in a way that is understandable to any audience.

I would like to thank Marc Liesa for his constant support and mentorship. Marc truly helped me become a better scientist and taught me how to analyze and truly interpret what the data is saying. Marc taught me how to properly plan experiments, and more importantly how to include the proper controls in order to confidently make conclusions. He is a brilliant scientists and is so humble and kind, which made working with him so rewarding.

I would also like to thank Rebeca Acín-Pérez for not only her mentorship in lab, but for her friendship and constant support in every aspect of my life, throughout these

past 5 years. She is an incredible scientists and constantly pushes the boundaries of what is possible. She has become my lab mom, and I am so grateful for everything she has taught me and all of the knowledge she has bestowed upon me. She brings such a positive presence everywhere she goes, and she taught me how to work hard and live life to the fullest.

I am grateful to my thesis committee, Dr. Alexander Van der Bliek, Dr. Ajit Divakaruni, Dr. Linsey Stiles and Dr. Ambre Bertholet for all of their support and guidance throughout my training. I would also like to thank all of the past and present members of the amazing Shirihai-Liesa lab for all of their help and guidance both at the bench and in the ways we think about science. This lab feels like family, and I am so grateful to have met so many amazing scientists and individuals through this experience. Their constant support, encouragement and desire to share and teach has allowed me to develop as a scientist and gain a diverse approach to addressing difficult questions. I know these relationships will be lifelong.

I would lastly like to thank my past mentors, Dr. Joshua Selsby and Dr, Michelle Parvitiyar who guided me in my early stages and constantly encouraged me to keep going and pursue my scientific endeavors.

Published work included in this thesis

Chapter two was originally published in Reviews in Endocrine and Metabolic Disorders.

Chapter three is currently in revision, and was submitted to life science alliance journal.

CURRICULUM VITAE

EDUCATION

Ph.D, Molecular, Cellular Integrative Physiology (Expected, July 2023)
University of California, Los Angeles, CA

Master of Science in Genetics and Genomics (2016)
Iowa State University, Ames, IA

Bachelor of Science in Ecology and Evolutionary Biology (2013)
University of California, Los Angeles, CA

RESEARCH EXPERIENCE

***University of California, Los Angeles,* 2019 –Present** *Orian S. Shirihai*
Graduate Student Researcher, Molecular Cellular Integrative Physiology

***University of California, Los Angeles,* 2016 –2018** *Rachelle H. Crosbie-Watson*
Laboratory Assistant, Department of Integrative Biology and Physiology

***Iowa State University, Ames IA,* 2014 – 2016** *Joshua T. Selsby*
Graduate Student, Interdepartmental Genetics and Genomics Program

PUBLICATIONS

Brownstein, A. J., Veliova, M., Acín-Perez, R., Villalobos, F., Petcherski, A., Tombolato, A., Liesa, M., Shirihai, O.S. (2023). Mitochondria isolated from lipid droplets reveal functional differences based on lipid droplet size. *Life Sci Alliance*. In Revision.

Petcherski, A., Tingley, B. M., Martin, A., Adams, S., **Brownstein, A. J.**, Steinberg, R. A., Shabane, B., Garcia-Jr, G., Veliova, M., Arumugaswami, V., Colby, A. H., Shirihai, O. S., Grinstaff, M. W. (2023). Endo-Lysosome-Targeted Nanoparticle delivery of Antiviral Therapy for Coronavirus Infections. *BioRxiv*. Submitted.

Desousa, B. R., Kim, K. K. O., Jones, A. E., Ball, A. B., Hsieh, W. Y., Swain, P., Morrow, D. H., **Brownstein, A. J.**, Ferrick, D. A., Shirihai, O. S., Neilson, A., Nathanson, D. A., Rogers, G. W., Dranka, D. P., Murphy, A. N., Affourtit, C., Bensinger, S. J., Stiles, L., Romero, N., and Divakaruni, A. S. (2023). Calculation of ATP production rates using the Seahorse XF Analyzer. *EMBO Rep*, accepted.

Acín-Pérez, R., Montales, K. P., Nguyen, K. B., **Brownstein, A. J**., Stiles, L., & Divakaruni, A. S. (2023). Isolation of Mitochondria from Mouse Tissues for Functional Analysis. *Methods Mol Biol, 2675*, 77-96.

Zeng, J., Acín-Pérez, R., Assali, E. A., Martin, A., **Brownstein, A. J.,** Petcherski, A., Fernández-Del-Rio, L., Xiao, R., Lo, C. H., Shum, M., Liesa, M., Han, X., Shirihai, O. S., & Grinstaff, M. W. (2023). Restoration of lysosomal acidification rescues autophagy and

metabolic dysfunction in non-alcoholic fatty liver disease. *Nature communications*, *14*(1), 2573.

Brownstein, A. J., Veliova, M., Acín-Pérez, R., Liesa, M., & Shirihai, O. S. (2022). ATP-consuming futile cycles as energy dissipating mechanisms to counteract obesity. *Rev Endocr Metab Disord, 23*(1), 121-131.

Acín-Perez, R., Petcherski, A., Veliova, M., Benador, I. Y., Assali, E. A., Colleluori, G., Cinti, S., **Brownstein, A. J.,** Baghdasarian, S., Livhits, M. J., Yeh, M. W., Krishnan, K. C., Vergnes, L., Winn, N. C., Padilla, J., Liesa, M., Sacks, H. S., & Shirihai, O. S. (2021). Recruitment and remodeling of peridroplet mitochondria in human adipose tissue. *Redox biology*, *46*, 102087.

Veliova, M., Ferreira, C. M., Benador, I. Y., Jones, A. E., Mahdaviani, K., **Brownstein, A. J.,** Desousa, B. R., Acín-Pérez, R., Petcherski, A., Assali, E. A., Stiles, L., Divakaruni, A. S., Prentki, M., Corkey, B. E., Liesa, M., Oliveira, M. F., & Shirihai, O. S. (2020). Blocking mitochondrial pyruvate import in brown adipocytes induces energy wasting via lipid cycling. *EMBO reports*, *21*(12), e49634.

Ngo, J., Benador, I. Y., **Brownstein, A. J.,** Vergnes, L., Veliova, M., Shum, M., Acín-Pérez, R., Reue, K., Shirihai, O. S., & Liesa, M. (2020). Isolation and functional analysis of peridroplet mitochondria from murine brown adipose tissue. *STAR protocols*, *2*(1), 100243.

Parvatiyar, M. S., **Brownstein, A. J.,** Kanashiro-Takeuchi, R. M., Collado, J. R., Dieseldorff Jones, K. M., Gopal, J., Hammond, K. G., Marshall, J. L., Ferrel, A., Beedle, A. M., Chamberlain, J. S., Renato Pinto, J., & Crosbie, R. H. (2019). Stabilization of the cardiac sarcolemma by sarcospan rescues DMD-associated cardiomyopathy. *JCI insight*, *5*(11), e123855.

Ganesan, S., **Brownstein, A. J**., Pearce, S. C., Hudson, M. B., Gabler, N. K., Baumgard, L. H., Rhoads, R. P., & Selsby, J. T. (2018). Prolonged environment-induced hyperthermia alters autophagy in oxidative skeletal muscle in Sus scrofa. *Journal of thermal biology*, *74*, 160–169.

Brownstein, A. J., Ganesan, S., Summers, C. M., Pearce, S., Hale, B. J., Ross, J. W., Gabler, N., Seibert, J. T., Rhoads, R. P., Baumgard, L. H., & Selsby, J. T. (2017). Heat stress causes dysfunctional autophagy in oxidative skeletal muscle. *Physiological reports*, *5*(12), e13317.

Ishak, W. W., Bagot, K., Thomas, S., Magakian, N., Bedwani, D., Larson, D., **Brownstein, A.,** & Zaky, C. (2012). Quality of life in patients suffering from insomnia. *Innovations in clinical neuroscience*, *9*(10), 13–26.

CHAPTER 1: INTRODUCTION

Obesity and the regulation of energy balance

Obesity prevalence worldwide is increasing at a rapid rate, and is a major risk factor for several chronic diseases, including cardiovascular disease, insulin resistance, type 2 diabetes, cancer and cognitive dysfunction. The fundamental cause of obesity is an energy imbalance between calories consumed and calories expended leading to their excessive accumulation in the form of triglycerides in white adipose tissue. Sustained lipid/nutrient overload can negatively affect adipose tissue function and overall metabolic homeostasis, highlighting the urgent need to find efficient approaches to combat a positive energy balance.

While improving lifestyle by increasing exercise and reducing food intake are viable option to counteract obesity for many patients, additional factors including genetic predisposition have been shown to play a major role in obesity. Thus, the consideration that obesity is a disease of lack of will or a fault of personality is scientifically unfounded. The current therapeutic options for obesity are limited, given the undesirable side effects presented by many of the therapies employed to date. Currently the anti-obesity medications approved by the FDA act to repress energy intake, either by suppressing appetite (Phentermine-Topiramte, benzphetamine, Liraglutide) or by inhibiting intestinal fat absorption (Orlistat) (Daneschvar *et al*, 2016; Filippatos *et al*, 2008). However, these drugs often elicit serious side effects including depression, and gastrointestinal problems, such as steatorrhea and oily bowel movements, highlighting the need for alternative strategies to treat obesity (Daneschvar *et al.*, 2016; Filippatos *et al.*, 2008).

In order to lose body weight or decrease adiposity, energy expenditure must exceed intake, either by decreasing caloric intake or increasing overall energy dissipation. Energy expenditure refers to the amount of energy an individual uses to maintain essential body functions (respiration, circulation, digestion), physical activity, and adaptive (non-shivering) thermogenesis (Heaney J. (2013) Energy: Expenditure; Spiegelman & Flier, 2001). Adaptive thermogenesis refers to the regulated dissipation of energy as heat, which occurs in shivering muscle, brown and beige adipocytes in response to environmental temperature and diet (Lowell & Spiegelman, 2000). Despite the existence of shivering thermogenesis, non-shivering thermogenesis still plays a major role in thermal homeostasis and maintenance of body temperature, being an essential mechanism for newborns to mitigate thermal stress (Foster & Frydman, 1978; Lowell & Spiegelman, 2000).

The obesity epidemic has increased interest in pathways that elevate energy expenditure, and brown and beige fat have become appealing therapeutic targets because of their ability to dissipate energy in the form of heat by mitochondrial uncoupling. Promoting brown adipose tissue thermogenesis and white adipose tissue “browning” have emerged as promising approaches that can offset the negative lipotoxic effects of obesity on metabolic health (Carobbio *et al*, 2017; Harms & Seale, 2013; Hussain *et al*, 2020; Seale & Lazar, 2009), counteracting fat accumulation and thus body weight gain.

Adipose tissue: physiology and function

Adipose tissue is an essential metabolic organ that plays a central role in regulating whole-body energy homeostasis. Humans have three types of adipose tissue; white, brown and beige fat, that serve distinct physiological functions. The main function of white adipose tissue (WAT) is to safely store excess nutrients as neutral triglycerides, and rapidly mobilize the stored nutrients in response to increased cellular energy demands (Peirce *et al*, 2014). Under conditions of nutrient shortage, WAT breaks down the stored triglycerides through lipolysis to produce free fatty acids (FFAs) and glycerol as fuel for the organism (Cinti, 2009). WAT plays an important role in buffering nutrient availability and demand, and the process of lipolysis and esterification is tightly regulated as high levels of non-esterified fatty acids (NEFA) can cause lipotoxicity.

The ability to both mobilize fat upon stimulation and store the fat by re-esterification enables the white adipose tissue to quickly control the levels of circulating fatty acids. The cycle of lipid breakdown and partial or full re-esterification of fatty acids into TAGs, diacylglycerols (DAGs) or Monoacylglycerols (MAGs) is a futile cycle consuming ATP. It has been shown by several studies that mitochondria in the white adipocyte provides the ATP required for lipolysis and fatty acid re-esterification, indicating the importance of WAT mitochondria in the control of whole body lipid levels (Carobbio *et al.*, 2017; Chitraju *et al*, 2017; Vernochet *et al*, 2014).

In addition to being a storage depot for excess nutrients, recent studies have demonstrated that WAT is a major endocrine organ that secretes a large number of metabolites and hormones, including leptin, adiponectin, tumor necrosis factor-*α*,

interleukin-6 that regulate diverse biological functions, such as glucose and lipid metabolism, insulin sensitivity, immunity, reproduction, angiogenesis and body weight homeostasis (Cinti, 2009; Coelho *et al*, 2013).

White adipocytes within WAT are spherical cells and contain a single lipid droplet composed of triglycerides that accounts for more than 90% of the cell volume (Cinti, 2009). White adipocytes contain few, small elongated mitochondria with randomly oriented cristae (Cinti, 2009). A major function of mitochondria in mature white adipocytes is to produce ATP, but without using fatty acid oxidation. The white adipocyte mitochondria represent the main source of ATP similar to that in other tissues, and they play critical roles in the biological processes of adipocytes such as differentiation, lipogenesis and lipolysis (Boudina & Graham, 2014; Cinti, 2009; Forner *et al*, 2009; Lee *et al*, 2019). Of note, during white adipocyte differentiation, fatty acid oxidation is increased to supply ATP, in marked contrast to a fully mature white adipocyte, in which fatty oxidation is inhibited(Boudina & Graham, 2014; De Pauw *et al*, 2009). Indeed, one of the features of mature WAT is that it has fewer mitochondria than BAT, with less expression of fatty acid oxidation-related enzymes such as acyl-CoA dehydrogenase (Forner *et al.*, 2009).

Brown Adipose Tissue (BAT) is composed of specialized, heat-producing adipocytes, and is the main site of non-shivering thermogenesis, a process resulting from mammalian evolution to regulate body temperature in cold environments (Cannon & Nedergaard, 2004). In addition, $UCP1^{+}$ 'brown-like' adipocytes, also known as beige cells, are thermogenically active adipocytes that can develop in white fat depots when mice are

exposed to cold or in response to hormonal stimuli such as catecholamines and other β-adrenergic agonists (Cannon & Nedergaard, 2004; Cohen & Spiegelman, 2015). Both thermogenic adipocytes play an important role in metabolic homeostasis and researchers have turned to strategies to induce the activity of these tissues as a possible therapeutic strategy for obesity and metabolic diseases.

A variety of adipose tissue dysfunctions have been demonstrated to play a role in development of obesity-related diseases. These include impairments in triglyceride storage in adipocytes and excessive release of fatty acids from adipocytes, alterations in "adipokines" and cytokines secretions, and negative effects overall of greater tissue mass. Given that mitochondria are essential for adipocyte-specific functions, impairments in mitochondrial function observed in adipose tissue of obese individuals negatively impact adipocyte differentiation, lipid metabolism, and insulin sensitivity (Chattopadhyay *et al*, 2011; Heinonen *et al*, 2015; Heinonen *et al*, 2020; Lee *et al.*, 2019). Moreover, it has been demonstrated that mitochondrial oxidative capacity is reduced in white adipocytes of obese adults (Yin *et al*, 2014). Further supporting that mitochondrial dysfunction in WAT contributes to metabolic syndrome, a recent study found a negative correlation between obesity and mitochondrial mass in WAT, where compared to lean age-matched control mice, white adipose tissue isolated from had significantly lower mitochondrial mass and oxygen consumption (Wilson-Fritch *et al*, 2003; Wilson-Fritch *et al*, 2004).

In addition, studies with pair-feeding of animals with lesions in neurons controlling energy expenditure and food intake (VMH) provide solid evidence that energy

expenditure is selectively impaired, even when food intake is normalized by pair feeding (Bray & York, 1979; Coleman, 1978; Cox & Powley, 1977, 1981; Ste Marie *et al*, 2000). In a mouse model of obesity, brown fat recruitment increased energy expenditure and reduced weight gain compared to controls, while BAT inactivation reduced energy expenditure resulting in obesity progression (Lowell *et al*, 1993). These data suggest adipose tissue plays a central role in regulating whole-body energy expenditure, not just storage (Roesler & Kazak, 2020).

Over the past several years, major advancements have been made in the field of brown adipose tissue biology, most notably the discovery that distinct and active BAT depots exist in adult humans (Cypess *et al*, 2009; Nedergaard *et al*, 2007). The existence of active brown adipose tissue in adult humans was initially revealed when researchers monitoring the uptake of the glucose analogue ^{18}F-fluorodeoxyglucose (^{18}F-FDG) with co-registered positron emission tomography (PET) and computed tomography (CT) imaging, identified regions corresponding to adipose tissue with high glucose uptake (Cohade *et al*, 2003; Cypess *et al.*, 2009; Hany *et al*, 2002; Nedergaard *et al.*, 2007; Yeung *et al*, 2003). FDG uptake was increased when patients were exposed to lower environmental temperatures (Christensen *et al*, 2006; Cohade *et al.*, 2003; Garcia *et al*, 2006) and reduced by pretreatment with β-adrenergic blockers such as propranolol or exposure to elevated temperature (Garcia *et al.*, 2006; Parysow *et al*, 2007; Söderlund *et al*, 2007). In addition, several studies have identified UCP1 protein and mRNA as well as high respiratory rate and low mitochondrial membrane potential in mitochondria isolated from tissue of perinephric and para-aortic depots of adult humans corresponding with FDG

uptake (Cunningham *et al*, 1985; Garruti & Ricquier, 1992; Kortelainen *et al*, 1993; Lean *et al*, 1986; Virtanen *et al*, 2009). These findings indicate that the FDG uptake in specific regions of adipose tissue reflects the metabolic activity of BAT (Nedergaard *et al.*, 2007). Additional studies have revealed that BAT FDG uptake is significantly lower in overweight and obese individuals compared with lean subjects, indicating a correlation between BAT activity and amount and metabolic health (Ouellet *et al*, 2011; Steinberg *et al*, 2017). Additionally, the amount of BAT is inversely correlated with body mass index (BMI) and percentage of body fat, suggesting individual variation in the amount or activity of brown adipose tissue is an important regulator of body weight, and a potential target for the treatment of obesity (Scheele & Wolfrum, 2020; Steinberg *et al.*, 2017; van Marken Lichtenbelt *et al*, 2009; Yeung *et al.*, 2003).

Since the discovery of BAT as the major site of non-shivering thermogenesis (Foster & Frydman, 1978), researchers have revealed that humans, similar to rodents, possess two types of UCP1-positive thermogenic adipocytes arising from developmentally distinct lineages: 1) Classical or developmentally programmed brown adipocytes and 2) Inducible, beige or brite cells that appear after thermogenic stimuli within white adipose tissue (Giralt & Villarroya, 2013). Both brown and beige fat cells are defined by their multilocular lipid droplet morphology, densely packed mitochondria and rich vascularization (Cinti, 2009; Cohen & Spiegelman, 2015). Despite their similarities, brown and beige fat come from different developmental lineages; classical brown fat cells arise from a myf5^{+} lineage shared with skeletal muscle, and UCP1^{+} beige cells induced in subcutaneous white fat depots come from a myf5^{-} lineage, that allow for distinction of

these two cell types (Cinti, 2009; Cohen & Spiegelman, 2015). The activation of classical BAT and the process of WAT "browning" share common mechanisms of induction (cold-mediated noradrenergic- induction), however the development of "inducible brown" adipocytes in WAT potentially involves a transdifferentiation processes of white-to-brown adipose tissue controlled by independent factors. Further understanding of WAT browning is a potential therapeutic strategy to increase energy expenditure.

Mitochondrial energy metabolism

Mitochondria play essential roles in cell physiology and energy metabolism; most notably they serve as the sites for the production of ATP through oxidative phosphorylation and support macromolecule biosynthesis. In addition to the production of energy, mitochondria also serve as hubs for Ca^{2+} handling, iron homeostasis, redox balance and importantly as signaling organelles that communicate the metabolic health status to the rest of the cell (Chandel, 2015). Mitochondria use the chemical energy harvested from the breakdown of sugars, amino acids, and fatty acids to generate reduced electron carriers NADH and $FADH_2$ through the tricarboxylic acid (TCA) cycle. NADH and $FADH_2$ are then passed through the respiratory chain (or electron transport chain ETC) where they donate their electrons down the ETC (complexes I through IV) through a series of favorable electron transfer reactions that are coupled to the pumping of protons against their concentration gradient into the mitochondrial intermembrane space. The final electron acceptor is molecular oxygen, which is reduced to H_2O ($½O_2$ to H_2O) at complex IV. The electron transfers through the respiratory chain result in both an electrostatic charge difference (positive outside) and a pH gradient from the pumping of

H+ (more acidic outside) across the inner mitochondrial membrane that generates a protonmotive force, and this potential energy is used to drive ATP synthesis (Rich & Maréchal, 2010). ATP-synthase, also known as respiratory complex V, uses the energy released by dissipating the proton gradient to drive the synthesis of ATP from ADP and Pi.

Moreover, under physiological conditions oxidative phosphorylation is incompletely coupled, as protons can leak across the inner membrane via carriers and activatable channels to dissipate the electrochemical proton gradient without the production of ATP (Bertholet *et al*, 2019; Bertholet *et al*, 2022; Divakaruni & Brand, 2011; Rich & Maréchal, 2010). Proton leak results in the dissipation or loss of potential energy, which might seem counterproductive but this mechanism has persisted throughout evolution, indicating a physiological role for mitochondrial inefficiency. The ability to uncouple oxidative phosphorylation from ATP production provides a mechanism to adjust energy metabolism and regulate metabolic homeostasis and body temperature (Brand, 2000; Divakaruni & Brand, 2011). The most well-known role for proton leak is thermogenesis, where specialized uncoupling proteins allow the flow of H+ down its concentration gradient dissipating the membrane potential to produce heat (Cannon & Nedergaard, 2004). Proton leak has also been shown to play a protective role against oxidative damage, where by decreasing the protonmotive force results in a lower rate of mitochondrial ROS production (Brand, 2000). The protonmotive force is also used to drive other endergonic mitochondrial processes such as the transport of ADP and P_i into the matrix, and the import of nuclear encoded proteins. Therefore, mitochondrial energetics

can be thought of as a balance between processes that contribute to the potential energy and those that consume it.

Energy dissipation and futile cycles

Chemical energy can be used to generate heat and perform work, which is transformed to ATP to generate work in biological systems. The proportion of heat versus work will determine the energetic efficiency of such a process. Thus, thermogenesis occurs through chemical reactions that liberate energy given off as heat, which would otherwise be used for work or captured by other molecules such as ATP or creatine phosphate (Cohen & Spiegelman, 2015). A system designed to be inefficient in terms of work is brown adipose tissue thermogenesis, where energy is purposely dissipated in the form of heat through the actions of UCP1, a key regulator of cold-mediated thermogenesis. Similarly, energy expenditure is triggered in response to caloric excess, and animals with reduced thermogenic fat function can succumb to diet-induced obesity.

A futile cycle occurs when a metabolic pathway concurrently runs in opposite directions, and as a result, energy is not produced but dissipated without any metabolic transformation or net gain (Cohen & Spiegelman, 2015; Qian & Beard, 2006). It was recently demonstrated that both beige and brown adipocytes have futile cycles of ATP consumption such as the futile creatine cycle, adding additional mechanisms by which beige and brown adipocytes promote energy expenditure. In this regard, mitochondria in all tissues are specialized in converting chemical energy derived from carbohydrates, lipids, and proteins into the high-energy phosphate bonds of ATP, or released as heat

(Lee *et al.*, 2019). Moreover, any chemical reaction including the production of ATP can generate heat as the by-product. Mitochondrial production of ATP is required for adipogenesis, as well as the synthesis of fatty acids and triglycerides (Boudina & Graham, 2014; Forner *et al.*, 2009; Johannsen & Ravussin, 2009; Lee *et al.*, 2019; Tormos *et al*, 2011). This raises the question regarding how adipocytes regulate fuel choice, as this might determine when adipocytes store lipids versus when adipocytes burn nutrients to generate heat.

Mechanisms controlling energy wasting versus energy storage in brown and beige adipocytes

Brown and beige adipose cells have the capacity to burn both glucose and fat to produce heat through the activation of the sympathetic nervous system (Harms & Seale, 2013; Kajimura *et al*, 2015). The sympathetic nervous system regulates the growth and development of BAT and its thermogenic function (Cannon & Nedergaard, 2004). Brown and beige adipocytes are innervated by sympathetic fibers, and upon cold-exposure, cold-sensitive thermoreceptors transmit afferent signals to the hypothalamus (Cannon & Nedergaard, 2004). These signals lead to the release of the sympathetic neurotransmitter norepinephrine (NE) from sympathetic nerves that innervate brown adipocytes to activate thermogenesis (Cannon & Nedergaard, 2004; Labbé *et al*, 2015; Morrison *et al*, 2014; Zhang & Bi, 2015). Norepinephrine binds β_3-adrenergic receptors in the membrane of brown adipocytes triggering PKA-cAMP and calcium signaling that results in lipid mobilization and lipolysis (Chernogubova *et al*, 2004; Dolgacheva *et al*, 2003). The

resultant free-fatty acids (FFAs) released from triglycerides activates the mitochondrial UCP1 (Azzu *et al*, 2010; Ježek *et al*, 2019). Activated UCP1 uncouples the electron transport of the respiratory chain, thereby blocking ATP production and dissipating energy from nutrient oxidation in the form of heat (Azzu *et al.*, 2010; Ježek *et al.*, 2019). Indeed, uncoupling allows a concurrent increase in TCA cycle and beta oxidation fluxes in the mitochondria, ensuring that sufficient reducing equivalents are generated to sustain proton extrusion, combating excessive depolarization.

Brown and beige adipose cells have the capacity to burn both glucose and fat to produce heat through the activation of the sympathetic nervous system (Harms & Seale, 2013; Kajimura *et al*, 2015). The sympathetic nervous system regulates the growth and development of BAT and its thermogenic function (Cannon & Nedergaard, 2004). Brown and beige adipocytes are innervated by sympathetic fibers, and upon cold-exposure, cold-sensitive thermoreceptors transmit afferent signals to the hypothalamus (Cannon & Nedergaard, 2004). These signals lead to the release of the sympathetic neurotransmitter norepinephrine (NE) from sympathetic nerves that innervate brown adipocytes to activate thermogenesis (Cannon & Nedergaard, 2004; Labbé *et al*, 2015; Morrison *et al*, 2014; Zhang & Bi, 2015). Norepinephrine binds β_3-adrenergic receptors in the membrane of brown adipocytes triggering PKA-cAMP and calcium signaling that results in lipid mobilization and lipolysis (Chernogubova *et al*, 2004; Dolgacheva *et al*, 2003). The resultant free-fatty acids (FFAs) released from triglycerides activates the mitochondrial UCP1 (Azzu *et al*, 2010; Ježek *et al*, 2019). Activated UCP1 uncouples the electron transport of the respiratory chain, thereby blocking ATP production and dissipating energy

from nutrient oxidation in the form of heat (Azzu *et al.*, 2010; Ježek *et al.*, 2019). Indeed, uncoupling allows a concurrent increase in TCA cycle and beta oxidation fluxes in the mitochondria, ensuring that sufficient reducing equivalents are generated to sustain proton extrusion, combating excessive depolarization. NE also induces a signaling cascade via PPARγ coactivator (PGC)-1 α that can stimulate transcriptional activation of mitochondrial genes to increase mitochondrial mass, as well as UCP1 itself , together with genes encoding proteins that control the uptake of lipids and glucose from the circulation, in order to sustain oxidation and thermogenesis (Giralt & Villarroya, 2013; Kajimura *et al.*, 2015).

Metabolic benefits induced by activating BAT and WAT energy expenditure

The primary activation of BAT was shown to impact systemic metabolism, by decreasing body weight and improving insulin sensitivity in mice (Stanford *et al*, 2013). Activation of UCP1 was shown to reduce elevated triglyceride concentrations and increase insulin sensitivity in mice subject to short-term cold exposure (4 hours) (Bartelt *et al*, 2011). Additional studies in transgenic mice with reduced brown fat have glucose intolerance and insulin resistance and are more susceptible to diet-induced obesity and diabetes (Hamann *et al*, 1995; Lowell & Flier, 1997), supporting the hypothesis that brown fat protects against obesity.

Numerous studies in rodents targeting the components upstream of BAT activation, by manipulating the sympathetic nervous system activity or inducing pharmacological stimulations targeting the β_3-adrenergic receptor (β_3-AR), have demonstrated an effective

means of dissipating excess energy (Berbée *et al*, 2015; Blondin *et al*, 2020; Mukherjee *et al*, 2016; Robidoux *et al*, 2004; Zaror-Behrens & Himms-Hagen, 1983). In humans, cold exposure has been known for several decades to activate BAT thermogenesis, and is currently the most effective way to stimulate BAT activity. Pharmacological strategies for BAT recruitment in humans have proven to be more complicated. Pharmacological stimulations targeting the β_3-adrenergic receptor (β_3-AR), the adrenergic receptor believed to mediate BAT thermogenesis, involve the use of use of β3-adrenergic receptor agonists, such as mirabegron (O'Mara *et al*, 2020). Although chronic mirabegron treatment was shown to increase BAT metabolic activity and improve insulin sensitivity, chronic treatment with adrenergic agonists can lead to undesirable off target side effects and presents too great a cardiovascular risk for clinical treatment of metabolic dysfunction in obese patients (Blondin *et al.*, 2020; O'Mara *et al.*, 2020). Importantly, it was revealed through this study using pharmacological stimulation and inhibition of the β_2-adrenergic receptor (β_2-AR) that human BAT activation is controlled by the β_2-AR, in contrast to BAT thermogenesis in rodents that is mediated by β_3-AR activation (Blondin *et al.*, 2020).

In addition, research related to the transcriptional control of brown adipocyte development, differentiation, and function have identified several regulators of brown adipocyte cell fate such as the PR domain containing 16 (PRDM16)(Seale *et al*, 2008; Seale *et al*, 2007) as well as Bone morphogenetic protein 7 (BMP7) which has been shown to specifically direct brown adipocyte differentiation (Tseng *et al*, 2008). Engineering synthetic chemicals or using endogenous known regulators of brown

adipocytes to promote brown adipocyte growth and development may be viable anti-obesity therapeutic.

On the other hand, the concept of WAT browning is extremely interesting as a potential therapeutic given the extreme amounts of excess WAT in obese individuals (Harms & Seale, 2013). Browning of WAT in many rodent models was found to result in resistance to diet-induced obesity and improvement in systemic energy metabolism (Kim & Plutzky, 2016; Seale *et al*, 2011; Vegiopoulos *et al*, 2010). WAT browning has been shown to be regulated by environmental factors including chronic cold exposure, physical activity, nutrition, and endocrine hormones and metabolites (Sidossis & Kajimura, 2015). WAT browning is impaired in obesity, and this has been associated with reduced energy expenditure, increased body weight and reduced insulin sensitivity (Sidossis & Kajimura, 2015). Chronic treatment of β_3-adrenergic activators or proliferator-activated receptor γ (PPARγ) agonist thiazolidinedione (TZD) in mice promotes WAT browning and thermogenic capacity by inducing mitochondrial biogenesis and UCP1 gene expression (Petrovic *et al*, 2010). Moreover, WAT browning by cold exposure was shown to play a role in increasing adipose tissue innervation, and this is a potential strategy to increase neurocrine-adipose signal integration (Bertholet *et al*, 2017; Christian, 2015; Guilherme *et al*, 2019). Furthermore, fibroblast growth factor 21 (FGF21) promotes white adipose tissue browning by increasing the expression of UCP1 and other thermogenic genes in white adipose tissue (Fisher *et al*, 2012). (UCP1 activation and mediated-uncoupling is not uncontrolled).

Studies with UCP1-KO mice demonstrate that these mice are resistant to diet-induced obesity at sub-thermoneutral temperatures (Enerbäck *et al*, 1997; Liu *et al*, 2003; Stefl *et al*, 1998). Additionally, it was found that UCP1-KO mice can adapt to tolerate cold, providing further evidence that BAT has alternative UCP1-independent thermogenic mechanisms to control energy expenditure (Enerbäck *et al.*, 1997; Hofmann *et al*, 2001; Ukropec *et al*, 2006).

Alternative approaches to increase energy expenditure independent of UCP1-mediated uncoupling involves the activation of ATP- consuming futile cycle**.** These mechanisms selectively consume specific ATP pools and offer an alternative to UCP1 dependent thermogenesis in brown and beige adipocytes. These UCP1 independent futile cycles prevent mitochondrial uncoupling, swelling and mitophagy. In chapter 2, we will review these alternative mechanisms of energy-dissipation with a focus on glycerolipid - free fatty acid cycling (GL/FFA or lipid cycling), as we recently identified a novel mechanism to induce a futile cycle of lipid breakdown and partial or full re-esterification in BAT by blocking the mitochondrial pyruvate carrier (MPC).

Mitochondrial heterogeneity and the control of lipid utilization

As described above, mitochondria morphology and function (energy generation and signaling) varies between different cell and tissue types. More recently, it has been demonstrated through advanced microscopy and isolation techniques that within individual cells, there are subpopulations of mitochondria with distinct characteristics indicating intercellular heterogeneity (Ngo *et al*, 2021). As mitochondrial morphology

relates to function, many of the differences in size, shape and cristae architecture relate to differences in subcellular localizations or microdomains in order to fulfill functions thar are required to meet specific needs (Kuznetsov & Margreiter, 2009).

Studies in brown adipose tissue have challenged views that mitochondria within a single cell are homogenous. Previously it was suggested that the entire population of mitochondria go through events of fusion and fission, with all mitochondria sharing the same content (Twig *et al*, 2008). Brown adipose tissue is a specialized organ that is responsible for maintaining body temperature through thermogenesis. One of the key characteristics of brown adipose tissue is its ability to both burn fat to produce heat, and to store fatty acids for fast mobilization. However it was not well understood if both the synthesis and oxidation of lipids can occur simultaneously, but recent reports in BAT have challenged our previous understanding and have explained how a cell can perform antagonistic metabolic processes.

Several studies in multiple tissue types including BAT and skeletal muscle have observed a unique population of mitochondria that are closely associated with lipid droplets and have a distinct morphology and cristae structure compared to the mitochondria in the cytoplasm (Benador *et al*, 2018; Boutant *et al*, 2017; Li *et al*, 2019; Wikstrom *et al*, 2014). By separating these unique populations from the same cell, Benador et al. discovered that the mitochondria attached to LDs have distinct bioenergetics, proteome, cristae organization and dynamics compared to cytoplasmic mitochondria (CM) that support lipid droplet expansion. Specifically, PDM tend to be more elongated with a higher capacity to oxidize pyruvate and malate, but lower capacity for

fat oxidation. Interestingly, PDM were shown to have a higher ATP synthesis capacity, that supports LD expansion by providing ATP for TAG synthesis. In contrast, CM are more fragmented and have increased fatty acid oxidation capacity (Benador *et al.*, 2018). Moreover, it was found that PDM and CM remain distinct populations as PDM do not fuse with CM and have limited motility. Overall, the finding that BAT maintains separate mitochondrial populations with distinct proteomes and fuel preference supports how brown adipose tissue maintains its metabolic flexibility and can undergo thermogenesis as well as lipid synthesis, to varying degrees concurrently (Benador *et al.*, 2018).

Although mitochondria-LD interaction has been observed in many cell and tissue types, the mechanisms that control their interaction are still not well understood. Several studies have identified mechanisms of mitochondria-LD interaction through the expression of proposed "linker" proteins, and this has enabled preliminary studies investigating the potential role of PDM in different cell types. One of the proposed PDM tethering proteins is Perilipin 5 (Plin5), which was shown to induce the formation of PDM by linking lipid droplets to mitochondria in multiple cell and tissue types including skeletal and cardiac muscle, liver, and pancreatic β-cells (Bosma *et al*, 2013; Laurens *et al*, 2016; Pollak *et al*, 2013; Sztalryd & Kimmel, 2014; Tan *et al*, 2019; Trevino *et al*, 2015b; Wang *et al*, 2011; Zhu *et al*, 2019). While Plin5 has demonstrated to be an efficient inducer of PDM, we must be careful in interpreting the results of the Plin5 OE and knockdown studies in the context of PDM. Plin5 is also a negative regulator of lipolysis through its interaction with ATGL (Adipose triglyceride lipase), making it difficult to separate the role of PDM directly in LD expansion with that of Plin5, blocking lipolysis (Sztalryd & Kimmel,

2014). Taking this into consideration, we have still learned a lot about PDM from Plin5 models.

Data in primary brown adipocytes using Plin5 overexpression demonstrated that inducing PDM formation shifts fuel utilization and lipid morphology and handling, suggesting that forcing mitochondria to attach to the LD is sufficient to give them their unique bioenergetics (Benador *et al.*, 2018). Plin5 overexpression in other metabolically active tissues was also shown to be protective against lipotoxicity and improve tissue specific functions in response to metabolic stress, for example by improving glucose tolerance and insulin secretion in pancreatic islets and β-cells (Trevino *et al*, 2015a; Zhu *et al.*, 2019). Moreover, Plin5 overexpression in HepG2 cells provided protection from H_2O_2 induced apoptosis, suggesting that PDM can confer resistance against cellular oxidative stress (Tan *et al.*, 2019). These results indicate that shifting mitochondrial heterogeneity in cells can contribute to differences in tissue function. Interestingly, under different cellular conditions, unique populations of mitochondria can be favorable or potentially pathologic, depending on the overall cellular and nutrient state. For example, increasing PDM in both conditions of starvation and nutrient excess can be protective. Under conditions of starvation, Nguyen et al. demonstrated that nutrient deprivation leads to LD expansion and increased PDM. Their model suggests that PDMs protect against lipotoxicity from starvation-induced autophagy by providing a lipid buffering system that sequesters FAs released by autophagic degradation (Nguyen *et al*, 2017). Moreover, overexpression of both Plin5 and DGAT2, another proposed mitochondria-LD tether shown to promote PDM formation, increased LD mass and protected against lipotoxic

liver injury in models of nutrient overload (Monetti *et al*, 2007; Stone *et al*, 2009; Wang *et al*, 2015a). Interestingly, it has also been shown in both obese individuals and trained athletes that lipid droplets expand in skeletal muscle in response to physical training and nutrient overload. However, opposite effects on insulin sensitivity are observed, where increasing lipid droplets in muscle is pathogenic in the obese state, but LD expansion by PDM in trained athletes has a beneficial physiological role (Laurens *et al.*, 2016; Li *et al.*, 2019).

In support of a tissue-specific role of PDM, recent studies in hepatocytes found that unique subpopulations of hepatic mitochondria support distinct lipid metabolic pathways. In conditions of starvation, fatty acids are selectively trafficked to cytosolic mitochondria (CM) for oxidation, while PDM are the major site of fatty acid trafficking and facilitate esterification under fed conditions or during excess fatty acid exposure. Moreover, Najt et al. found that the proportion of these populations is altered under different metabolic states such as nutrient deprivation, enabling fine tune control of cellular adaptation (Najt *et al*, 2023).

Mitophagy and adaptation to the nutritional state regulate mitochondrial dynamics

Recent studies linking mitochondrial architecture and the balance of energy supply and demand suggest that changes in mitochondrial dynamics may reflect a bioenergetic adaptation to fuel availability and metabolic status (Brooks *et al*, 2009; Liesa & Shirihai,

2013; Ngo *et al*, 2023). Mitochondria normally go through frequent fusion and fission events that allow mitochondria to reorganize and dispose damaged elements through mitophagy; however the balance between fusion and fission is disrupted by altered nutrient exposure (Gao *et al*, 2014; Stiles & Shirihai, 2012). Mitochondrial dynamics maintains the pool of metabolically efficient mitochondria, and disruption of either fusion or fission alters mitochondrial morphology and functionality (Liesa *et al*, 2009; Liesa & Shirihai, 2013). Under conditions of nutrient excess, the balance between fusion and fission leans in favor of fission and reduction in fusion resulting in an increase in fragmented mitochondria, whereas under starvation mitochondria shift towards an elongated state through increased fusion (Brooks *et al.*, 2009; Gao *et al.*, 2014; Liesa & Shirihai, 2013; Ngo *et al.*, 2023; Stiles & Shirihai, 2012). Mitochondrial fragmentation under conditions of metabolic stress was previously thought to be maladaptive, however it was recently shown in several cell types including hepatocytes and HepG2 cells, beta cells and cancer cells that fragmentation in response to excess nutrients increases both lipid oxidation capacity and preference for lipids as a fuel (Gao *et al.*, 2014; Martinez-Lopez *et al*, 2023; Molina *et al*, 2009; Ngo *et al.*, 2023; Supale *et al*, 2012). Moreover, adrenergic stimulation in brown adipose tissue induces mitochondrial fragmentation that promotes fatty acid utilization, suggesting fragmentation may have an adaptive role in regulating fuel preference and utilization (Liesa & Shirihai, 2013).

Although changes to mitochondrial morphology in response to nutrient stress are adaptive, over time these adaptive changes to mitochondria can produce a state of de-compensation, where the adaptive changes, over time compromise other essential

functions, such as mitochondrial quality control (Ngo *et al.*, 2021). In pancreatic beta-cells, chronic exposure to excess glucose and free fatty acids resulted in heterogeneity in mitochondrial morphology and membrane potential, resulting in pathological fragmentation, impaired glucose-stimulated insulin secretion and increased apoptosis (Molina *et al.*, 2009; Wikstrom *et al*, 2007). Mitochondrial fission was also shown to play a vital role in the progression of nonalcoholic fatty liver disease (NAFLD). Because of these findings, several studies aimed to determine if fragmentation was compensatory or pathogenic in NAFLD by removing DRP1 and investigating if inhibiting mitochondrial fission was protective. Although some studies found that decreasing mitochondrial fission was protective and prevented body fat gain, glucose intolerance and hepatic triglyceride accumulation in models of NAFLD (Galloway *et al*, 2014; Wang *et al*, 2015b), these studies were not translational as Drp1 was knocked out or decreased prior to high fat diet feeding. A similar study induced Drp1 knockdown in hepatocytes of adult mice with established NASH and found that loss of Drp1 exacerbated inflammation, NASH-induced ER stress, fibrosis and necrosis, arguing that fission might indeed play a protective role (Steffen *et al*, 2022).

Increased mitochondrial fragmentation has also been observed in several models of kidney injury and in kidney biopsies from diabetic human patients, resulting in an increase in the population of fragmented mitochondria that maintain reduced fatty acid oxidation (Kang *et al*, 2015; Zhan *et al*, 2013). Energy depletion by impaired fatty acid oxidation is a key contributor to the development of several kidney diseases, suggesting a role of mitochondrial fragmentation through increased morphological heterogeneity in

the pathogenesis of renal diseases (Brooks *et al.*, 2009; Ngo *et al.*, 2021; Zhan *et al.*, 2013). Interestingly, while increased mitochondrial fragmentation resulted in reduced mitochondrial fatty acid oxidation in the kidney, in the beta cell and liver increased fatty acid utilization was induced by fragmentation, demonstrating how increased heterogeneity can alter mitochondrial function in various ways dependent on their specific tissue function.

The role of PDM and mitochondrial heterogeneity in WAT

Manipulating the subpopulations of mitochondria within cells has the potential to provide a novel mechanism to control the metabolic state, fuel preference and nutrient availability vs utilization. Moreover, little is known about the existence of unique mitochondrial populations, such as PDM in white adipose tissue and whether these levels change throughout adipogenesis or in response to stress. PDM have been proposed to play a role in LD building during the early stages of adipogenesis, where increased ATP is required to support de novo lipogenesis and LD synthesis.

Being the main tissue for lipid storage, WAT has an important role in buffering nutrient availability and demand by storing excess calories and preventing the toxic accumulation of excess nutrients in non-adipose tissues. During the development of obesity, increased nutrient intake can exceed the capacity of WAT to safely store the excess lipids, leading to lipotoxicity. Although it may seem counterintuitive to increase LD content as a therapy for obesity, triglyceride accumulation in response to lipid overload was shown to protect against fatty-acid induced lipotoxicity (Listenberger *et al*, 2003).

Thus increasing PDM content may represent an approach to prevent lipotoxicity by securing free fatty acids into TAGs. In chapter 3, we will further explore whether PDM exist in white adipocytes, and their potential role in lipid expansion vs utilization.

References

Azzu V, Jastroch M, Divakaruni AS, Brand MD (2010) The regulation and turnover of mitochondrial uncoupling proteins. *Biochim Biophys Acta* 1797: 785-791

Bartelt A, Bruns OT, Reimer R, Hohenberg H, Ittrich H, Peldschus K, Kaul MG, Tromsdorf UI, Weller H, Waurisch C *et al* (2011) Brown adipose tissue activity controls triglyceride clearance. *Nat Med* 17: 200-205

Benador IY, Veliova M, Mahdaviani K, Petcherski A, Wikstrom JD, Assali EA, Acín-Pérez R, Shum M, Oliveira MF, Cinti S *et al* (2018) Mitochondria Bound to Lipid Droplets Have Unique Bioenergetics, Composition, and Dynamics that Support Lipid Droplet Expansion. *Cell Metab* 27: 869-885.e866

Berbée JF, Boon MR, Khedoe PP, Bartelt A, Schlein C, Worthmann A, Kooijman S, Hoeke G, Mol IM, John C *et al* (2015) Brown fat activation reduces hypercholesterolaemia and protects from atherosclerosis development. *Nat Commun* 6: 6356

Bertholet AM, Chouchani ET, Kazak L, Angelin A, Fedorenko A, Long JZ, Vidoni S, Garrity R, Cho J, Terada N *et al* (2019) H(+) transport is an integral function of the mitochondrial ADP/ATP carrier. *Nature* 571: 515-520

Bertholet AM, Kazak L, Chouchani ET, Bogaczyńska MG, Paranjpe I, Wainwright GL, Bétourné A, Kajimura S, Spiegelman BM, Kirichok Y (2017) Mitochondrial Patch Clamp of Beige Adipocytes Reveals UCP1-Positive and UCP1-Negative Cells Both Exhibiting Futile Creatine Cycling. *Cell Metab* 25: 811-822.e814

Bertholet AM, Natale AM, Bisignano P, Suzuki J, Fedorenko A, Hamilton J, Brustovetsky T, Kazak L, Garrity R, Chouchani ET *et al* (2022) Mitochondrial

uncouplers induce proton leak by activating AAC and UCP1. *Nature* 606: 180-187

Blondin DP, Nielsen S, Kuipers EN, Severinsen MC, Jensen VH, Miard S, Jespersen NZ, Kooijman S, Boon MR, Fortin M *et al* (2020) Human Brown Adipocyte Thermogenesis Is Driven by β2-AR Stimulation. *Cell Metab* 32: 287-300.e287

Bosma M, Sparks LM, Hooiveld GJ, Jorgensen JA, Houten SM, Schrauwen P, Kersten S, Hesselink MK (2013) Overexpression of PLIN5 in skeletal muscle promotes oxidative gene expression and intramyocellular lipid content without compromising insulin sensitivity. *Biochim Biophys Acta* 1831: 844-852

Boudina S, Graham TE (2014) Mitochondrial function/dysfunction in white adipose tissue. *Exp Physiol* 99: 1168-1178

Boutant M, Kulkarni SS, Joffraud M, Ratajczak J, Valera-Alberni M, Combe R, Zorzano A, Cantó C (2017) Mfn2 is critical for brown adipose tissue thermogenic function. *Embo j* 36: 1543-1558

Brand MD (2000) Uncoupling to survive? The role of mitochondrial inefficiency in ageing. *Exp Gerontol* 35: 811-820

Bray GA, York DA (1979) Hypothalamic and genetic obesity in experimental animals: an autonomic and endocrine hypothesis. *Physiol Rev* 59: 719-809

Brooks C, Wei Q, Cho SG, Dong Z (2009) Regulation of mitochondrial dynamics in acute kidney injury in cell culture and rodent models. *J Clin Invest* 119: 1275-1285

Cannon B, Nedergaard J (2004) Brown adipose tissue: function and physiological significance. *Physiol Rev* 84: 277-359

Carobbio S, Pellegrinelli V, Vidal-Puig A (2017) Adipose Tissue Function and Expandability as Determinants of Lipotoxicity and the Metabolic Syndrome. *Adv Exp Med Biol* 960: 161-196

Chandel NS (2015) Evolution of Mitochondria as Signaling Organelles. *Cell Metab* 22: 204-206

Chattopadhyay M, Guhathakurta I, Behera P, Ranjan KR, Khanna M, Mukhopadhyay S, Chakrabarti S (2011) Mitochondrial bioenergetics is not impaired in nonobese subjects with type 2 diabetes mellitus. *Metabolism* 60: 1702-1710

Chernogubova E, Cannon B, Bengtsson T (2004) Norepinephrine increases glucose transport in brown adipocytes via beta3-adrenoceptors through a cAMP, PKA, and PI3-kinase-dependent pathway stimulating conventional and novel PKCs. *Endocrinology* 145: 269-280

Chitraju C, Mejhert N, Haas JT, Diaz-Ramirez LG, Grueter CA, Imbriglio JE, Pinto S, Koliwad SK, Walther TC, Farese RV (2017) Triglyceride Synthesis by DGAT1 Protects Adipocytes from Lipid-Induced ER Stress during Lipolysis. *Cell Metab* 26: 407-418.e403

Christensen CR, Clark PB, Morton KA (2006) Reversal of hypermetabolic brown adipose tissue in F-18 FDG PET imaging. *Clin Nucl Med* 31: 193-196

Christian M (2015) Transcriptional fingerprinting of "browning" white fat identifies NRG4 as a novel adipokine. *Adipocyte* 4: 50-54

Cinti S (2009) Transdifferentiation properties of adipocytes in the adipose organ. *Am J Physiol Endocrinol Metab* 297: E977-986

Coelho M, Oliveira T, Fernandes R (2013) Biochemistry of adipose tissue: an endocrine organ. *Arch Med Sci* 9: 191-200

Cohade C, Mourtzikos KA, Wahl RL (2003) "USA-Fat": prevalence is related to ambient outdoor temperature-evaluation with 18F-FDG PET/CT. *J Nucl Med* 44: 1267-1270

Cohen P, Spiegelman BM (2015) Brown and Beige Fat: Molecular Parts of a Thermogenic Machine. *Diabetes* 64: 2346-2351

Coleman DL (1978) Obese and diabetes: two mutant genes causing diabetes-obesity syndromes in mice. *Diabetologia* 14: 141-148

Cox JE, Powley TL (1977) Development of obesity in diabetic mice pair-fed with lean siblings. *J Comp Physiol Psychol* 91: 347-358

Cox JE, Powley TL (1981) Intragastric pair feeding fails to prevent VMH obesity or hyperinsulinemia. *Am J Physiol* 240: E566-572

Cunningham S, Leslie P, Hopwood D, Illingworth P, Jung RT, Nicholls DG, Peden N, Rafael J, Rial E (1985) The characterization and energetic potential of brown adipose tissue in man. *Clin Sci (Lond)* 69: 343-348

Cypess AM, Lehman S, Williams G, Tal I, Rodman D, Goldfine AB, Kuo FC, Palmer EL, Tseng YH, Doria A *et al* (2009) Identification and importance of brown adipose tissue in adult humans. *N Engl J Med* 360: 1509-1517

Daneschvar HL, Aronson MD, Smetana GW (2016) FDA-Approved Anti-Obesity Drugs in the United States. *Am J Med* 129: 879.e871-876

De Pauw A, Tejerina S, Raes M, Keijer J, Arnould T (2009) Mitochondrial (dys)function in adipocyte (de)differentiation and systemic metabolic alterations. *Am J Pathol* 175: 927-939

Divakaruni AS, Brand MD (2011) The regulation and physiology of mitochondrial proton leak. *Physiology (Bethesda)* 26: 192-205

Dolgacheva LP, Abzhalelov BB, Zhang SJ, Zinchenko VP, Bronnikov GE (2003) Norepinephrine induces slow calcium signalling in murine brown preadipocytes through the beta-adrenoceptor/cAMP/protein kinase A pathway. *Cell Signal* 15: 209-216

Enerbäck S, Jacobsson A, Simpson EM, Guerra C, Yamashita H, Harper ME, Kozak LP (1997) Mice lacking mitochondrial uncoupling protein are cold-sensitive but not obese. *Nature* 387: 90-94

Filippatos TD, Derdemezis CS, Gazi IF, Nakou ES, Mikhailidis DP, Elisaf MS (2008) Orlistat-associated adverse effects and drug interactions: a critical review. *Drug Saf* 31: 53-65

Fisher FM, Kleiner S, Douris N, Fox EC, Mepani RJ, Verdeguer F, Wu J, Kharitonenkov A, Flier JS, Maratos-Flier E *et al* (2012) FGF21 regulates PGC-1α and browning of white adipose tissues in adaptive thermogenesis. *Genes Dev* 26: 271-281

Forner F, Kumar C, Luber CA, Fromme T, Klingenspor M, Mann M (2009) Proteome differences between brown and white fat mitochondria reveal specialized metabolic functions. *Cell Metab* 10: 324-335

Foster DO, Frydman ML (1978) Brown adipose tissue: the dominant site of nonshivering thermogenesis in the rat. *Experientia Suppl* 32: 147-151

Galloway CA, Lee H, Brookes PS, Yoon Y (2014) Decreasing mitochondrial fission alleviates hepatic steatosis in a murine model of nonalcoholic fatty liver disease. *Am J Physiol Gastrointest Liver Physiol* 307: G632-641

Gao AW, Cantó C, Houtkooper RH (2014) Mitochondrial response to nutrient availability and its role in metabolic disease. *EMBO Mol Med* 6: 580-589

Garcia CA, Van Nostrand D, Atkins F, Acio E, Butler C, Esposito G, Kulkarni K, Majd M (2006) Reduction of brown fat 2-deoxy-2-[F-18]fluoro-D-glucose uptake by controlling environmental temperature prior to positron emission tomography scan. *Mol Imaging Biol* 8: 24-29

Garruti G, Ricquier D (1992) Analysis of uncoupling protein and its mRNA in adipose tissue deposits of adult humans. *Int J Obes Relat Metab Disord* 16: 383-390

Giralt M, Villarroya F (2013) White, brown, beige/brite: different adipose cells for different functions? *Endocrinology* 154: 2992-3000

Guilherme A, Henriques F, Bedard AH, Czech MP (2019) Molecular pathways linking adipose innervation to insulin action in obesity and diabetes mellitus. *Nat Rev Endocrinol* 15: 207-225

Hamann A, Benecke H, Le Marchand-Brustel Y, Susulic VS, Lowell BB, Flier JS (1995) Characterization of insulin resistance and NIDDM in transgenic mice with reduced brown fat. *Diabetes* 44: 1266-1273

Hany TF, Gharehpapagh E, Kamel EM, Buck A, Himms-Hagen J, von Schulthess GK (2002) Brown adipose tissue: a factor to consider in symmetrical tracer uptake in the neck and upper chest region. *Eur J Nucl Med Mol Imaging* 29: 1393-1398

Harms M, Seale P (2013) Brown and beige fat: development, function and therapeutic potential. *Nat Med* 19: 1252-1263

Heaney J. (2013) Energy: Expenditure I, Lack of. In: Gellman M.D., Turner J.R. (eds) Encyclopedia of Behavioral Medicine. Springer, New York, NY. https://doi.org/10.1007/978-1-4419-1005-9_454.

Heinonen S, Buzkova J, Muniandy M, Kaksonen R, Ollikainen M, Ismail K, Hakkarainen A, Lundbom J, Lundbom N, Vuolteenaho K *et al* (2015) Impaired Mitochondrial Biogenesis in Adipose Tissue in Acquired Obesity. *Diabetes* 64: 3135-3145

Heinonen S, Jokinen R, Rissanen A, Pietiläinen KH (2020) White adipose tissue mitochondrial metabolism in health and in obesity. *Obes Rev* 21: e12958

Hofmann WE, Liu X, Bearden CM, Harper ME, Kozak LP (2001) Effects of genetic background on thermoregulation and fatty acid-induced uncoupling of mitochondria in UCP1-deficient mice. *J Biol Chem* 276: 12460-12465

Hussain MF, Roesler A, Kazak L (2020) Regulation of adipocyte thermogenesis: mechanisms controlling obesity. *Febs j* 287: 3370-3385

Ježek P, Jabůrek M, Porter RK (2019) Uncoupling mechanism and redox regulation of mitochondrial uncoupling protein 1 (UCP1). *Biochim Biophys Acta Bioenerg* 1860: 259-269

Johannsen DL, Ravussin E (2009) The role of mitochondria in health and disease. *Curr Opin Pharmacol* 9: 780-786

Kajimura S, Spiegelman BM, Seale P (2015) Brown and Beige Fat: Physiological Roles beyond Heat Generation. *Cell Metab* 22: 546-559

Kang HM, Ahn SH, Choi P, Ko YA, Han SH, Chinga F, Park AS, Tao J, Sharma K, Pullman J *et al* (2015) Defective fatty acid oxidation in renal tubular epithelial cells has a key role in kidney fibrosis development. *Nat Med* 21: 37-46

Kim SH, Plutzky J (2016) Brown Fat and Browning for the Treatment of Obesity and Related Metabolic Disorders. *Diabetes Metab J* 40: 12-21

Kortelainen ML, Pelletier G, Ricquier D, Bukowiecki LJ (1993) Immunohistochemical detection of human brown adipose tissue uncoupling protein in an autopsy series. *J Histochem Cytochem* 41: 759-764

Labbé SM, Caron A, Lanfray D, Monge-Rofarello B, Bartness TJ, Richard D (2015) Hypothalamic control of brown adipose tissue thermogenesis. *Front Syst Neurosci* 9: 150

Laurens C, Bourlier V, Mairal A, Louche K, Badin PM, Mouisel E, Montagner A, Marette A, Tremblay A, Weisnagel JS *et al* (2016) Perilipin 5 fine-tunes lipid oxidation to metabolic demand and protects against lipotoxicity in skeletal muscle. *Sci Rep* 6: 38310

Lean ME, James WP, Jennings G, Trayhurn P (1986) Brown adipose tissue uncoupling protein content in human infants, children and adults. *Clin Sci (Lond)* 71: 291-297

Lee JH, Park A, Oh KJ, Lee SC, Kim WK, Bae KH (2019) The Role of Adipose Tissue Mitochondria: Regulation of Mitochondrial Function for the Treatment of Metabolic Diseases. *Int J Mol Sci* 20

Li X, Li Z, Zhao M, Nie Y, Liu P, Zhu Y, Zhang X (2019) Skeletal Muscle Lipid Droplets and the Athlete's Paradox. *Cells* 8

Liesa M, Palacín M, Zorzano A (2009) Mitochondrial dynamics in mammalian health and disease. *Physiol Rev* 89: 799-845

Liesa M, Shirihai OS (2013) Mitochondrial dynamics in the regulation of nutrient utilization and energy expenditure. *Cell Metab* 17: 491-506

Listenberger LL, Han X, Lewis SE, Cases S, Farese RV, Jr., Ory DS, Schaffer JE (2003) Triglyceride accumulation protects against fatty acid-induced lipotoxicity. *Proc Natl Acad Sci U S A* 100: 3077-3082

Liu X, Rossmeisl M, McClaine J, Riachi M, Harper ME, Kozak LP (2003) Paradoxical resistance to diet-induced obesity in UCP1-deficient mice. *J Clin Invest* 111: 399-407

Lowell BB, Flier JS (1997) Brown adipose tissue, beta 3-adrenergic receptors, and obesity. *Annu Rev Med* 48: 307-316

Lowell BB, Spiegelman BM (2000) Towards a molecular understanding of adaptive thermogenesis. *Nature* 404: 652-660

Lowell BB, V SS, Hamann A, Lawitts JA, Himms-Hagen J, Boyer BB, Kozak LP, Flier JS (1993) Development of obesity in transgenic mice after genetic ablation of brown adipose tissue. *Nature* 366: 740-742

Martinez-Lopez N, Mattar P, Toledo M, Bains H, Kalyani M, Aoun ML, Sharma M, McIntire LBJ, Gunther-Cummins L, Macaluso FP *et al* (2023) mTORC2-NDRG1-CDC42 axis couples fasting to mitochondrial fission. *Nat Cell Biol* 25: 989-1003

Molina AJ, Wikstrom JD, Stiles L, Las G, Mohamed H, Elorza A, Walzer G, Twig G, Katz S, Corkey BE *et al* (2009) Mitochondrial networking protects beta-cells from nutrient-induced apoptosis. *Diabetes* 58: 2303-2315

Monetti M, Levin MC, Watt MJ, Sajan MP, Marmor S, Hubbard BK, Stevens RD, Bain JR, Newgard CB, Farese RV, Sr. *et al* (2007) Dissociation of hepatic steatosis and insulin resistance in mice overexpressing DGAT in the liver. *Cell Metab* 6: 69-78

Morrison SF, Madden CJ, Tupone D (2014) Central neural regulation of brown adipose tissue thermogenesis and energy expenditure. *Cell Metab* 19: 741-756

Mukherjee J, Baranwal A, Schade KN (2016) Classification of Therapeutic and Experimental Drugs for Brown Adipose Tissue Activation: Potential Treatment Strategies for Diabetes and Obesity. *Curr Diabetes Rev* 12: 414-428

Najt CP, Adhikari S, Heden TD, Cui W, Gansemer ER, Rauckhorst AJ, Markowski TW, Higgins L, Kerr EW, Boyum MD *et al* (2023) Organelle interactions compartmentalize hepatic fatty acid trafficking and metabolism. *Cell Rep* 42: 112435

Nedergaard J, Bengtsson T, Cannon B (2007) Unexpected evidence for active brown adipose tissue in adult humans. *Am J Physiol Endocrinol Metab* 293: E444-452

Ngo J, Choi DW, Stanley IA, Stiles L, Molina AJA, Chen PH, Lako A, Sung ICH, Goswami R, Kim MY *et al* (2023) Mitochondrial morphology controls fatty acid utilization by changing CPT1 sensitivity to malonyl-CoA. *EMBO J* 42: e111901

Ngo J, Osto C, Villalobos F, Shirihai OS (2021) Mitochondrial Heterogeneity in Metabolic Diseases. *Biology (Basel)* 10

Nguyen TB, Louie SM, Daniele JR, Tran Q, Dillin A, Zoncu R, Nomura DK, Olzmann JA (2017) DGAT1-Dependent Lipid Droplet Biogenesis Protects Mitochondrial Function during Starvation-Induced Autophagy. *Dev Cell* 42: 9-21.e25

O'Mara AE, Johnson JW, Linderman JD, Brychta RJ, McGehee S, Fletcher LA, Fink YA, Kapuria D, Cassimatis TM, Kelsey N *et al* (2020) Chronic mirabegron treatment increases human brown fat, HDL cholesterol, and insulin sensitivity. *J Clin Invest* 130: 2209-2219

Ouellet V, Routhier-Labadie A, Bellemare W, Lakhal-Chaieb L, Turcotte E, Carpentier AC, Richard D (2011) Outdoor temperature, age, sex, body mass index, and diabetic status determine the prevalence, mass, and glucose-uptake activity of 18F-FDG-detected BAT in humans. *J Clin Endocrinol Metab* 96: 192-199

Parysow O, Mollerach AM, Jager V, Racioppi S, San Roman J, Gerbaudo VH (2007) Low-dose oral propranolol could reduce brown adipose tissue F-18 FDG uptake in patients undergoing PET scans. *Clin Nucl Med* 32: 351-357

Peirce V, Carobbio S, Vidal-Puig A (2014) The different shades of fat. *Nature* 510: 76-83

Petrovic N, Walden TB, Shabalina IG, Timmons JA, Cannon B, Nedergaard J (2010) Chronic peroxisome proliferator-activated receptor gamma (PPARgamma)

activation of epididymally derived white adipocyte cultures reveals a population of thermogenically competent, UCP1-containing adipocytes molecularly distinct from classic brown adipocytes. *J Biol Chem* 285: 7153-7164

Pollak NM, Schweiger M, Jaeger D, Kolb D, Kumari M, Schreiber R, Kolleritsch S, Markolin P, Grabner GF, Heier C *et al* (2013) Cardiac-specific overexpression of perilipin 5 provokes severe cardiac steatosis via the formation of a lipolytic barrier. *J Lipid Res* 54: 1092-1102

Qian H, Beard DA (2006) Metabolic futile cycles and their functions: a systems analysis of energy and control. *Syst Biol (Stevenage)* 153: 192-200

Rich PR, Maréchal A (2010) The mitochondrial respiratory chain. *Essays Biochem* 47: 1-23

Robidoux J, Martin TL, Collins S (2004) Beta-adrenergic receptors and regulation of energy expenditure: a family affair. *Annu Rev Pharmacol Toxicol* 44: 297-323

Roesler A, Kazak L (2020) UCP1-independent thermogenesis. *Biochem J* 477: 709-725

Scheele C, Wolfrum C (2020) Brown Adipose Crosstalk in Tissue Plasticity and Human Metabolism. *Endocr Rev* 41: 53-65

Seale P, Bjork B, Yang W, Kajimura S, Chin S, Kuang S, Scimè A, Devarakonda S, Conroe HM, Erdjument-Bromage H *et al* (2008) PRDM16 controls a brown fat/skeletal muscle switch. *Nature* 454: 961-967

Seale P, Conroe HM, Estall J, Kajimura S, Frontini A, Ishibashi J, Cohen P, Cinti S, Spiegelman BM (2011) Prdm16 determines the thermogenic program of subcutaneous white adipose tissue in mice. *J Clin Invest* 121: 96-105

Seale P, Kajimura S, Yang W, Chin S, Rohas LM, Uldry M, Tavernier G, Langin D, Spiegelman BM (2007) Transcriptional control of brown fat determination by PRDM16. *Cell Metab* 6: 38-54

Seale P, Lazar MA (2009) Brown fat in humans: turning up the heat on obesity. *Diabetes* 58: 1482-1484

Sidossis L, Kajimura S (2015) Brown and beige fat in humans: thermogenic adipocytes that control energy and glucose homeostasis. *J Clin Invest* 125: 478-486

Spiegelman BM, Flier JS (2001) Obesity and the regulation of energy balance. *Cell* 104: 531-543

Stanford KI, Middelbeek RJ, Townsend KL, An D, Nygaard EB, Hitchcox KM, Markan KR, Nakano K, Hirshman MF, Tseng YH *et al* (2013) Brown adipose tissue regulates glucose homeostasis and insulin sensitivity. *J Clin Invest* 123: 215-223

Ste Marie L, Miura GI, Marsh DJ, Yagaloff K, Palmiter RD (2000) A metabolic defect promotes obesity in mice lacking melanocortin-4 receptors. *Proc Natl Acad Sci U S A* 97: 12339-12344

Steffen J, Ngo J, Wang SP, Williams K, Kramer HF, Ho G, Rodriguez C, Yekkala K, Amuzie C, Bialecki R *et al* (2022) The mitochondrial fission protein Drp1 in liver is required to mitigate NASH and prevents the activation of the mitochondrial ISR. *Mol Metab* 64: 101566

Stefl B, Janovská A, Hodný Z, Rossmeisl M, Horáková M, Syrový I, Bémová J, Bendlová B, Kopecký J (1998) Brown fat is essential for cold-induced thermogenesis but not for obesity resistance in aP2-Ucp mice. *Am J Physiol* 274: E527-533

Steinberg JD, Vogel W, Vegt E (2017) Factors influencing brown fat activation in FDG PET/CT: a retrospective analysis of 15,000+ cases. *Br J Radiol* 90: 20170093

Stiles L, Shirihai OS (2012) Mitochondrial dynamics and morphology in beta-cells. *Best Pract Res Clin Endocrinol Metab* 26: 725-738

Stone SJ, Levin MC, Zhou P, Han J, Walther TC, Farese RV, Jr. (2009) The endoplasmic reticulum enzyme DGAT2 is found in mitochondria-associated membranes and has a mitochondrial targeting signal that promotes its association with mitochondria. *J Biol Chem* 284: 5352-5361

Supale S, Li N, Brun T, Maechler P (2012) Mitochondrial dysfunction in pancreatic β cells. *Trends Endocrinol Metab* 23: 477-487

Sztalryd C, Kimmel AR (2014) Perilipins: lipid droplet coat proteins adapted for tissue-specific energy storage and utilization, and lipid cytoprotection. *Biochimie* 96: 96-101

Söderlund V, Larsson SA, Jacobsson H (2007) Reduction of FDG uptake in brown adipose tissue in clinical patients by a single dose of propranolol. *Eur J Nucl Med Mol Imaging* 34: 1018-1022

Tan Y, Jin Y, Wang Q, Huang J, Wu X, Ren Z (2019) Perilipin 5 Protects against Cellular Oxidative Stress by Enhancing Mitochondrial Function in HepG2 Cells. *Cells* 8

Tormos KV, Anso E, Hamanaka RB, Eisenbart J, Joseph J, Kalyanaraman B, Chandel NS (2011) Mitochondrial complex III ROS regulate adipocyte differentiation. *Cell Metab* 14: 537-544

Trevino MB, Machida Y, Hallinger DR, Garcia E, Christensen A, Dutta S, Peake DA, Ikeda Y, Imai Y (2015a) Perilipin 5 regulates islet lipid metabolism and insulin secretion in a cAMP-dependent manner: implication of its role in the postprandial insulin secretion. *Diabetes* 64: 1299-1310

Trevino MB, Mazur-Hart D, Machida Y, King T, Nadler J, Galkina EV, Poddar A, Dutta S, Imai Y (2015b) Liver Perilipin 5 Expression Worsens Hepatosteatosis But Not Insulin Resistance in High Fat-Fed Mice. *Mol Endocrinol* 29: 1414-1425

Tseng YH, Kokkotou E, Schulz TJ, Huang TL, Winnay JN, Taniguchi CM, Tran TT, Suzuki R, Espinoza DO, Yamamoto Y *et al* (2008) New role of bone morphogenetic protein 7 in brown adipogenesis and energy expenditure. *Nature* 454: 1000-1004

Twig G, Elorza A, Molina AJ, Mohamed H, Wikstrom JD, Walzer G, Stiles L, Haigh SE, Katz S, Las G *et al* (2008) Fission and selective fusion govern mitochondrial segregation and elimination by autophagy. *EMBO J* 27: 433-446

Ukropec J, Anunciado RP, Ravussin Y, Hulver MW, Kozak LP (2006) UCP1-independent thermogenesis in white adipose tissue of cold-acclimated Ucp1-/- mice. *J Biol Chem* 281: 31894-31908

van Marken Lichtenbelt WD, Vanhommerig JW, Smulders NM, Drossaerts JM, Kemerink GJ, Bouvy ND, Schrauwen P, Teule GJ (2009) Cold-activated brown adipose tissue in healthy men. *N Engl J Med* 360: 1500-1508

Vegiopoulos A, Müller-Decker K, Strzoda D, Schmitt I, Chichelnitskiy E, Ostertag A, Berriel Diaz M, Rozman J, Hrabe de Angelis M, Nüsing RM *et al* (2010)

Cyclooxygenase-2 controls energy homeostasis in mice by de novo recruitment of brown adipocytes. *Science* 328: 1158-1161

Vernochet C, Damilano F, Mourier A, Bezy O, Mori MA, Smyth G, Rosenzweig A, Larsson NG, Kahn CR (2014) Adipose tissue mitochondrial dysfunction triggers a lipodystrophic syndrome with insulin resistance, hepatosteatosis, and cardiovascular complications. *FASEB J* 28: 4408-4419

Virtanen KA, Lidell ME, Orava J, Heglind M, Westergren R, Niemi T, Taittonen M, Laine J, Savisto NJ, Enerbäck S *et al* (2009) Functional brown adipose tissue in healthy adults. *N Engl J Med* 360: 1518-1525

Wang C, Zhao Y, Gao X, Li L, Yuan Y, Liu F, Zhang L, Wu J, Hu P, Zhang X *et al* (2015a) Perilipin 5 improves hepatic lipotoxicity by inhibiting lipolysis. *Hepatology* 61: 870-882

Wang H, Sreenivasan U, Hu H, Saladino A, Polster BM, Lund LM, Gong DW, Stanley WC, Sztalryd C (2011) Perilipin 5, a lipid droplet-associated protein, provides physical and metabolic linkage to mitochondria. *J Lipid Res* 52: 2159-2168

Wang L, Ishihara T, Ibayashi Y, Tatsushima K, Setoyama D, Hanada Y, Takeichi Y, Sakamoto S, Yokota S, Mihara K *et al* (2015b) Disruption of mitochondrial fission in the liver protects mice from diet-induced obesity and metabolic deterioration. *Diabetologia* 58: 2371-2380

Wikstrom JD, Katzman SM, Mohamed H, Twig G, Graf SA, Heart E, Molina AJ, Corkey BE, de Vargas LM, Danial NN *et al* (2007) beta-Cell mitochondria exhibit

membrane potential heterogeneity that can be altered by stimulatory or toxic fuel levels. *Diabetes* 56: 2569-2578

Wikstrom JD, Mahdaviani K, Liesa M, Sereda SB, Si Y, Las G, Twig G, Petrovic N, Zingaretti C, Graham A *et al* (2014) Hormone-induced mitochondrial fission is utilized by brown adipocytes as an amplification pathway for energy expenditure. *EMBO J* 33: 418-436

Wilson-Fritch L, Burkart A, Bell G, Mendelson K, Leszyk J, Nicoloro S, Czech M, Corvera S (2003) Mitochondrial biogenesis and remodeling during adipogenesis and in response to the insulin sensitizer rosiglitazone. *Mol Cell Biol* 23: 1085-1094

Wilson-Fritch L, Nicoloro S, Chouinard M, Lazar MA, Chui PC, Leszyk J, Straubhaar J, Czech MP, Corvera S (2004) Mitochondrial remodeling in adipose tissue associated with obesity and treatment with rosiglitazone. *J Clin Invest* 114: 1281-1289

Yeung HW, Grewal RK, Gonen M, Schöder H, Larson SM (2003) Patterns of (18)F-FDG uptake in adipose tissue and muscle: a potential source of false-positives for PET. *J Nucl Med* 44: 1789-1796

Yin X, Lanza IR, Swain JM, Sarr MG, Nair KS, Jensen MD (2014) Adipocyte mitochondrial function is reduced in human obesity independent of fat cell size. *J Clin Endocrinol Metab* 99: E209-216

Zaror-Behrens G, Himms-Hagen J (1983) Cold-stimulated sympathetic activity in brown adipose tissue of obese (ob/ob) mice. *Am J Physiol* 244: E361-366

Zhan M, Brooks C, Liu F, Sun L, Dong Z (2013) Mitochondrial dynamics: regulatory mechanisms and emerging role in renal pathophysiology. *Kidney Int* 83: 568-581

Zhang W, Bi S (2015) Hypothalamic Regulation of Brown Adipose Tissue Thermogenesis and Energy Homeostasis. *Front Endocrinol (Lausanne)* 6: 136

Zhu Y, Zhang X, Zhang L, Zhang M, Li L, Luo D, Zhong Y (2019) Perilipin5 protects against lipotoxicity and alleviates endoplasmic reticulum stress in pancreatic β-cells. *Nutr Metab (Lond)* 16: 50

CHAPTER 2: ATP-CONSUMING FUTILE CYCLES AS ENERGY DISSIPATING MECHANISMS TO COUNTERACT OBESITY

The work described in this chapter has been reproduced from:

Brownstein, A. J., Veliova, M., Acín-Pérez, R., Liesa, M., & Shirihai, O. S. (2022). ATP-consuming futile cycles as energy dissipating mechanisms to counteract obesity. *Reviews in endocrine & metabolic disorders*, *23*(1), 121–131. doi: 10.1007/s11154-021-09690-w

ATP-consuming futile cycles as energy dissipating mechanisms to counteract obesity

Alexandra J Brownstein[1,2], Michaela Veliova[1,3], Rebeca Acín-Pérez [1,4], Marc Liesa[1,2,3,4,5], Orian S Shirihai[1,2,3,4#]

Affiliations

[1] Metabolism Theme, David Geffen School of Medicine, University of California, Los Angeles, CA, 90095, USA

[2] Molecular Cellular Integrative Physiology, University of California, Los Angeles, CA, 90095, USA

[3] Department of Molecular and Medical Pharmacology, University of California, Los Angeles, CA, 90095, USA

[4] Department of Medicine, Endocrinology, David Geffen School of Medicine, University of California, Los Angeles, CA, 90095 USA

[5] Molecular Biology Institute, University of California, Los Angeles, CA, 90095, USA

[#], to whom correspondence should be addressed: Tel: +1 310 825 5160; Email: Oshirihai@mednet.ucla.edu

Keywords

Brown adipose tissue, futile cycle, malate aspartate shuttle, energy metabolism, thermogenesis, energy expenditure

Funding

O.S.S. is funded by NIH-NIDDK 5-RO1DK099618-02.

M.L. is funded by the Department of Medicine chair commitment at UCLA, Pilot and Feasibility grants from NCATS UL1TR001881 (CTSI), NIDDK P30 DK063491 (UCSD-UCLA DERC), NIDDK P30 41301 (CURE:Digestive Diseases Research Center) and 1R01AA026914-01A1

Acknowledgments

We would like to thank Dr. Dani Dagan, Dr. Marcus F. Oliveira, Dr. Ambre Bertholet, Dr. Ajit S. Divakaruni, Dr. Ilan Y. Benador, Dr. Anton Petcherski, Dr. Michael Shum, Dr. Essam A Assali and Jennifer Ngo for helpful discussions and advice. Figures created with BioRender.com

Abbreviations

white adipose tissue	WAT
brown adipose tissue	BAT
free fatty acids	FFAs
norepinephrine	NE
uncoupling protein 1	UCP1
body mass index	BMI
^{18}F-fluorodeoxyglucose	^{18}F-FDG
positron emission tomography	PET
computed tomography	CT

electron transport chain	ETC
mitochondrial ADP/ATP carrier	AAC
sarco/endoplasmic reticulum Ca^{2+}-ATPase	SERCA1/2b
phosphoenolpyruvate carboxykinase	PEPCK-C
glycerolipid - free fatty acid cycling	GL/FFA or lipid cycling
glycerol-3-phosphate	G3P
triglycerides	TGs
diacylglycerols	DAGs
monoacylglycerols	MAGs
adipose triglyceride lipase	*ATGL*
hormone-sensitive lipase	*HSL*
monoacylglycerol lipase	*MAGL*
dihydroxyacetone phosphate	DHAP
glycerol-3-phosphate dehydrogenase	GPDH
ryanodine receptor 2	RyR2
β_2-adrenergic receptor	β_2-AR
β_3-adrenergic receptor	β_3-AR
sarcolipin	SLN
creatine kinase	CK
phosphocreatine	PCr
malate-aspartate shuttle	MaSH
lysophosphatidic	LPA
α-Ketoglutarate	αKG
oxaloacetate	OA
glutamate	Glu
aspartate	Asp
mitochondrial pyruvate carrier	MPC
lactate dehydrogenase	LDH

nicotinamide nucleotide transhydrogenase	NNT
Thiazolidinediones	TZDs

ABSTRACT

Obesity results from an imbalance in energy homeostasis, whereby excessive energy intake exceeds caloric expenditure. Energy can be dissipated out of an organism by producing heat (thermogenesis), explaining the long-standing interest in exploiting thermogenic processes to counteract obesity. Mitochondrial uncoupling is a process that expends energy by oxidizing nutrients to produce heat, instead of ATP. Energy can also be dissipated through mechanisms that do not involve mitochondrial uncoupling. Such mechanisms include futile cycles described as metabolic reactions that consume ATP to produce a product from a substrate but then converting the product back into the original substrate, releasing the energy as heat. Energy dissipation driven by cellular ATP demand can be regulated by adjusting the speed and number of futile cycles. Energy consuming futile cycles that are reviewed here are lipolysis/fatty acid re-esterification cycle, creatine/phosphocreatine cycle, and the SERCA-mediated calcium import and export cycle. Their reliance on ATP emphasizes that mitochondrial oxidative function coupled to ATP synthesis, and not just uncoupling, can play a role in thermogenic energy dissipation. Here, we review ATP consuming futile cycles, the evidence for their function in humans, and their potential employment as a strategy to dissipate energy and counteract obesity.

INTRODUCTION

The prevalence of obesity worldwide has substantially increased, concurrently with the vast array of obesity-associated diseases, including type 2 diabetes, dyslipidemia, hypertension heart disease, and cancer. Obesity develops when calorie intake chronically exceeds total energy expenditure, leading to a rise in the proportion of calories that remain in storage. A therapy for weight loss must, therefore, involve a decrease in calorie intake and/or an increase in energy dissipation out of the organism. While efforts have been put into increasing energy expenditure by increasing exercise, this only worked for a small portion of the population. Similarly, low caloric diet offers only a transient reduction in weight that is followed by weight re-gain (Leibel *et al*, 1995). This dynamic nature of weight loss, where a low caloric diet is very successful in the first two weeks, but eventually weight loss stops as the body tends to compensate for the decrease in energy intake, is where the most interesting opportunity lies in (Fothergill *et al*, 2016; Johannsen *et al*, 2012). What molecular mechanisms are responsible for blocking weight loss after a couple of weeks of low caloric diet?

For the body to stop losing weight under low caloric diet, energy expenditure must go down. Indeed, recent studies in humans have demonstrated that weight loss by caloric restriction results in a decline in basal metabolic rate (BMR), beyond changes attributed to decreased body weight (Corbett *et al*, 1986; Dulloo & Calokatisa, 1991; Elliot *et al*, 1989; Kaiyala *et al*, 2010; Leibel *et al.*, 1995; Maclean *et al*, 2011; Valtueña *et al*, 1995). This adaptive reduction in BMR is a regulated mechanism that limits energy dissipation to conserve tissue mass, mostly by suppressing thermogenesis (Dulloo & Jacquet, 1998).

This adaptation highlights the ability to preserve energy balance when caloric intake is reduced (Leibel *et al.*, 1995). The question remains, can we use the same pathways to increase energy dissipation and to counteract obesity? Can defects in the mechanisms regulating energy expenditure be responsible for obesity?

Thermogenesis, which is the production of heat in living organisms, is a regulated process that largely contributes to energy dissipation. Two major processes are responsible for thermoregulatory heat production in mammals – shivering and nonshivering thermogenesis. Shivering, the involuntary contraction of skeletal muscles induced by cold exposure results in heat production that involves ATP-dependent movement. Non-shivering thermogenesis is defined as an increase in metabolic heat production that is not associated with muscle activity and occurs in response to environmental temperature (Himms-Hagen, 1984). Non-shivering thermogenesis occurs in several systems, including skeletal muscle and most notably brown adipose tissue (Cypess *et al*, 2009; Himms-Hagen, 1984).

Mitochondrial uncoupling is considered a central component of non-shivering thermogenesis by brown adipose tissue. UCP1, an anion/H^+ symporter, is an uncoupling protein unique to brown adipose tissue and beige adipocytes. (Table 1)(Fedorenko *et al*, 2012; Jastroch *et al*, 2010; Parker *et al*, 2009) UCP1 allows for the re-entry of protons into the mitochondrial matrix bypassing ATP-synthase, thereby uncoupling oxygen consumption from ATP synthesis and dissipating the energy of the proton gradient into heat. (Fedorenko *et al.*, 2012; Jastroch *et al.*, 2010; Parker *et al.*, 2009). Uncoupling is activated in response to decreased environmental temperature (cold-induced

thermogenesis) and, with some conflicting evidence, to overfeeding (diet-induced thermogenesis) (Cannon & Nedergaard, 2004; Foster & Frydman, 1978; Rothwell & Stock, 1979; Saito *et al*, 2009). In addition, UCP1^{+} 'brown-like' white adipocytes, also named beige cells, are thermogenically active adipocytes that can emerge in white fat when mice are exposed to cold, as well as in response to catecholamines and other β-adrenergic agonists (Cannon & Nedergaard, 2004; Cohen & Spiegelman, 2015). Several lines of evidence suggest that beige adipocytes, despite carrying UCP1, also dissipate energy through ATP-consuming processes. (Chouchani *et al*, 2019; Ikeda *et al*, 2017; Ikeda & Yamada, 2020; Kazak *et al*, 2015).

Numerous studies have characterized the role and regulation of UCP1-mediated thermogenesis in brown and beige adipose tissue and we will do it a disservice by trying to review it in one paragraph. The role of UCP1 in thermogenesis has been recently reviewed (Chouchani *et al.*, 2019; Nedergaard & Cannon, 2018). BAT thermogenesis and UCP1 activity can decrease body fat accumulation, improving insulin sensitivity and glycemic control in diet-induced obese mice (Stanford *et al*, 2013). Accordingly, short-term cold exposure (4 hours) decreases circulating triglyceride concentrations and increases insulin sensitivity in mice (Bartelt *et al*, 2011). Moreover, mice with genetic ablation of BAT are more susceptible to diet-induced obesity and insulin resistance (Hamann *et al*, 1995; Lowell & Flier, 1997). Similarly, mice lacking beige fat function caused by the adipocyte-specific deletion of PRDM16 develop obesity and insulin resistance (Cohen *et al*, 2014).

It was previously hypothesized that the action of UCP1 primarily mediates the "anti-obesity" and "anti-diabetic" actions of brown and beige fat. Surprisingly, UCP1-knock out mice maintained normal resting energy expenditure and were resistant to diet-induced obesity at sub-thermoneutral temperatures (Enerbäck *et al*, 1997; Liu *et al*, 2003; Stefl *et al*, 1998). Additionally, it was shown that UCP1-deficient mice can adapt to a cold environment, highlighting the presence of UCP1-independent mechanisms of adaptive thermogenesis and regulation of whole-body energy homeostasis (Liu *et al.*, 2003; Ukropec *et al*, 2006). UCP1-knock out mice are protected from diet-induced obesity at sub-thermoneutral temperatures, because the alternative thermogenic mechanisms consume more calories to produce the same amount of heat needed for thermoregulation (Enerbäck *et al.*, 1997; Liu *et al.*, 2003; Stefl *et al.*, 1998). Furthermore, deletion of the mitochondrial protein, Mfn2, in brown adipose tissue protected from insulin resistance and obesity, despite impairing cold-induced thermogenesis. In this regard, BAT-specific Mfn2 deletion decreased the animal energy efficiency and increased coupled fat oxidation in BAT, explaining protection from obesity and hyperglycemia (Mahdaviani *et al*, 2017). Altogether, these studies suggest that outside UCP1 mediated uncoupling, other mechanisms may affect energy expenditure by changing energy efficiency.

While some of the animal studies were translated to humans, others were not. Earlier clinical observations in humans demonstrated that both cold exposure (Ouellet *et al*, 2012; Saito *et al.*, 2009; Yoneshiro *et al*, 2011) and treatment with mitochondrial uncouplers (Cutting *et al*, 1933; Parascandola, 1974; Tainter *et al*, 1934) result in increased energy expenditure and weight loss (Yoneshiro & Saito, 2015). More recent

BAT-targeted pharmacological studies have failed to demonstrate that BAT activation results in a significant weight loss by increasing overall energy expenditure (Chen *et al*, 2020; Larson, 2019; O'Mara *et al*, 2020). For example, treatment of human subjects with a B-3 adrenergic receptor agonist Mirabegron did not result in a significant weight loss although it successfully activated thermogenesis by BAT (O'Mara *et al.*, 2020). The lack of success of Mirabegron was hypothesized to be explained by the lower mass of BAT in humans when compared to mice. An alternative hypothesis could be that increased energy expenditure by adaptive thermogenesis is compensated for by an increase in energy efficiency in other tissues, leading to an overall unchanged or reduced BMR.

UCP1-independent Mechanisms of Mitochondrial Uncoupling

The mitochondrial ADP/ATP carrier, (ACC), acts as a mitochondrial uncoupler under certain conditions, fueling a futile cycle of proton diffusion across the inner mitochondrial membrane (Bertholet *et al*, 2019) (Figure 1, Table 1). AAC is a member of the solute carrier family (SLC25) that exchanges ATP and ADP between the mitochondria matrix and the cytosol (Bertholet *et al.*, 2019). However, ACC has additional key functions: ACC is a fatty-acid induced proton channel that explains endogenous proton leak, as well as regulating the opening of the permeability transition pore and the removal of mitochondria by mitophagy (Bertholet *et al.*, 2019; Kreiter *et al*, 2021). Remarkably, both ACC-controlled leak and PTP opening can be stimulated by free fatty acids, similarly to how fatty acids activate UCP1 (Bertholet *et al.*, 2019). This connection by fatty acids highlights the importance of nutrients as active regulators of energy

dissipation, by determining the relative proportion that is directed to mitochondrial ATP synthesis versus leak.

Another mechanism that uncouples oxygen consumption from ATP synthesis by allowing protons to enter the mitochondrial matrix is mediated by the mitochondrial Nicotinamide nucleotide transhydrogenase (NNT) (Hoek & Rydström, 1988; Jackson *et al*, 2015; Kampjut & Sazanov, 2019). NNT uses the electrons in NADH to reduce $NADP^+$ to NADPH, with this transhydrogenation being coupled to proton translocation across the inner membrane (Hoek & Rydström, 1988; Jackson *et al.*, 2015; Kampjut & Sazanov, 2019). The energy consumed by NNT-mediated proton translocation generates NADPH . Therefore, although the NNT uncouples the mitochondria respiration from ATP synthesis, energy consumed by the NNT is not directly transformed into heat and thus will not be dissipated out of the organism (Rydström, 2006).

The Two Categories of Thermogenic Energy Expenditure: ATP-Consuming Futile Cycles and Uncoupling

Recent evidence demonstrated that BAT and beige adipocytes can increase energy expenditure by activating ATP-consuming futile cycles. This need for ATP means that mitochondria can remain coupled to sustain ATP demand and fuel these futile cycles, which prevents the potential risks associated with large depolarization characteristic of mitochondrial uncoupling (Table 1). Remarkably, these ATP-consuming futile cycles recently identified in BAT and beige adipocytes were already shown to promote energy expenditure in skeletal muscle.

A futile cycle consists of a set of biochemical reactions that concurrently run in opposite directions, consuming ATP in one of the directions. As the product of the first reaction is the substrate of the second reaction, and the product of the second reaction is the substrate of the first reaction, such a cycle will lead to a net decrease in ATP (Newsholme, 1978). While we use the word futile, this does not mean there is no use for these cycles. Outcomes of futile cycles include the consumption of excess nutrients and the generation of heat. Furthermore, futile cycles are characterized by the continuous production of the cycle's intermediates allowing for the maintenance of a steady pool of metabolites comprising the cycle and the active enzymes producing them. As such, futile cycles allow for a quick response to cellular events requiring the production or processing of the cycle intermediates.

The capacity of energy-wasting mechanisms based on futile cycles to decrease body weight loss will be mostly dependent on their abundancy and/or frequency of execution. Therefore, the extent of energy expenditure achieved by each of these mechanisms per cell at a given time is unlikely to be a reliable predictor of their impact on weight loss.

Calcium Futile Cycles in Beige and Brown Adipocytes

A UCP1-independent thermogenic pathway that involves an ATP-consuming Ca^{2+} futile cycling was shown to contribute to beige fat energy expenditure and systemic glucose homeostasis (Figure 1, Table 1) (Gamu & Tupling, 2017; Ikeda *et al.*, 2017; Ukropec *et al.*, 2006). In response to cold exposure, NE binds to α1-AR (adrenergic receptor) and β3-AR to increase intracellular Ca^{2+} cycling by activating the ryanodine

receptor 2 (RyR2) and promoting the extrusion of ER-calcium. Calcium extrusion then increases the activity of the sarco(endo) plasmic reticulum Ca^{2+} (SERCA2b), which brings the calcium back to the ER of beige adipocytes (Gamu & Tupling, 2017; Ikeda *et al.*, 2017; Mottillo *et al*, 2018). As SERCA2b consumes ATP to transport calcium back to the ER, the activation of this calcium cycle leads to a futile consumption of ATP that is responsible for energy dissipation. In addition, decreased efficiency of SERCA2b importing calcium leads to an increase in Ca^{2+} levels in the cytosol, which enter the mitochondria to activate pyruvate dehydrogenase activity and ATP synthesis (Ikeda *et al.*, 2017; Mottillo *et al.*, 2018). Thus, calcium itself activates mitochondria to cover this increase ATP demand more efficiently. This calcium cycle explained why UCP1 KO beige adipocytes utilize glucose-derived pyruvate as the primary fuel source for mitochondrial respiration (Ikeda *et al.*, 2017; Mottillo *et al.*, 2018). In all, SERCA2-mediated calcium cycling increases energy dissipation while elevating glucose oxidation, which counteracts hyperglycemia (Ikeda *et al.*, 2017).

Intriguingly, the SERCA2b-mediated Ca^{2+} cycling thermogenic mechanism is necessary for beige adipocyte thermogenesis but is dispensable in brown adipocytes that express high levels of UCP1. It is hypothesized that this pathway is unique to beige fat due to the high expression of ATP synthase not found in brown adipose tissue, enabling beige fat to dissipate energy by increasing ATP consumption in a futile manner (Cannon & Vogel, 1977; Ikeda *et al*, 2018; Lindberg *et al*, 1967).

Although regulators of SERCA2 activity in beige adipocytes have yet to be established, the regulatory protein sarcolipin (SLN) has been shown to promote

uncoupling of ATP hydrolysis of SERCA1a from calcium transport in skeletal muscle, resulting in muscle nonshivering thermogenesis (Autry *et al*, 2016; Bal *et al*, 2012; Sahoo *et al*, 2013). Unphosphorylated SLN induces conformational changes in SERCA structure which decreases the affinity of SERCA to bind calcium (Autry *et al.*, 2016). This decrease in affinity causes SERCA to hydrolyze more ATP to transport less calcium, meaning that more ATP will be consumed to perform the same transport process. Accordingly, it was shown that SLN enhances energy dissipation and heat production in skeletal muscle, concurrent with a sustained elevation of cytoplasmic Ca^{2+}.

Interestingly, SERCA1 was recently identified in the inner mitochondrial membranes (IMM) of BAT and was shown to induce SERCA/RyR mediated Ca^{2+} futile cycling in BAT mitochondria (Table 1)(de Meis, 2003). Calcium is pumped from the matrix to the inner mitochondrial space (IMS) by SERCA1 and returns to the mitochondrial matrix through the RyR (de Meis *et al*, 2006; de Meis *et al*, 2010; de Meis *et al*, 2005). The ATP hydrolysis activity of SERCA1 was shown to absorb part of the ATP derived from the electron flux activated by Ca^{2+}, contributing to brown adipose tissue energy expenditure (de Meis *et al.*, 2010).

Creatine-Phosphocreatine Futile Cycle

A Creatine-dependent ATP-consuming cycle has been shown to promote energy dissipation in beige fat and brown adipocytes (Figure 1, Table 1)(Bertholet *et al*, 2017; Kazak *et al.*, 2015; Kazak *et al*, 2017; Kazak *et al*, 2019; Rahbani *et al*; Sun *et al*, 2021). This cycle was initially identified in mitochondria isolated from beige fat of cold-exposed

animals under ADP-limited conditions and was further confirmed to exist in both mouse and human brown adipocytes (Kazak *et al.*, 2015; Rahbani *et al.*). Preliminary studies demonstrated that creatine stimulates substrate cycling and increases ADP-dependent respiration in beige fat mitochondria when ADP is limiting (Kazak *et al.*, 2015). When UCP1 is deleted, genes involved in creatine metabolism including creatine kinase B (CKB) are upregulated by thermogenic cAMP signaling (Kazak *et al.*, 2015; Rahbani *et al.*). Moreover, depleting creatine levels in thermogenic adipocytes of mice by deleting the rate-limiting enzyme of creatine biosynthesis, glycine amidinotransferase (GATM), impairs energy expenditure due to reduced thermogenesis and causes diet-induced obesity (Kazak *et al.*, 2017; Kazak *et al.*, 2019). The existence of this cycle in BAT supports the concept that increasing mitochondrial ATP synthesis can be used as an approach to promote energy dissipation.

Lipid Cycling as a Futile Cycle Consuming ATP.

Lipid cycling consists of a catabolic segment and an anabolic segment. The catabolic segment refers to the hydrolysis of triglycerides (TAGs) into free fatty acids (FFAs) and glycerol (Guan *et al*, 2002; Prentki & Madiraju, 2008; Reshef *et al*, 2003). Adipose triglyceride lipase (*ATGL*), *hormone-sensitive lipase* (*HSL*), and monoacylglycerol lipase (*MAGL*) are the main enzymes catalyzing this hydrolysis, namely lipolysis. The free glycerol that is generated during the breakdown of triglycerides can potentially be reused by the anabolic segment, constituted by glycerol kinase, which consumes ATP to regenerate glycerol-3-P that can be utilized to rebuild triglycerides (Reshef *et al.*, 2003).

In cells with low glycerol kinase activity, glycerol can be released into the bloodstream, preventing this ATP-consuming lipid cycle (Guan *et al.*, 2002). However, glucose can be consumed to make new triglycerides by fueling glyceroneogenesis, a process controlled by phosphoenolpyruvate carboxykinase (GTP) (PEPCK-C) (Table 1) (Ballard *et al*, 1967; Guan *et al.*, 2002; Reshef *et al.*, 2003). Glyceroneogenesis is active in liver, white and brown adipose tissue. Therefore, re-esterification and futile ATP consumption can still occur in cells with low glycerol kinase activity via PEPCK-C. In BAT, glyceroneogenesis has an important role in determining the rate of triglyceride re-esterification after norepinephrine stimulation (Feldman & Hirst, 1978). It has been reported that cold exposure promotes a decrease in PEPCK-C in BAT, which is accompanied by a decrease in re-esterification as the FFAs need to be delivered to the mitochondria to maintain thermogenesis (Feldman & Hirst, 1978).

Glycerol metabolism is not the only ATP-consuming process that can increase energy dissipation in adipocytes. Glycerolipid-free fatty acid cycling (GL/FFA or lipid cycling) is a futile cycle that consumes ATP via the partial or full re-esterification of free fatty acids into TAGs, *diacylglycerols* (DAGs), or *Monoacylglycerols* (MAGs) (Table 1)(Prentki & Madiraju, 2008; Reshef *et al.*, 2003). The reason is that lipolysis removes CoA from fatty acids and the addition of CoA to fatty acids consumes ATP, with CoA addition to FFA being essential for esterification. Each GL/FFA cycle consumes 7 ATP molecules (Prentki & Madiraju, 2012).

The functional role of lipid cycling can range from facilitating a rapid provision of FFA for oxidation, to cell signaling regulation and detoxification from excess free fatty acids

(Chouchani & Kajimura, 2019). Importantly, the anabolic and catabolic segments of lipid cycling can concurrently occur in the same cell or in different tissues; for example between the liver and white adipose tissue (Figure 2). Abnormalities in the function of lipid cycling are associated with insulin resistance, type 2 diabetes, fatty liver disease, and cancer (Larter *et al*, 2010; Nomura *et al*, 2010; Prentki & Madiraju, 2008).

A significant amount of basal energy expenditure in white adipose tissue is attributed to lipid cycling (Bertin, 1976). The reason is that mature white adipocytes do not oxidize fatty acids but are a major source of free fatty acids for surrounding tissues (Hammond, 1987; Harper & Saggerson, 1975; Wang *et al*, 2010). In cultured white adipocytes from humans, around 40% of released fatty acids are recycled back into lipid droplets (Hammond, 1987). In vivo, Wolfe *et al.* showed that in humans at rest around 70% of fatty acids are re-esterified in the adipose tissue (Wolfe *et al*, 1990). Especially at the beginning of physical exercise, re-esterification is reduced to 25%, suggesting that decreased re-esterification is explained by fatty acids consumption in muscle and liver (Wolfe *et al.*, 1990). This suggests that lipid cycling enables the adipose tissue to be ready to deliver oxidizable fatty acids to muscle and liver, while the esterification component protects the adipocytes from lipotoxicity when fatty acids are not oxidized (Wolfe *et al.*, 1990).

Mechanisms Inducing Lipid Cycling

While the majority of heat in activated brown adipocytes is generated via UCP1 mediated proton leak, part of thermogenesis is attributed to lipid cycling (Mottillo *et al*,

2014). Recently, Veliova et al proposed a novel mechanism to activate lipid cycling and increase energy dissipation in non-stimulated brown adipocytes, by blocking the mitochondrial pyruvate carrier (MPC) (Figure 1)(Veliova *et al*, 2020). Inhibition of the MPC results in increased ATP demand and coupled mitochondrial fat oxidation to support fatty acid esterification, as energy expenditure was sensitive to the ACSL inhibitor Triacsin C. Consequently, MPC blockage increases fat oxidation and energy expenditure bypassing the need for adrenergic stimulation or mitochondrial uncoupling to oxidize fat (Veliova *et al.*, 2020). It remains to be determined whether lipid cycling can be induced in white adipocytes by a similar mechanism, which would be particularly interesting as a way to promote energy-wasting and possibly weight loss.

Aside from its role in maintaining the availability of free fatty acids, lipid cycling has an essential role in cell signaling, In pancreatic beta cells, lipid species can act as signaling molecules that modulate insulin secretion (Nolan *et al*, 2006; Prentki & Madiraju, 2012; Reshef *et al.*, 2003). Furthermore, the increased energy demand caused by lipid cycling has been linked to AMPK activation in adipocytes and beta cells, as lipid cycling can increase the AMP/ATP ratio (Gauthier *et al*, 2008; Prentki & Madiraju, 2012). In addition, lipid cycling can play an important role in signaling from fatty acids and glucose to promote cell growth and modulate gene expression (Faergeman & Knudsen, 1997). It was proposed that high glycolysis rates that support cancer proliferation could be maintained by *Glycerol-3-phosphate dehydrogenase* (GPDH), which regenerates NAD+ by transforming G-3-P to DHAP (Przybytkowski *et al*, 2007).

Moreover, it has been demonstrated that the type 2 diabetes drugs, Thiazolidinediones (TZDs), which are agonists for peroxisome proliferator-activated receptor-gamma (PPARγ) and block MPC activity, induce changes in fatty acid esterification (Tordjman *et al*, 2003). TZDs induced the expression of PEPCK, a key regulator of the glyceroneogenesis pathway (Tordjman *et al.*, 2003). The activation of glyceroneogenesis in adipose tissue by TZDs allows the re-esterification of fatty acids via lipid cycling, thus lowering fatty acid release into the plasma (Tordjman *et al.*, 2003). Importantly, reduced fatty acid levels in the plasma may be important for the insulin-sensitizing action of thiazolidinediones (Tordjman *et al.*, 2003). However, whether some of the actions on fatty acid cycling induced by TZDs are mediated by their actions on MPC has not been characterized.

Futile Cycles That Connect Multiple Subcellular Compartments and Tissues

To avoid uncontrolled dissipation of energy, some futile cycles have their core steps occurring in different tissues or even in different subcellular compartments. An example is the hexokinase/glucose-6-phosphatase reaction, wherein the liver hexokinase is replaced by glucokinase (GK), which is regulated by glucokinase regulatory protein (GKRP) (Raimondo *et al*, 2015; van Schaftingen *et al*, 1992). Under fasting, GKRP inactivates and sequesters GK in the nucleus to prevent futile cycles of glucose phosphorylation during gluconeogenesis (Raimondo *et al.*, 2015; van Schaftingen *et al.*, 1992).

Interestingly, the same mechanism used to induce lipid cycling in adipose tissue was shown to contribute to the Cori cycle that communicates between muscle and liver (Figure 2). Skeletal muscle-specific deletion of the mitochondrial pyruvate carrier (MPC) in mice increases flux through the Cori cycle, leading to an increase in whole-body energy expenditure (Sharma *et al*, 2019). Muscle-specific MPC deletion (MPC SkmKO) promoted the conversion of pyruvate to lactate in the muscle and its release of lactate into the circulation (Sharma *et al.*, 2019). This lactate provides carbons for glucose production in the liver, which resupplies glucose to the muscle. The Cori cycle is futile because each round produces two skeletal muscle ATP molecules and consumes six in the liver, for a net consumption of 4 ATP equivalents. Cori cycling is energetically supported by fatty acid oxidation in the liver for gluconeogenesis, as well as in the muscle to support muscle ATP demand. This increase in mitochondrial fat oxidation was shown to account for a decrease in body weight in mice with skeletal muscle-specific deletion of the MPC (Sharma *et al.*, 2019).

CONCLUSIONS

Energy homeostasis is maintained by a balance of energy intake and energy dissipation. The basal metabolic rate can be regulated to decrease energy dissipation during periods of decreased nutrient intake. The existence of these compensatory mechanisms means that cells can fine-tune the amount of energy required to sustain the same essential metabolic processes. Understanding the regulation of energy-dissipating

processes modulated by food intake can potentially lead to therapeutic strategies that serve to promote weight loss among individuals with obesity.

It has been shown through the use of chemical uncouplers that increasing the metabolic rate can cause weight loss and supports the hypothesis that increasing energy expenditure by decreasing metabolic efficiency is a potential mechanism to induce a negative energy balance (Parascandola, 1974; Tainter *et al.*, 1934). However, chemical uncouplers and adrenergic inducers of thermogenesis have several disadvantages and risks related to their safety, including their lack of tissue specificity and the potential disruption of other functions of mitochondria that are membrane potential-dependent (Duchen, 2004; Grundlingh *et al*, 2011). Specifically, treatment with uncouplers can result in large enough mitochondrial depolarization that will impair charge-dependent transport processes required for metabolite import as well as calcium buffering. Depolarization can also increase the propensity for permeability transition and apoptosis. On the other hand, mechanisms that increase ATP demand through futile cycles dissipate energy through pathways that can be more easily made tissue-specific and that are less disruptive to mitochondrial functions. By increasing ATP demand, ATP-consuming futile cycles can induce mild depolarization that is unlikely to affect other mitochondrial functions. Conversely, whether the adaptive response of the organisms to the induction of futile cycles may consist of either transient or persistent change in BMR and sustainable reduction in weight remains to be seen.

In conditions where ATP production is compromised, an ATP-consuming futile cycle can be deleterious. By blocking ATP-consuming futile cycles, it is possible we can

prevent cell death or dysfunctionality in conditions such as ischemia and mitochondrial respiratory chain diseases, where ATP demand exceeds the synthesis rate.

Overall, ATP-consuming futile cycles hold promise both as an intervention to treat obesity-related diseases as well as conditions of unmet ATP demand. Further elucidating mechanisms that control ATP-consuming futile cycles may allow for the development of drugs that can modify the ATP demand in a tissue-specific manner.

FIGURES AND TABLES

Futile Cycle	Tissue	Physiological Role	Protein Involved	ATP-Dependent	References
UCP1-mediated uncoupling	BAT	Thermogenesis	UCP1	—	[13, 14, 16, 17, 95]
Calcium cycling	BAT, Skeletal muscle	Thermogenesis	SERCA1, RyR1, SLN	✓	[58-63, 96, 97]
Endogenous mitochondrial uncoupling	BAT	ATP production and thermogenesis	AAC	✓	[45, 46]
Calcium cycling	Beige Fat	Thermogenesis and glucose homeostasis	SERCA2b, RyR2	✓	[24, 34, 52, 53]
Creatine-dependent ADP/ATP cycling	Beige Fat	Thermogenesis	CK, AAC	✓	[21, 64-68]
Glycerolipid-free fatty acid cycle	WAT, BAT, Islet β-cell	Lipolysis and triglyceride synthesis	ATGL, HSL, MAGL, GK, MPC	✓	[70, 71, 74, 79, 83, 84]
Glyceroneogenesis-lipid cycle	Liver, WAT, BAT	G3P formation and triglyceride synthesis	PEPCK-C, Glycerol Kinase	✓	[69, 70, 72, 73, 78]
Cori Cycle	Skeletal Muscle and Liver	Lactate and glucose production	LDH	✓	[92]

Table 1-1: ATP-consuming processes that contribute to energy expenditure

Non-shivering thermogenesis through UCP1-mediated proton gradient dissipation is the main mechanism of BAT-mediated energy expenditure. Additional futile cycles dependent

on ATP synthesis and consumption have been demonstrated to contribute to energy dissipation in a UCP1 independent manner in different tissues. UCP1, uncoupling protein 1; AAC, mitochondrial ADP/ATP carrier; SERCA1/2b, sarco/endoplasmic reticulum Ca^{2+}-ATPase; RyR, *Ryanodine* receptor; SLN, Sarcolipin; CK, Creatine Kinase; PEPCK-C, Phosphoenolpyruvate carboxykinase; MPC, mitochondrial pyruvate carrier; LDH, Lactate dehydrogenase; *ATGL,* Adipose triglyceride lipase; HSL, *hormone-sensitive lipase*; *MAGL,* monoacylglycerol lipase; GK, glycerol kinase.

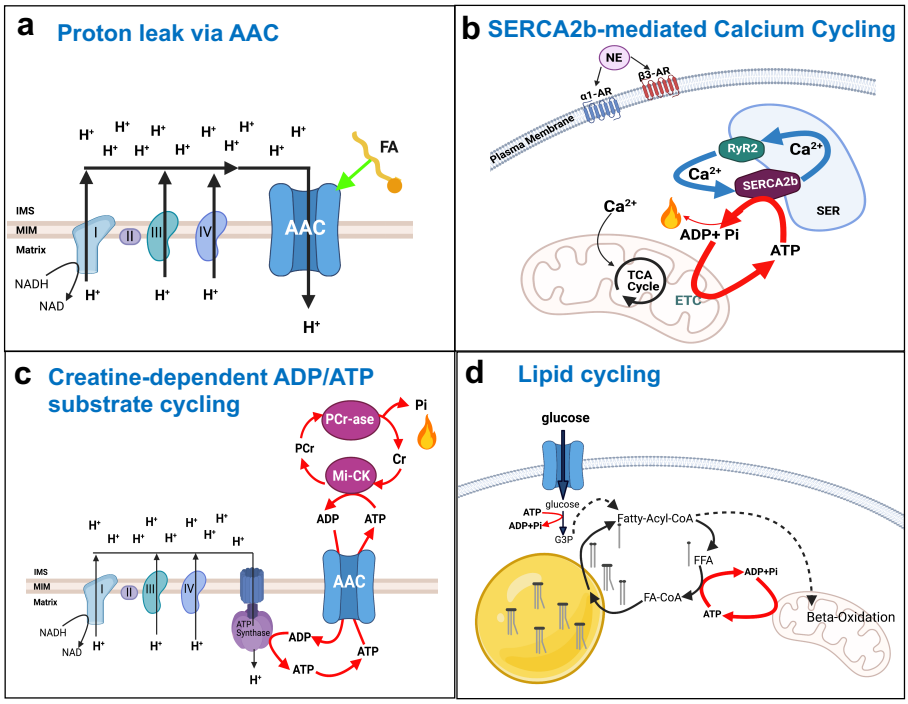

Figure 1-1: ATP-Dependent Futile Cycles

(a) The mitochondrial ADP/ATP carrier (ACC) can act as H+ transporter, in addition to its function as ADP/ATP exchanger. ACC-mediated proton leak requires the presence of free fatty acids and is negatively regulated by ADP/ATP exchange. Thereby, ACC provides an alternative mechanism to induce mitochondrial proton leak**. (b)** In beige adipocytes norepinephrine (NE)–mediated stimulation of adrenergic receptors stimulates futile Ca2+ cycling through activation of sarco/endoplasmic reticulum Ca^{2+}-ATPase 2b (SERCA2b) and ryanodine receptor 2 (RyR2). SER, sarco/endoplasmic reticulum**. (c)** In

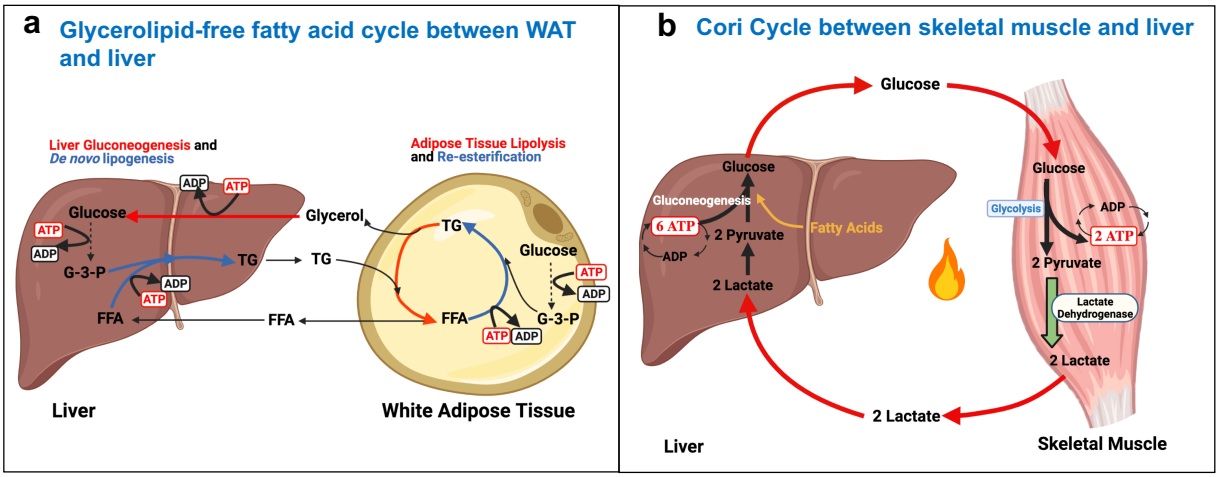

UCP1-deficient adipocytes creatine (Cr) and creatine and CK-mediated hydrolysis of ATP stimulates cycling of ATP production and consumption when ADP is limiting through the ATP/ADP carrier (AAC). The mitochondrial AAC localizes to the mitochondrial inner membrane and functions as an ADP/ATP exchanger to control the cellular ATP pool. MI-CK, mitochondrial-creatine kinase; PCr, phosphor-creatine; PCr-ase, phosphor-creatine kinase. **(d)** In the absence of mitochondrial pyruvate import, brown adipocytes activate lipolysis, which induces futile lipid cycling and β-oxidation. Additional details about the malate aspartate shuttle as a mechanism to induce lipid cycling appear in the text. FFA, free fatty acid; G3P, glycerol-3-phosphate.

Figure 1-2: Futile Cycles That Connect Multiple Subcellular Compartments and Tissues

(a) Glycerolipid-free fatty acid cycle between white adipose tissue and the liver. Triglycerides (TGs) are broken down to glycerol and free fatty acids (FFAs), which are either re-esterified in the adipose tissue or released into the bloodstream. The liver converts the glycerol from the bloodstream to glucose through gluconeogenesis, and this glucose can then be used to make glucose-3-phosphate (G-3-P) needed for triglyceride synthesis. Free fatty acids picked up by the liver are used along with glucose-3-phosphate for *de novo* triglyceride synthesis also called *de novo* lipogenesis. **(b)** Cori cycle between skeletal muscle and the liver. Glucose in the muscle is metabolized to pyruvate and ATP through glycolysis and then converted to lactate by lactate dehydrogenase (LDH), which is released into the blood and picked up by the liver. The liver uses the lactate to produce glucose, utilizing ATP, and the glucose is then released back into the circulation. Overall this futile cycle results in a net loss of 4 ATPs.

REFERENCES

Autry JM, Thomas DD, Espinoza-Fonseca LM (2016) Sarcolipin Promotes Uncoupling of the SERCA Ca(2+) Pump by Inducing a Structural Rearrangement in the Energy-Transduction Domain. *Biochemistry* 55: 6083-6086

Bal NC, Maurya SK, Sopariwala DH, Sahoo SK, Gupta SC, Shaikh SA, Pant M, Rowland LA, Bombardier E, Goonasekera SA *et al* (2012) Sarcolipin is a newly

identified regulator of muscle-based thermogenesis in mammals. *Nat Med* 18: 1575-1579

Ballard FJ, Hanson RW, Leveille GA (1967) Phosphoenolpyruvate carboxykinase and the synthesis of glyceride-glycerol from pyruvate in adipose tissue. *J Biol Chem* 242: 2746-2750

Bartelt A, Bruns OT, Reimer R, Hohenberg H, Ittrich H, Peldschus K, Kaul MG, Tromsdorf UI, Weller H, Waurisch C *et al* (2011) Brown adipose tissue activity controls triglyceride clearance. *Nat Med* 17: 200-205

Bertholet AM, Chouchani ET, Kazak L, Angelin A, Fedorenko A, Long JZ, Vidoni S, Garrity R, Cho J, Terada N *et al* (2019) H(+) transport is an integral function of the mitochondrial ADP/ATP carrier. *Nature* 571: 515-520

Bertholet AM, Kazak L, Chouchani ET, Bogaczyńska MG, Paranjpe I, Wainwright GL, Bétourné A, Kajimura S, Spiegelman BM, Kirichok Y (2017) Mitochondrial Patch Clamp of Beige Adipocytes Reveals UCP1-Positive and UCP1-Negative Cells Both Exhibiting Futile Creatine Cycling. *Cell Metab* 25: 811-822.e814

Bertin R (1976) Glycerokinase activity and lipolysis regulation in brown adipose tissue of cold acclimated rats. *Biochimie* 58: 431-434

Cannon B, Nedergaard J (2004) Brown adipose tissue: function and physiological significance. *Physiol Rev* 84: 277-359

Cannon B, Vogel G (1977) The mitochondrial ATPase of brown adipose tissue. Purification and comparison with the mitochondrial ATPase from beef heart. *FEBS Lett* 76: 284-289

Chen KY, Brychta RJ, Abdul Sater Z, Cassimatis TM, Cero C, Fletcher LA, Israni NS, Johnson JW, Lea HJ, Linderman JD *et al* (2020) Opportunities and challenges in the therapeutic activation of human energy expenditure and thermogenesis to manage obesity. *J Biol Chem* 295: 1926-1942

Chouchani ET, Kajimura S (2019) Metabolic adaptation and maladaptation in adipose tissue. *Nat Metab* 1: 189-200

Chouchani ET, Kazak L, Spiegelman BM (2019) New Advances in Adaptive Thermogenesis: UCP1 and Beyond. *Cell Metab* 29: 27-37

Cohen P, Levy JD, Zhang Y, Frontini A, Kolodin DP, Svensson KJ, Lo JC, Zeng X, Ye L, Khandekar MJ *et al* (2014) Ablation of PRDM16 and beige adipose causes metabolic dysfunction and a subcutaneous to visceral fat switch. *Cell* 156: 304-316

Cohen P, Spiegelman BM (2015) Brown and Beige Fat: Molecular Parts of a Thermogenic Machine. *Diabetes* 64: 2346-2351

Corbett SW, Stern JS, Keesey RE (1986) Energy expenditure in rats with diet-induced obesity. *Am J Clin Nutr* 44: 173-180

Cutting WC, Mehrtens HG, Tainter ML (1933) Actions and Uses of Dinitrophenol: Promising Metabolic Applications. *JAMA*

Cypess AM, Lehman S, Williams G, Tal I, Rodman D, Goldfine AB, Kuo FC, Palmer EL, Tseng YH, Doria A *et al* (2009) Identification and importance of brown adipose tissue in adult humans. *N Engl J Med* 360: 1509-1517

de Meis L (2003) Brown adipose tissue Ca2+-ATPase: uncoupled ATP hydrolysis and thermogenic activity. *J Biol Chem* 278: 41856-41861

de Meis L, Arruda AP, da Costa RM, Benchimol M (2006) Identification of a Ca2+-ATPase in brown adipose tissue mitochondria: regulation of thermogenesis by ATP and Ca2+. *J Biol Chem* 281: 16384-16390

de Meis L, Ketzer LA, da Costa RM, de Andrade IR, Benchimol M (2010) Fusion of the endoplasmic reticulum and mitochondrial outer membrane in rats brown adipose tissue: activation of thermogenesis by Ca2+. *PLoS One* 5: e9439

de Meis L, Oliveira GM, Arruda AP, Santos R, Costa RM, Benchimol M (2005) The thermogenic activity of rat brown adipose tissue and rabbit white muscle Ca2+-ATPase. *IUBMB Life* 57: 337-345

Duchen MR (2004) Roles of mitochondria in health and disease. *Diabetes* 53 Suppl 1: S96-102

Dulloo AG, Calokatisa R (1991) Adaptation to low calorie intake in obese mice: contribution of a metabolic component to diminished energy expenditures during and after weight loss. *Int J Obes* 15: 7-16

Dulloo AG, Jacquet J (1998) Adaptive reduction in basal metabolic rate in response to food deprivation in humans: a role for feedback signals from fat stores. *Am J Clin Nutr* 68: 599-606

Elliot DL, Goldberg L, Kuehl KS, Bennett WM (1989) Sustained depression of the resting metabolic rate after massive weight loss. *Am J Clin Nutr* 49: 93-96

Enerbäck S, Jacobsson A, Simpson EM, Guerra C, Yamashita H, Harper ME, Kozak LP (1997) Mice lacking mitochondrial uncoupling protein are cold-sensitive but not obese. *Nature* 387: 90-94

Faergeman NJ, Knudsen J (1997) Role of long-chain fatty acyl-CoA esters in the regulation of metabolism and in cell signalling. *Biochem J* 323 (Pt 1): 1-12

Fedorenko A, Lishko PV, Kirichok Y (2012) Mechanism of fatty-acid-dependent UCP1 uncoupling in brown fat mitochondria. *Cell* 151: 400-413

Feldman D, Hirst M (1978) Glucocorticoids and regulation of phosphoenolpyruvate carboxykinase activity in rat brown adipose tissue. *Am J Physiol* 235: E197-202

Foster DO, Frydman ML (1978) Brown adipose tissue: the dominant site of nonshivering thermogenesis in the rat. *Experientia Suppl* 32: 147-151

Fothergill E, Guo J, Howard L, Kerns JC, Knuth ND, Brychta R, Chen KY, Skarulis MC, Walter M, Walter PJ *et al* (2016) Persistent metabolic adaptation 6 years after "The Biggest Loser" competition. *Obesity (Silver Spring)* 24: 1612-1619

Gamu D, Tupling AR (2017) Fattening the role of Ca(2+) cycling in adaptive thermogenesis. *Nat Med* 23: 1403-1404

Gauthier MS, Miyoshi H, Souza SC, Cacicedo JM, Saha AK, Greenberg AS, Ruderman NB (2008) AMP-activated protein kinase is activated as a consequence of lipolysis in the adipocyte: potential mechanism and physiological relevance. *J Biol Chem* 283: 16514-16524

Grundlingh J, Dargan PI, El-Zanfaly M, Wood DM (2011) 2,4-dinitrophenol (DNP): a weight loss agent with significant acute toxicity and risk of death. *J Med Toxicol* 7: 205-212

Guan HP, Li Y, Jensen MV, Newgard CB, Steppan CM, Lazar MA (2002) A futile metabolic cycle activated in adipocytes by antidiabetic agents. *Nat Med* 8: 1122-1128

Hamann A, Benecke H, Le Marchand-Brustel Y, Susulic VS, Lowell BB, Flier JS (1995) Characterization of insulin resistance and NIDDM in transgenic mice with reduced brown fat. *Diabetes* 44: 1266-1273

Hammond VAJ, Desmond G., 1987. Substrate cycling between triglyceride and fatty acid in human adipocytes. Metabolism, pp. 308-313.

Harper RD, Saggerson ED (1975) Some aspects of fatty acid oxidation in isolated fat-cell mitochondria from rat. *Biochem J* 152: 485-494

Himms-Hagen J (1984) Nonshivering thermogenesis. *Brain Res Bull* 12: 151-160

Hoek JB, Rydström J (1988) Physiological roles of nicotinamide nucleotide transhydrogenase. *Biochem J* 254: 1-10

Ikeda K, Kang Q, Yoneshiro T, Camporez JP, Maki H, Homma M, Shinoda K, Chen Y, Lu X, Maretich P *et al* (2017) UCP1-independent signaling involving SERCA2b-mediated calcium cycling regulates beige fat thermogenesis and systemic glucose homeostasis. *Nat Med* 23: 1454-1465

Ikeda K, Maretich P, Kajimura S (2018) The Common and Distinct Features of Brown and Beige Adipocytes. *Trends Endocrinol Metab* 29: 191-200

Ikeda K, Yamada T (2020) UCP1 Dependent and Independent Thermogenesis in Brown and Beige Adipocytes. *Front Endocrinol (Lausanne)* 11: 498

Jackson JB, Leung JH, Stout CD, Schurig-Briccio LA, Gennis RB (2015) Review and Hypothesis. New insights into the reaction mechanism of transhydrogenase: Swivelling the dIII component may gate the proton channel. *FEBS Lett* 589: 2027-2033

Jastroch M, Divakaruni AS, Mookerjee S, Treberg JR, Brand MD (2010) Mitochondrial proton and electron leaks. *Essays Biochem* 47: 53-67

Johannsen DL, Knuth ND, Huizenga R, Rood JC, Ravussin E, Hall KD (2012) Metabolic slowing with massive weight loss despite preservation of fat-free mass. *J Clin Endocrinol Metab* 97: 2489-2496

Kaiyala KJ, Morton GJ, Leroux BG, Ogimoto K, Wisse B, Schwartz MW (2010) Identification of body fat mass as a major determinant of metabolic rate in mice. *Diabetes* 59: 1657-1666

Kampjut D, Sazanov LA (2019) Structure and mechanism of mitochondrial proton-translocating transhydrogenase. *Nature* 573: 291-295

Kazak L, Chouchani ET, Jedrychowski MP, Erickson BK, Shinoda K, Cohen P, Vetrivelan R, Lu GZ, Laznik-Bogoslavski D, Hasenfuss SC *et al* (2015) A creatine-driven substrate cycle enhances energy expenditure and thermogenesis in beige fat. *Cell* 163: 643-655

Kazak L, Chouchani ET, Lu GZ, Jedrychowski MP, Bare CJ, Mina AI, Kumari M, Zhang S, Vuckovic I, Laznik-Bogoslavski D *et al* (2017) Genetic Depletion of Adipocyte

Creatine Metabolism Inhibits Diet-Induced Thermogenesis and Drives Obesity. *Cell Metab* 26: 660-671.e663

Kazak L, Rahbani JF, Samborska B, Lu GZ, Jedrychowski MP, Lajoie M, Zhang S, Ramsay LC, Dou FY, Tenen D *et al* (2019) Ablation of adipocyte creatine transport impairs thermogenesis and causes diet-induced obesity. *Nat Metab* 1: 360-370

Kreiter J, Rupprecht A, Škulj S, Brkljača Z, Žuna K, Knyazev DG, Bardakji S, Vazdar M, Pohl EE (2021) ANT1 Activation and Inhibition Patterns Support the Fatty Acid Cycling Mechanism for Proton Transport. *Int J Mol Sci* 22

Kuznetsov AV, Margreiter R (2009) Heterogeneity of mitochondria and mitochondrial function within cells as another level of mitochondrial complexity. *Int J Mol Sci* 10: 1911-1929

Larson CJ (2019) Translational Pharmacology and Physiology of Brown Adipose Tissue in Human Disease and Treatment. *Handb Exp Pharmacol* 251: 381-424

Larter CZ, Chitturi S, Heydet D, Farrell GC (2010) A fresh look at NASH pathogenesis. Part 1: the metabolic movers. *J Gastroenterol Hepatol* 25: 672-690

Leibel RL, Rosenbaum M, Hirsch J (1995) Changes in energy expenditure resulting from altered body weight. *N Engl J Med* 332: 621-628

Lindberg O, de Pierre J, Rylander E, Afzelius BA (1967) Studies of the mitochondrial energy-transfer system of brown adipose tissue. *J Cell Biol* 34: 293-310

Liu X, Rossmeisl M, McClaine J, Riachi M, Harper ME, Kozak LP (2003) Paradoxical resistance to diet-induced obesity in UCP1-deficient mice. *J Clin Invest* 111: 399-407

Lowell BB, Flier JS (1997) Brown Adipose Tissue, β3-Adrenergic Receptors, and Obesity. *Annual Review of Medicine* 48 : 1: 307-316

Maclean PS, Bergouignan A, Cornier MA, Jackman MR (2011) Biology's response to dieting: the impetus for weight regain. *Am J Physiol Regul Integr Comp Physiol* 301: R581-600

Mahdaviani K, Benador IY, Su S, Gharakhanian RA, Stiles L, Trudeau KM, Cardamone M, Enríquez-Zarralanga V, Ritou E, Aprahamian T *et al* (2017) Mfn2 deletion in brown adipose tissue protects from insulin resistance and impairs thermogenesis. *EMBO Rep* 18: 1123-1138

Mottillo EP, Balasubramanian P, Lee YH, Weng C, Kershaw EE, Granneman JG (2014) Coupling of lipolysis and de novo lipogenesis in brown, beige, and white adipose tissues during chronic β3-adrenergic receptor activation. *J Lipid Res* 55: 2276-2286

Mottillo EP, Ramseyer VD, Granneman JG (2018) SERCA2b Cycles Its Way to UCP1-Independent Thermogenesis in Beige Fat. *Cell Metab* 27: 7-9

Nedergaard J, Cannon B (2018) Brown adipose tissue as a heat-producing thermoeffector. *Handb Clin Neurol* 156: 137-152

Newsholme EA (1978) Substrate cycles: their metabolic, energetic and thermic consequences in man. *Biochem Soc Symp*: 183-205

Ngo J, Benador IY, Brownstein AJ, Vergnes L, Veliova M, Shum M, Acín-Pérez R, Reue K, Shirihai OS, Liesa M (2021) Isolation and functional analysis of peridroplet mitochondria from murine brown adipose tissue. *STAR Protoc* 2: 100243

Nolan CJ, Madiraju MS, Delghingaro-Augusto V, Peyot ML, Prentki M (2006) Fatty acid signaling in the beta-cell and insulin secretion. *Diabetes* 55 Suppl 2: S16-23

Nomura DK, Long JZ, Niessen S, Hoover HS, Ng SW, Cravatt BF (2010) Monoacylglycerol lipase regulates a fatty acid network that promotes cancer pathogenesis. *Cell* 140: 49-61

O'Mara AE, Johnson JW, Linderman JD, Brychta RJ, McGehee S, Fletcher LA, Fink YA, Kapuria D, Cassimatis TM, Kelsey N *et al* (2020) Chronic mirabegron treatment increases human brown fat, HDL cholesterol, and insulin sensitivity. *J Clin Invest* 130: 2209-2219

Ouellet V, Labbé SM, Blondin DP, Phoenix S, Guérin B, Haman F, Turcotte EE, Richard D, Carpentier AC (2012) Brown adipose tissue oxidative metabolism contributes to energy expenditure during acute cold exposure in humans. *J Clin Invest* 122: 545-552

Parascandola J (1974) Dinitrophenol and bioenergetics: an historical perspective. *Mol Cell Biochem* 5: 69-77

Parker N, Crichton PG, Vidal-Puig AJ, Brand MD (2009) Uncoupling protein-1 (UCP1) contributes to the basal proton conductance of brown adipose tissue mitochondria. *J Bioenerg Biomembr* 41: 335-342

Prentki M, Madiraju SR (2008) Glycerolipid metabolism and signaling in health and disease. *Endocr Rev* 29: 647-676

Prentki M, Madiraju SR (2012) Glycerolipid/free fatty acid cycle and islet β-cell function in health, obesity and diabetes. *Mol Cell Endocrinol* 353: 88-100

Przybytkowski E, Joly E, Nolan CJ, Hardy S, Francoeur AM, Langelier Y, Prentki M (2007) Upregulation of cellular triacylglycerol - free fatty acid cycling by oleate is associated with long-term serum-free survival of human breast cancer cells. *Biochem Cell Biol* 85: 301-310

Rahbani JF, Roesler A, Hussain MF, Samborska B, Dykstra CB, Tsai L, Jedrychowski MP, Vergnes L, Reue K, Spiegelman BM *et al* Creatine kinase B controls futile creatine cycling in thermogenic fat.

Raimondo A, Rees MG, Gloyn AL (2015) Glucokinase regulatory protein: complexity at the crossroads of triglyceride and glucose metabolism. *Curr Opin Lipidol* 26: 88-95

Reshef L, Olswang Y, Cassuto H, Blum B, Croniger CM, Kalhan SC, Tilghman SM, Hanson RW (2003) Glyceroneogenesis and the triglyceride/fatty acid cycle. *J Biol Chem* 278: 30413-30416

Rothwell NJ, Stock MJ (1979) A role for brown adipose tissue in diet-induced thermogenesis. *Nature* 281: 31-35

Rydström J (2006) Mitochondrial transhydrogenase--a key enzyme in insulin secretion and, potentially, diabetes. *Trends Biochem Sci* 31: 355-358

Sahoo SK, Shaikh SA, Sopariwala DH, Bal NC, Periasamy M (2013) Sarcolipin protein interaction with sarco(endo)plasmic reticulum Ca2+ ATPase (SERCA) is distinct from phospholamban protein, and only sarcolipin can promote uncoupling of the SERCA pump. *J Biol Chem* 288: 6881-6889

Saito M, Okamatsu-Ogura Y, Matsushita M, Watanabe K, Yoneshiro T, Nio-Kobayashi J, Iwanaga T, Miyagawa M, Kameya T, Nakada K *et al* (2009) High incidence of metabolically active brown adipose tissue in healthy adult humans: effects of cold exposure and adiposity. *Diabetes* 58: 1526-1531

Sharma A, Oonthonpan L, Sheldon RD, Rauckhorst AJ, Zhu Z, Tompkins SC, Cho K, Grzesik WJ, Gray LR, Scerbo DA *et al* (2019) Impaired skeletal muscle mitochondrial pyruvate uptake rewires glucose metabolism to drive whole-body leanness. *Elife* 8

Stanford KI, Middelbeek RJ, Townsend KL, An D, Nygaard EB, Hitchcox KM, Markan KR, Nakano K, Hirshman MF, Tseng YH *et al* (2013) Brown adipose tissue regulates glucose homeostasis and insulin sensitivity. *J Clin Invest* 123: 215-223

Stefl B, Janovská A, Hodný Z, Rossmeisl M, Horáková M, Syrový I, Bémová J, Bendlová B, Kopecký J (1998) Brown fat is essential for cold-induced thermogenesis but not for obesity resistance in aP2-Ucp mice. *Am J Physiol* 274: E527-533

Stone SJ, Levin MC, Zhou P, Han J, Walther TC, Farese RV, Jr. (2009) The endoplasmic reticulum enzyme DGAT2 is found in mitochondria-associated

membranes and has a mitochondrial targeting signal that promotes its association with mitochondria. *J Biol Chem* 284: 5352-5361

Sun Y, Rahbani JF, Jedrychowski MP, Riley CL, Vidoni S, Bogoslavski D, Hu B, Dumesic PA, Zeng X, Wang AB *et al* (2021) Mitochondrial TNAP controls thermogenesis by hydrolysis of phosphocreatine. *Nature* 593: 580-585

Tainter ML, Cutting WC, Stockton AB (1934) Use of Dinitrophenol in Nutritional Disorders : A Critical Survey of Clinical Results. *Am J Public Health Nations Health* 24: 1045-1053

Tordjman J, Chauvet G, Quette J, Beale EG, Forest C, Antoine B (2003) Thiazolidinediones block fatty acid release by inducing glyceroneogenesis in fat cells. *J Biol Chem* 278: 18785-18790

Ukropec J, Anunciado RP, Ravussin Y, Hulver MW, Kozak LP (2006) UCP1-independent thermogenesis in white adipose tissue of cold-acclimated Ucp1-/- mice. *J Biol Chem* 281: 31894-31908

Valtueña S, Blanch S, Barenys M, Solà R, Salas-Salvadó J (1995) Changes in body composition and resting energy expenditure after rapid weight loss: is there an energy-metabolism adaptation in obese patients? *Int J Obes Relat Metab Disord* 19: 119-125

van Schaftingen E, Vandercammen A, Detheux M, Davies DR (1992) The regulatory protein of liver glucokinase. *Adv Enzyme Regul* 32: 133-148

Veliova M, Ferreira CM, Benador IY, Jones AE, Mahdaviani K, Brownstein AJ, Desousa BR, Acín-Pérez R, Petcherski A, Assali EA *et al* (2020) Blocking mitochondrial

pyruvate import in brown adipocytes induces energy wasting via lipid cycling. *EMBO Rep*: e49634

Wang T, Si Y, Shirihai OS, Si H, Schultz V, Corkey RF, Hu L, Deeney JT, Guo W, Corkey BE (2010) Respiration in adipocytes is inhibited by reactive oxygen species. *Obesity (Silver Spring)* 18: 1493-1502

Wolfe RR, Klein S, Carraro F, Weber JM (1990) Role of triglyceride-fatty acid cycle in controlling fat metabolism in humans during and after exercise. *Am J Physiol* 258: E382-389

Yoneshiro T, Aita S, Matsushita M, Kameya T, Nakada K, Kawai Y, Saito M (2011) Brown adipose tissue, whole-body energy expenditure, and thermogenesis in healthy adult men. *Obesity (Silver Spring)* 19: 13-16

Yoneshiro T, Saito M (2015) Activation and recruitment of brown adipose tissue as anti-obesity regimens in humans. *Ann Med* 47: 133-141

CHAPTER 3: MITOCHONDRIA ISOLATED FROM LIPID DROPLETS IN WAT REVEAL FUNCTIONAL DIFFERENCES BASED ON LIPID DROPLET SIZE

The work described in this chapter has been submitted to Life Science Alliance Journal and is currently under revision:

Alexandra J. Brownstein, Michaela Veliova, Rebeca Acín-Pérez, Frankie Villalobos, Alberto Tombolato, Anton Petcherski, Marc Liesa[#], Orian S. Shirhai[#]. (2023) Mitochondria isolated from lipid droplets in WAT reveal functional differences based on lipid droplet size. *Life Science Alliance*.

# these authors contributed equally

Running Title: WAT Peridroplet Mitochondria

Mitochondria isolated from lipid droplets in WAT reveal functional differences based on lipid droplet size

Alexandra J. Brownstein[1, 2], Michaela Veliova[1], Rebeca Acín-Pérez [1], Frankie Villalobos[1], Alberto Tombolato[1], Anton Petcherski[1], Marc Liesa[3 #], Orian S. Shirhai[1,2, #]

1. David Geffen School of Medicine, Department of Endocrinology and Department of Molecular and Medical Pharmacology, University of California, Los Angeles, CA, 90095, United States
2. Molecular Cellular Integrative Physiology Interdepartmental Graduate Program, University of California, Los Angeles, CA, 90095, United States
3. Department of Cells and Tissues, Institut de Biologia Molecular de Barcelona, IBMB, CSIC, Barcelona, Spain, 08028

# these authors contributed equally

ABSTRACT

Recent studies in brown adipose tissue (BAT) described a unique subpopulation of mitochondria bound to lipid droplets (LDs), peridroplet mitochondria (PDM). PDMs can be isolated from BAT by differential centrifugation and salt washes (Benador *et al*, 2018). Contrary to BAT, this approach has so far not led to successful isolation of PDMs from white adipose tissue (WAT). Here, we developed a method to isolate PDM from WAT with high yield and purity by an optimized proteolytic treatment that preserves the respiratory function of mitochondria. Using this approach, we show that, contrary to BAT, WAT PDM have lower respiratory and ATP synthesis capacity compared to WAT CM. Furthermore, by isolating PDM from LDs of different sizes, we find a negative correlation between LD size and the respiratory capacity of their PDM in WAT. Thus, our new isolation method reveals tissue-specific characteristics of PDM and establishes the existence of heterogeneity in PDM function determined by LD size.

Key Words

white adipose tissue / lipid droplet / mitochondria / peridroplet mitochondria / brown adipose tissue

GRAPHICAL SYNOPSIS

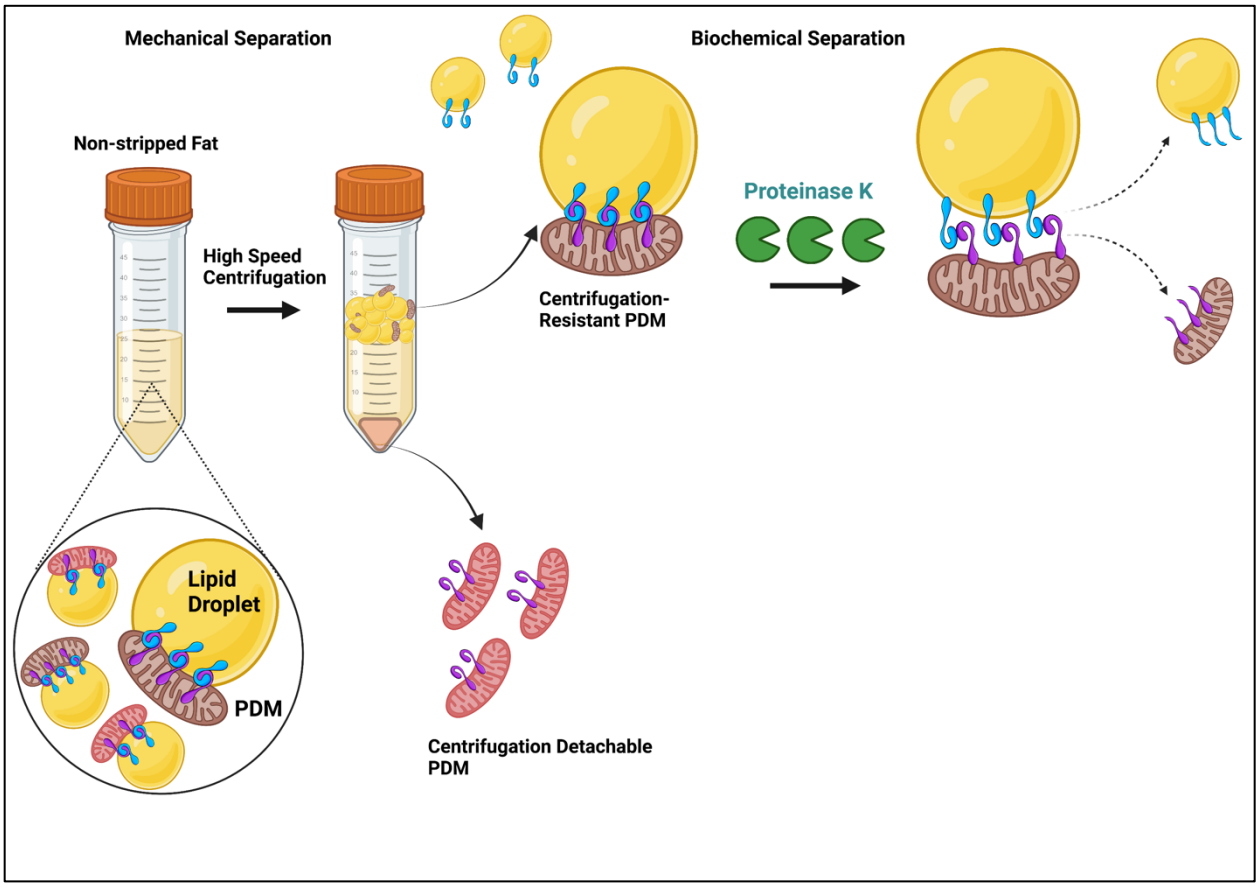

INTRODUCTION

Mitochondria attached to lipid droplets (LD), or peridroplet mitochondria (PDM), were shown to expand lipid droplets in brown adipose tissue (BAT) (Benador *et al.*, 2018). Mechanistically, BAT PDM are specialized to oxidize pyruvate and provide ATP to fuel the esterification of fatty acids into triglycerides (Benador *et al.*, 2018). Whether this specialized function of PDM is conserved in tissues different from BAT is unknown, mostly due to a lack of available protocols to isolate PDM efficiently from other tissues. The role of PDM promoting the esterification of fatty acids into triglycerides was hypothesized to be especially relevant in white adipose tissue (WAT), as esterification can protect from lipotoxicity of NEFA (non-esterified fatty acids) (Kuramoto *et al*, 2012; Laurens *et al*, 2016; Listenberger *et al*, 2003; Tan *et al*, 2019; Veliova *et al*, 2020; Wang *et al*, 2015; Zheng *et al*, 2017). It has been hypothesized that both PDM and cytoplasmic mitochondria (CM) contribute to the removal of NEFA, with CM oxidizing NEFA and PDM securing them into neutral triglycerides (Veliova *et al.*, 2020). Finding ways in which we can manipulate or offset different mitochondrial populations has the potential to regulate lipid metabolism.

WAT has been shown to have lower mitochondrial mass per cell when compared to BAT. Moreover, per mitochondrial mass, WAT has a lower capacity to oxidize fatty acids when compared to BAT (Cannon & Nedergaard, 2004; Cinti, 2018). Nonetheless, recent studies have shown that mitochondria from WAT not only support adipocyte-specific functions, but play essential roles in maintaining whole-body energy homeostasis, control

of insulin sensitivity, glucose metabolism, and crosstalk between muscles and adipose tissues (Boudina & Graham, 2014; Lee *et al*, 2019; Vernochet *et al*, 2014). Electron microscopy images of human white adipose tissue support the existence of a unique population of mitochondria that are in contact with lipid droplets in WAT; however the function of these mitochondria within the cell, and the changes associated with the development of obesity is still unknown (Cinti, 2018; Cushman, 1970; Freyre *et al*, 2019). In order to better understand the role of PDM in WAT, it is crucial to develop an optimized protocol that allows for PDM isolation with a high yield.

The PDM isolation protocols published to date utilize differential centrifugation. However, these protocols differ in the composition of the homogenization and isolation buffers used, more specifically in salt concentrations and the presence of detergents (Cui *et al*, 2019; Ngo *et al*, 2021; Yu *et al*, 2015; Zhang *et al*, 2016). Benador et al. showed successful stripping of a large proportion of mitochondria attached to lipid droplets in BAT by centrifuging the fraction enriched with lipid droplets at high speed(Benador *et al.*, 2018; Ngo *et al.*, 2021). However, not all lipid-bound mitochondria were removed by this centrifugation (Benador *et al.*, 2018). This may reflect on the heterogeneity of the mechanisms adhering mitochondria to lipid droplets and may represent functional diversity of PDM. To explore the diversity of PDM, a more powerful approach to detach mitochondria from lipid droplets needs to be applied. We rationalized that digestion of the proteins that link mitochondria to LDs could enhance the detachment of PDM from lipid droplets, while addressing the potential for damage induced by the proteolytic activity.

Accordingly, several studies in oxidative tissues, including skeletal and cardiac muscle, used protease treatments to disperse the tissue in the process of mitochondrial isolation (Kras *et al*, 2016; Lai *et al*, 2019; Sánchez-González & Formentini, 2021).

Here, we describe a new approach to isolate PDM that combines protease treatment and centrifugation. The combined protease and centrifugation method successfully detaches mitochondria from WAT lipid droplets, revealing that BAT and WAT PDM differ in the strength of attachment to lipid droplets as well as in their bioenergetic characteristics. Moreover, using our new approach we detached PDM from small and large lipid droplets, uncovering the functional diversity of PDM segregated by their lipid droplet size.

RESULTS

The attachment of mitochondria to lipid droplets is stronger in WAT compared to BAT.

Previously published protocols to isolate peridroplet mitochondria from BAT demonstrated that the centrifugal force applied to lipid droplets (LDs) was sufficient to strip a significant portion of the PDM in BAT **(Fig 1C-D).** (Acín-Perez *et al*, 2021; Benador *et al.*, 2018; Ngo *et al.*, 2021). In WAT, PDM isolation was historically low. By using our previously published protocol to image mitochondria in fat layers (Acín-Perez *et al.*, 2021), we found that there is a major fraction of PDMs in WAT fat layers that remain attached to the LDs after centrifugation **(Fig 1A-B).** This result suggested that attachment of PDM to

LDs in WAT is more resistant to centrifugation than in BAT, highlighting that the interaction between PDM and LDs is stronger in WAT.

Protein-protein interactions explain the stronger attachment of PDM in WAT versus BAT.

Mitochondria-LD interactions are mediated by a variety of protein tethers and complexes, whose composition seems to be tissue-specific (Boutant *et al*, 2017; Freyre *et al.*, 2019; Stone *et al*, 2009; Wang *et al*, 2011). In this regard, PLIN5 mediates attachment of mitochondria to lipid droplets (LDs) and its expression is higher in BAT, when compared to WAT (Wang *et al.*, 2011; Wolins *et al*, 2006). Thus, there is a possibility that the composition and/or number of tethers are different in BAT and WAT. We therefore hypothesized that stronger protein-protein interactions explained both the inefficiency of centrifugation to strip mitochondria from WAT **(Fig 1A and 1B)**, as well as the presence of some PDM in BAT that remained attached to LDs after centrifugation **(Fig 1C and 1D)**. To test our hypothesis, we treated the fat layers of WAT with Proteinase K (Prot K), with the goal to digest the protein tethers anchoring mitochondria to LDs and potentially strip mitochondria that are resistant to stripping by centrifugation.

With the aim to confine degradation to the protein tethers in the LD and outer mitochondrial membrane, we inactivated Prot K with phenylmethylsulfonyl fluoride (PMSF) right before separating PDM from the LDs by centrifugation **(Fig 1E)** (Badugu *et al*, 2008; Gold, 1965; Gold & Fahrney, 1964; Koncsos *et al*, 2018). Furthermore, PMSF

addition would allow long term storage of the fractions by freezing them, as Prot K is still active after freeze and thaw cycles. Prot K is widely used to identify the domains of outer mitochondrial membranes exposed to the cytosol, as Prot K cannot diffuse across intact mitochondrial membranes. Therefore, Prot K cannot degrade matrix, inner membrane proteins or even integral outer membrane proteins facing the intermembrane space in intact mitochondria; only if membranes are pierced by freeze thawing (Badugu *et al.*, 2008; Denuc *et al*, 2016).

To establish the efficacy of protease treatment on the yield and function of isolated PDM, we performed paired comparisons of protease-treated LD fractions with their respective controls. To this end, we split the WAT homogenates into four groups **(Fig 1E)**: in the first group, PDM were isolated exclusively by centrifuging the LD fraction as was previously published (Benador *et al.*, 2018). In the second group, the LD fraction was treated with Prot K before centrifugation and in the third group, the LD fraction was treated with Prot K, and then incubated with PMSF before centrifugation. Lastly, the fourth fraction was treated only with PMSF, to establish whether PMSF itself could change PDM isolation and function. As an additional control, we added Prot K to the supernatant from which cytosolic mitochondria (CM) are isolated **(Fig 1E)**. The rationale was that cytosolic mitochondria were expected to have less protein tethers and thus Prot K actions would be harder to confine on CM .

We found that Prot K treatment significantly increased the amount of protein in the PDM fraction of WAT, demonstrating an improvement in the yield of PDM isolation **(Fig 1F)**. Prot K treatment also increased the yield of CM isolated from WAT **(Fig 1F),** suggesting that the CM in WAT were potentially tethered via protein-mediated interactions to other membranes (ER or nucleus) that were disrupted with Prot K. In BAT, we also found that Prot K treatment significantly increased the yield of PDM isolation, but not of BAT CM **(Fig 1G)**. These data suggest that both WAT PDM and WAT CM potentially have different mechanisms regulating their tethering to other organelles and membranes.

We next sought to confirm whether the increase in total protein observed in the PDM fraction was associated with an increase in mitochondrial content, as well as with an increase in the purity of mitochondrial fractions. To determine purity, we used Western blot to quantify the amount of mitochondrial proteins per microgram of protein in PDM and CM fractions isolated from WAT and BAT. As PDM isolation is a long procedure, we could not perform the Western blots in freshly isolated mitochondria. Complicating the analysis of frozen samples, proteins inserted in the outer membrane (VDAC), as well as inner membrane proteins (OXPHOS) can be degraded by Prot K when mitochondrial membranes are damaged by freeze-thaw cycles (Badugu *et al.*, 2008; Zhang *et al*, 2015).

In agreement with these published findings, we found that the content of VDAC and OXPHOS subunits was dramatically decreased in PDM and CM fractions frozen and thawed after isolation from WAT and BAT that did not contain PMSF **(Fig 1H and 1I).**

Treatment with PMSF prevented the decreases in VDAC and OXPHOS protein content and preserved the proteins of freeze-thawed mitochondria isolated with Prot K **(Fig 1H and 1I)**. Quantification of VDAC and OXPHOS proteins by Western blot revealed no differences in their content per microgram of protein **(Supplementary Fig 1)**, which showed that Prot K treatment proportionally increase the yield of mitochondrial and contaminant proteins in PDM fractions. The effects of PMSF confirm that the decrease in VDAC and OXPHOS content were caused by the persistence of Prot K activity in PDM and CM fractions even after washes and freeze-thawing. Finally, PMSF treatment by itself did not result in any significant differences in VDAC and OXPHOS protein content **(Supplementary Fig 1)**. This latter result supports that the inhibitory actions of PMSF on respiration were not caused by a decrease in OXPHOS protein content nor in the purity of the isolated fraction.

The finding that Prot K treatment facilitates the separation of mitochondria from LDs was further confirmed by our plate-reader based assay quantifying PDM (Acín-Perez *et al.*, 2021; Benador *et al.*, 2018; Ngo *et al.*, 2021). The lipid droplet fractions were stained with BODIPY493/503 (BD493), a dye staining neutral lipids, and MitoTracker DeepRed (MTDR), a dye staining mitochondria (Acín-Perez *et al.*, 2021). We chose to use MTDR because we have previously verified its membrane potential dependency is minimal and does not impose a significant bias over mitochondrial mass with the concentration and duration of staining required (Acín-Perez *et al.*, 2021). To evaluate the amount of mitochondria per LD, the LD fractions were stained before and after separating

the mitochondria. The reduction in the ratio of MTDR/BD493 fluorescence after separating the mitochondria by centrifugation was used to quantify PDM content (Acín-Perez *et al.*, 2021). In WAT, centrifugation alone was unable to strip a significant amount of PDM **(Fig 1J)**, confirming the confocal imaging, where we see PDM retained after centrifugation **(Fig 1A and 1B**). We were only able to strip the PDM from WAT when LD fractions were treated with Prot K **(Fig 1J)**. In BAT, the ratio of MTDR/BD493 was significantly reduced by centrifugation alone and was further reduced, although not significantly, when Prot K was added **(Fig 1K)**. Together these data suggest that Prot K treatment enhances PDM isolation from WAT, and can increase the yield of PDM isolated from BAT.

Isolation of PDM with Proteinase K does not inhibit mitochondrial respiratory function.

Despite Prot K not being able to access the inner membrane of intact mitochondria, both PMSF and Prot K treatments were reported to impact oxygen consumption measured in intact mitochondria (Cole *et al*, 2015; Koncsos *et al.*, 2018; Marcillat *et al*, 1988; Ruiz-Meana *et al*, 2014). Thus, we wanted to verify whether our treatments with Prot K, without PMSF, were affecting respiratory function of freshly isolated mitochondria. In addition, we determined whether PMSF treatment at 2 mM affected mitochondrial respiratory function by itself. Lower concentrations (below 2 mM) of PMSF were previously shown to have marginal or no effects on mitochondrial respiration (Koncsos *et al.*, 2018), but these lower concentrations of PMSF cannot block Prot K effectively.

Respiratory function of isolated PDM and CM using Prot K was determined by quantifying oxygen consumption rates (OCR) using the XF96 flux analyzer. We measured state 3 respiration, which reflects coupled respiration associated with maximal ATP synthesis, and separately, maximal complex IV (CoxIV) activity. CoxIV activity is measured by providing TMPD/Ascorbate to directly to isolated mitochondria, as TMPD donates electrons directly to complex CoxIV. Prot K +/- PMSF treated CM and PDM respiration data was normalized as fold change to respiration of untreated mitochondria isolated from the same tissue sample.

A significant increase in state 3 OCR was observed in WAT CM isolated using Prot K **(Fig 2A)**. PMSF treatment prevented the increase in state 3 induced by Prot K treatment. However, PMSF alone decreased respiration rates to the same levels as mitochondria treated with Prot K + PMSF. Therefore, the decrease associated with PMSF is explained by an autonomous effect of PMSF decreasing state 3 respiration, rather than by blocking protein degradation. A similar inhibitory effect of PMSF on respiration was observed when providing electrons directly to CoxIV **(Fig 2B)**. On the other hand , CoxIV-driven respiration was not increased in mitochondria isolated using Prot K, supporting the notion that increased state 3 respiration was reflecting a specific increase in ATP-synthesizing activity. To confirm this possibility, we measured ATP synthesis rates in isolated mitochondria using firefly luciferase luminescence. We find that Prot K treatment increased ATP synthesis rates in WAT CM **(Fig 2C)**, further supporting the idea that the

addition of Prot K results in a mitochondrial fraction enriched with functional, non-damaged mitochondria.

The effects of Prot K on WAT PDM respiratory function showed some similarities to WAT CM. Isolating PDM using Prot K increased both state 3 respiration **(Fig 2D)** and ATP synthesis rates **(Fig 2F)**, as in WAT CM. PMSF resulted in decreased ATP synthesis rates in PDM as well. The major difference induced by Prot K treatment in PDM was an increase in CoxIV activity, which was not observed in CM **(Fig 2E)**. In all, isolating either CM or PDM using Prot K yielded higher respiratory capacity.

Because we observed that Prot K treatment selectively increased ATP synthesizing respiration in some mitochondrial preparations, it was still possible that Prot K induced a mild damage to the outer membrane, to cause mild cytochrome C leakage. If mild leakage was present, we should see a larger increase in respiration induced by cytochrome C supplementation in mitochondria isolated with proteinase K, when compared to cytochrome c supplementation in mitochondria isolated without proteinase K. It is important to note that cytochrome c supplementation can increase oxygen consumption independently of complex IV activity as well. We found that cytochrome c supplementation did not induce a larger increase in respiration in Prot K treated mitochondria, with this effect being even of lower magnitude than the effect in control mitochondria **(Supplementary Figure 2A)**. In this regard, the largest portion of cytochrome c-induced increase in respiration observed in both control and Prot K treated

mitochondria was preserved in azide-treated mitochondria **(Supplementary Figure 2B)**. This latter result shows that cytochrome c-induced increase in respiration is not caused by an increase in the availability of cytochrome c for mitochondrial respiration. These new data show that proteinase K treatment did not induce a mild damage in the outer membrane to cause a small leak in cytochrome c.

Our protocol allowed us to compare the respiratory capacity between CM and PDM in WAT, which revealed remarkable differences from PDM and CM in BAT. PDM showed lower respiratory capacity than CM in WAT, as demonstrated by decreased state 3 and CoxIV driven respiration **(Fig 2G)**. These results might suggest that the demand for CM pyruvate oxidation in WAT can be higher than in BAT, as CM in BAT are specialized in fatty acid oxidation (Benador *et al.*, 2018). Confirming the decrease in state 3 respiration fueled by pyruvate, WAT PDM also showed lower ATP-synthesis rates than CM **(Fig 2H)**.

We next determined whether Prot K treatment altered the function of PDM isolated from BAT, and preserved the previously published distinct bioenergetic and proteomic makeup of BAT PDM (Benador *et al.*, 2018). First, we found that, as in WAT, using Prot K to isolate CM from BAT did not decrease state 3 CoxIV driven respiration or ATP synthesis rates **(Fig 3A-3C)**. Similarly, Prot K treatment did not decrease the respiratory function of PDM fractions from BAT **(Fig 3D)**. Indeed, Prot K treatment even increased state 3 respiration in PDM fractions from BAT, as observed in WAT. We also found that PMSF treatment by itself decreased state 3 respiration in PDM. No significant differences

were observed in the measures of CoxIV driven respiration or ATP-linked respiration in BAT PDM, although PMSF treatment trended towards decreased CoxIV respiration **(Fig 3E and 3F)**.

The side-by-side comparison of BAT PDM and CM function revealed that Prot K treatment preserved the unique characteristics of BAT PDM, which we previously published (Benador *et al.*, 2018). BAT PDM fueled by pyruvate and malate show higher state 3 and CoxIV stimulated maximal respiration than CM **(Fig 3G)**. Furthermore, we were able to reproduce the previous observation that BAT PDM have higher ATP synthesis rates than BAT CM **(Fig 3H)** (Benador *et al.*, 2018). Overall, these data suggest that Prot K-assisted isolation does not inhibit mitochondrial respiratory function and that PMSF treatments are only needed to analyze the mitochondrial proteome for further characterization of mitochondrial subpopulations (Benador *et al.*, 2018; Forner *et al*, 2009; Mirza *et al*, 2021; Najt *et al*, 2023).

PDM isolation from lipid droplets with different diameters reveals that lipid droplet size sets PDM functional heterogeneity.

Previous studies have shown that LDs vary in size within individual cells and that these differently sized LDs can have distinct metabolic functions (Herms *et al*, 2013; Olzmann & Carvalho, 2019; Zhang *et al.*, 2016). Furthermore, changes in lipid droplet size are a response to cycles of nutrient availability and overload, as lipid droplets buffer

NEFAs to protect from lipotoxicity (Hariri *et al*, 2018; Hariri *et al*, 2019; Herms *et al.*, 2013; Nguyen *et al*, 2017; Olzmann & Carvalho, 2019; Rambold *et al*, 2015; Renne & Hariri, 2021).

Electron microscopy images of WAT and BAT show that while WAT has larger sized lipid droplets, it has fewer mitochondria per total lipid droplet perimeter per cell. In contrast, BAT contains smaller sized lipid droplet and has more mitochondria per total lipid perimeter (Cinti, 2000, 2001; Cinti, 2007, 2018; Cushman, 1970). We hypothesized that small LDs recruited more mitochondria, despite showing less perimeter of contact area. In order to decipher if recruitment of mitochondria to LDs is determined by the size of the LD, and if this regulation is tissue specific, we developed an approach to obtain separated LD fractions that differed in the average size of their LDs by performing two consecutive centrifugations (Brasaemle & Wolins, 2016; Zhang *et al.*, 2016). The approach required us to be as gentle as possible in order to yield functional isolated mitochondria.

The first centrifugation at 500 x g, yields a fat layer that contains large LDs (LG-LD). This was followed by a second centrifugation step at 2000 x g, resulting in a fat layer that consists of smaller LDs (SM-LD) **(Fig 4A)**. To confirm that these centrifugation steps indeed separated two fractions with differently sized LDs, we stained the LG-LD and SM-LD fractions with BD493 and used confocal microscopy to visualize the LD size **(Fig 4B and 4C)**. More specifically, we measured the perimeter and size distribution by surface

area of each individual LD imaged in the large and small LD fractions isolated from WAT and BAT. We found that the difference in area between the large and small fractions is more pronounced in the WAT, with LG-LD having an average area of 328.6, μm^2, while SM-LD had an average area of 1.9 μm^2 **(Fig 4B and 4D)**. In contrast, the range between the LG and SM-LD average area is smaller in the BAT: the average area of LG-LD was 40.2 μm^2, while 3.4 μm^2 was the average of SM-LD **(Fig 4C and 4E)**. Accordingly, the average LD perimeter of the LG-LD in WAT is 37.6 μm, and 2.5 μm in SM-LD **(Fig 4F)**. In BAT, the average LD perimeter in the LG-LD fraction is 18.6 μm, and 5.4 μm in SM-LD **(Fig 4G)**. Of note, the large lipid droplet fraction isolated from the WAT still contains a significant amount of smaller LDs **(Fig 4F)**. Moreover, the lipid droplet sizes we observed in the isolated fat layers are consistent with what has been reported in vivo in previous studies (Swift *et al*, 2017).

To measure whether small lipid droplets had more mitochondria bound to them, we compared the amount of PDM between LG-LD and SM-LD fractions, by quantifying the ratio of MTDR/BD493 fluorescence using our published plate reader assay of PDM quantification (Acín-Perez *et al.*, 2021). Our data shows that the SM-LD fraction contains more mitochondria per lipid content when compared to the LG-LD fraction in WAT **(Fig 4H)**. However, we found that in BAT the LG-LD fraction has more mitochondria attached to them when compared to SM-LD fraction **(Fig 4I)**.

Mitochondria attached to small and large lipid droplets have different respiratory capacities in WAT and BAT

Separation of lipid droplets by size from mouse BAT revealed diverse protein profiles between the subpopulations of lipid droplets, indicating different interactions with mitochondria and the ER (Zhang *et al.*, 2016). In intact primary brown adipocytes, we observed heterogeneity in PDM function and composition; some PDM showed higher ATP synthase content and membrane potential than others (Benador *et al.*, 2018). Here, we have observed that PDM from WAT have lower ATP-synthesizing respiration and CoxIV activity than CM, which is the opposite behavior of BAT PDM **(Fig 2 and 3).** We find that WAT harbors very large lipid droplets (>100 μm perimeter) that do not exist in BAT from mice housed at room temperature and fed a standard chow diet **(Fig 4E)**. Based on these observations, we sought to test our hypothesis that LD size might determine the intracellular and tissue-specific heterogeneity of PDM function,

To test this hypothesis, we stripped PDM from SM-LD and LG-LD fractions and analyzed them separately by respirometry. In WAT, PDM isolated from SM-LD had significantly higher state 3 OCR when respiring under pyruvate and malate, as well as higher CoxIV driven respiration per mitochondria when compared to PDM isolated from LG-LD **(Fig 5A)**. Under palmitoyl carnitine as the oxidative fuel, the differences in mitochondrial respiration disappeared between WAT PDM isolated from LG vs. SM-LD **(Fig 5B)**.

Interestingly, we find that PDM isolated from BAT LG-LDs show higher state 3 respiration, proton leak-driven respiration, and ATP-synthesizing respiration when compared to PDM from SM-LDs under pyruvate malate **(Fig 5C)**. In marked contrast to WAT, CoxIV driven respiration in BAT was similar in PDM from LG-LD and SM-LD fractions. Furthermore, BAT PDM from LG-LD fractions preserved increased state 3, leak and ATP-synthesizing respiration, in addition to increased CoxIV when palmitoyl-carnitine was provided as a fuel **(Fig 5D)**.

To validate that the differences in respirometry between the two fractions in BAT and WAT are due to bioenergetic differences rather than differences in fraction purity, we measured the content of mitochondrial proteins (VDAC and OXPHOS subunits) per total protein of PDM fraction by Western blot. PDM isolated from WAT SM-LD fractions had significantly higher content of VDAC. In addition, WAT PDM isolated from SM-LD had increased levels of respiratory complexes as determined by the expression of representative proteins in 4 out of 5 OXPHOS complexes (NDUFB8, SDHB, UQCRC2, MTC01) **(Fig 5E and 5F)**. Therefore the respirometry data for WAT **(Fig 5A and B)** was normalized by VDAC, as a marker for total mitochondrial content (Camara *et al*, 2017). On the other hand**,** BAT PDM isolated from large and small LDs did not show differences in VDAC or OXPHOS subunit protein content and the respirometry did not need to be re-normalized **(Fig 5G and 5H)**.

Together these data suggest that in both WAT and BAT, there are separate populations of PDM with unique bioenergetic functions, which may be related to their distinct subcellular localization and heterogeneity of LD function.

DISCUSSION

Here we describe the development of the first method allowing for the isolation of peridroplet mitochondria (PDM) from white adipose tissue (WAT). Benador et al. previously described the isolation and characterization of PDM from BAT using high speed centrifugation (Benador *et al.*, 2018). However, we found that centrifugation was not efficient in isolating PDM from WAT. The main novelty of our new method is the treatment of lipid droplet fractions, containing PDM, with a protease. This step was inspired by previous studies supporting that proteins are key molecules tethering mitochondria to lipid droplets (Boutant *et al.*, 2017; Freyre *et al.*, 2019; Stone *et al.*, 2009; Wang *et al.*, 2011). We used Proteinase K (Prot K), a serine endopeptidase that remains active in the presence of different detergents and temperature ranges, and digests a wide variety of proteins. The dependence upon Prot K to isolate sufficient WAT PDM supports the notion that the interaction of mitochondria with lipid droplets in WAT might be more resilient to mechanical forces than in BAT. Moreover the difference in strength between mitochondria and LDs can be mediated either by a different composition of protein tethers, as supported by differences in PLIN5 and MIGA2 between BAT and WAT, and/or by a larger number of other uncharacterized tethers shared between WAT and BAT (Freyre *et al.*, 2019; Wolins *et al.*, 2006).

In the current protocol, we find that the use of Prot K results in PDM and CM fractions with higher respiratory capacity, when compared to those obtained by high-speed centrifugation alone. We propose that this increase can be explained by Prot K degrading few contaminant components that decrease mitochondrial function. This hypothesis is consistent with several studies in which isolation of interfibrillar mitochondria from both cardiac and skeletal muscle with the protease nagarse resulted in increased mitochondrial function and energetic coupling (Koncsos *et al.*, 2018; Kras *et al.*, 2016).

We show that Prot K does not digest respiratory complexes in intact mitochondria. However, Prot K inactivation by PMSF is required to prevent degradation in freeze-thawed PDM. Membrane disrupting processes enable Prot K to access inner membrane proteins and Prot K itself is resistant to detergents and freeze-thawing procedures. Thus, the addition of PMSF is needed to analyze the protein composition of PDM, as time-constraints prevented protein analyses on the same day of PDM isolation.

We find that respirometry of PDM isolated with Prot K in BAT recapitulated our previous findings: higher maximal ATP synthesis fueled by pyruvate oxidation, when compared to cytosolic mitochondria (Benador *et al.*, 2018). In marked contrast, WAT PDM have lower respiratory capacity and ATP synthesis rates as compared to WAT CM. Indeed, BAT CM are specialized in oxidizing fatty acids for thermogenesis, a function absent in CM from mature white adipocytes. These data suggest that the functional

specialization of PDM in WAT may not be the same as in BAT, and this difference between WAT and BAT may be related to the specific capacity of BAT to perform thermogenesis and fatty acid oxidation. Future studies will determine the function of WAT PDM in esterification of NEFA, versus *de novo* lipogenesis and LD homeostasis.

Differences in the size and location of intracellular lipid droplets, as well as the architecture of their contact sites, are thought to be key determinants of LD function (Renne & Hariri, 2021). These differences in size and location vary depending on the type of cell, nutrient availability and metabolic state (Thiam & Beller, 2017). The diversity in the multifunctional lipid droplet populations is reflected by the recent characterization of their heterogeneous proteomes and lipid compositions (Hsieh *et al*, 2012; Larsson *et al*, 2012; Martin *et al*, 2005; Qian *et al*, 2023; Thiam & Beller, 2017; Wilfling *et al*, 2013). A novel integral endoplasmic reticulum membrane protein expressed selectively in brown adipose tissue, CLSTN3β, was recently shown to regulate LD form and function, as forced expression in both BAT and WAT was shown to induce multilocularity and promote fatty acid oxidation, as observed in thermogenic adipocytes (Qian *et al.*, 2023). Moreover, the expression of lipid-droplet associated proteins including ATGL, Plin5 and several CIDE proteins known to regulate BAT multilocular thermogenic phenotype, were induced in WAT upon cold stimulation, highlighting the relationship between lipid droplet morphology and energy metabolism (Barneda *et al*, 2013).

Our data demonstrates that in WAT, PDM attached to smaller LDs have higher respiratory capacity under pyruvate and malate. In contrast**,** PDM attached to larger LDs in BAT are the ones that have higher ATP synthesizing capacity, which is the opposite from what we observed in WAT. The discrepancy between BAT and WAT could be explained by the fact that LDs in BAT have a larger capacity for *de novo* lipogenesis and TAG turnover, which is dependent on ATP synthesizing respiration. Moreover, Benador et al. previously showed that PDM support LD expansion by providing ATP for fatty acid esterification into triglycerides, which would explain why PDM attached to larger LDs have higher ATP synthesizing capacity (Benador *et al.*, 2018). Indeed, BAT is a more dynamic tissue which is reflected in its multilocular LD-morphology as BAT is constantly undergoing cycles of lipolysis for *β*-oxidation and re-esterification.

On the other hand, differentiating adipocytes in WAT undergo lipogenesis which requires a large amount of ATP as their LDs expand. Morphologically, these differentiating white adipocytes have multi-locular LDs, which are indeed more similar to brown adipocytes as reflected by their function. PDM from small LDs in WAT have increased pyruvate oxidation and ATP-synthase capacity, supporting the idea that PDM from small LDs provide ATP necessary for lipid droplet expansion. This is also supported by the report that white adipocytes increase mitochondrial biogenesis during differentiation, in order to meet the increased energy demand of differentiation as cells and their lipid droplets mature (De Pauw *et al*, 2009; Wilson-Fritch *et al*, 2003).

We show that fat oxidation capacity is higher in PDM isolated from large lipid droplets in BAT, when compared to smaller BAT lipid droplets. On the other hand, we did not see differences in fat oxidation capacity of WAT PDM from large and small lipid droplets. Remarkably, large-lipid droplet fraction in BAT contain lipid droplets of the same size as small lipid droplet fraction in WAT. This may reflect a relationship between fat utilization efficiency and LD size, where fat oxidation capacity is maximal at a certain lipid droplet size and does not further increase after a certain threshold of size.

From the current experiments, we cannot definitively say whether the higher respiratory capacity induces PDM to bind preferentially to smaller LDs or if the higher respiratory capacity of PDMs fueling the oxidation of fatty acids leads to the observation of more active PDM on smaller LDs in WAT. However, fat oxidation is minimal in WAT. This suggests that when mitochondria interact with small LDs in WAT, they are not oxidizing these fatty acids. At the same time, as previously described, the small LDs in WAT are the ones that can expand and are thus more active esterifying and breaking lipids. Therefore, we suggest that in WAT, the interaction of PDM with small LDs and the higher capacity for ATP-synthesis supports a higher activity of TG esterification in small LDs compared to large LD.

Consistent with our data, it was recently shown that white pre-adipocytes lacking MIGA2, the protein linker that binds mitochondria to LDs in WAT, had reduced adipocyte differentiation, decreased LD abundance, and diminished TAG synthesis (Freyre *et al.*,

2019). The increased surface area of small multilocular LDs can promote increased lipolysis and the subsequent release of NEFA (Nishimoto & Tamori, 2017). Furthermore, in MIGA-2 knockout pre-adipocytes, radio-labelled glucose is not enriched in TAGs, suggesting that PDM-association to LDs is essential for the expansion of small lipid droplets through *de novo* lipogenesis and pyruvate oxidation in WAT (Freyre *et al.*, 2019). Once white adipocytes have fully matured and increased their LD size to form a single unilocular LD, they reduce their need for ATP to actively perform TAG synthesis, which is one of the roles of PDM described in BAT.

When PDM from large and small LDs are isolated together, as they were in our initial experiments, the functional differences between the PDM from different populations are averaged together, concealing their unique properties. The new isolation protocol presented here allows us to explore open questions related to mitochondria-LD interaction and will help us better understand PDM function within individual cells and between different adipose tissue depots. Overall, we show data supporting the existence of at least two different populations of PDM, distinguished by their association with LDs of varying size. The differences in mitochondrial function observed between the subpopulations potentially reflect local LD environments with specific needs. We show that in order to isolate PDM from WAT, Proteinase K treatment is needed regardless of the size of the LD that is being used for the preparation. As the yield of PDM isolated from SM-LD and LG-LD by centrifugation is similar, we can conclude that the strength of PDM attachment to different size LDs is similar in BAT. We do however, observe more PDM

attached to smaller LDs in WAT, and the opposite in BAT. This discrepancy between BAT and WAT supports that other tissue-specific factors beyond lipid droplet size determine mitochondria-LD interaction.

Understanding what controls the diversity of lipid droplet biology can help us better understand how and why such diversity exists, and shed new light on the role of LD biology in determining the function of PDM.

A limitation of the approach presented here is in the utilization of crude isolated mitochondrial fractions for the respirometry studies. Crude isolated mitochondria may include diverse levels of contamination by other organelles. A caveat to alternative purification methods which may include ultracentrifugation is that they are time consuming and although they result in ultrapure mitochondrial fractions, they compromise mitochondrial function and impair bioenergetics. Biochemical studies, for example, might require different isolation protocols depending on the main aim of the study. Another limitation of our approach is our incomplete understanding of the enzymatic impact of Prot K on mitochondria. While we show here that mitochondria exposed to Prot K have comparable and even higher state 3 and ATP-synthesizing respiration, this does not preclude that regulatory systems that are dependent on outer membrane proteins are disabled by the Prot K. Further studies would be required to better understand the effect of Prot K on respiration and on individual outer membrane proteins.

In this study we developed a new method to isolate PDM from WAT and improved the isolation of PDM from BAT by adding proteolytic treatment. We demonstrate that the addition of Prot K to PDM isolation protocol does not impair mitochondrial OCR and ATP synthesis capacity in both CM and PDM. Using our new protocol to isolate PDM from WAT, we show that WAT PDM have a lower respiratory capacity than WAT CM, in contrast to our previously published findings on PDM in BAT. We also show that different sized lipid droplets in both BAT and WAT are associated with unique populations of PDM, highlighting the heterogeneity in PDM function. These data suggest PDM have distinct roles in maintaining LD homeostasis, which is determined by the association with LDs and the local cellular needs.

MATERIALS AND METHODS

Mice

Mitochondria were isolated from the interscapular brown adipose tissue and both left and right epididymal white adipose fat pads from 12-week-old male C57BL6/J mice (Jackson lab, Bar Harbor, ME). Animals were fed standard chow (mouse diet 9F, PMI Nutrition International, Brentwood, MO) and maintained under controlled conditions (19–22°C and a 14:10 hr light-dark cycle) until euthanasia by isoflurane. All animal procedures were performed in accordance with the Guide for Care and Use of Laboratory Animals of the NIH, and were approved by the Animal Subjects Committee of the University of California, Los Angeles Institutional Guidelines for Animal Care.

Peridroplet mitochondria isolation

Peridroplet mitochondria were isolated as previously described in detail (Benador *et al.*, 2018; Ngo *et al.*, 2021) with some modifications. BAT was isolated from the inter-scapular BAT depot, and WAT was isolated from both perigonadal fat pads, also known as the epididymal fat from each mouse. BAT was homogenized using a glass-teflon dounce homogenizer, and WAT has homogenized using a glass-glass dounce homogenizer in Sucrose-HEPES-EGTA buffer supplemented with BSA (SHE+BSA; 250 mM sucrose, 5 mM HEPES, 2 mM EGTA, 1% fatty acid-free BSA, pH 7.2). Homogenate was split into four equal parts to test protocol optimizations side-by side. Homogenates were centrifuged at 1000 x g for 10 min at 4°C. Supernatant was poured into a new tube and fat layer was scraped into a second tube and resuspended in SHE+BSA buffer. Fat layers and supernatant were left either untreated or treated with Proteinase K at 2ug/mL for 15 minutes (Proteinase K, Invitrogen 25530-049 20mg/mL). All fat-layers were incubated for 15 minutes at 4°C under constant rotation. For protocol including PMSF, 2 mM PMSF was added for an additional 20 minutes of incubation on ice while inverting the samples every 2 minutes (PMSF, Sigma 78830). Then all the samples were centrifuged again at 10,000 x g for 10 min at 4°C. The pellets were then re-suspended in SHE+BSA and centrifuged with the same settings once more. The pellets were then re-suspended in SHE without BSA and again centrifuged with the same settings. Final pellets were resuspended in SHE without BSA and protein concentration was determined by BCA (Thermo Fisher Scientific, Waltham, Massachusetts).

Isolation of Peridroplet Mitochondria from Large and Small Lipid Droplets

Fat tissue was homogenized as described above for the PDM isolation. Homogenates were first sieved through a 630 μm mesh (Genesee Scientific, San Diego, CA), and transferred into ice-cold tubes. Homogenates were then centrifuged at 500 x g for 3 min at 4ºC which created a fat layer made up of the larger lipid droplets (LG-LD). Supernatant was carefully poured into a new tube and centrifuged at 2000 x g for 10 min at 4ºC which created a second fat layer consisting of smaller lipid droplets (SM-LD). The supernatant, which contained the cytoplasmic mitochondria was transferred into a new tube by carefully pipetting underneath the fat layer. LG-LDs and SM-LDs were resuspended in SHE+BSA. LG-LDs were centrifuged again at 500 x g for 5 min at 4ºC and SM-LGs were centrifuged at 2000 x g for 10 min at 4ºC. Both large and small LDs were resuspended in 1 ml SHE+BSA and incubated with Prot K as described above. All fractions including the supernatant containing the CM were centrifuged at 10,000 x g for 10 min at 4ºC to pellet the mitochondria. Mitochondrial pellets were resuspended in SHE without BSA, and spun one more time with the same conditions. Mitochondrial pellets were resuspended in SHE without BSA and protein concentrations were determined by BCA (Thermo Fisher Scientific, Waltham, Massachusetts).

Isolated Mitochondria Respirometry

Respirometry in isolated mitochondria was performed as previously described in detail (Ngo *et al.*, 2021). Briefly, isolated mitochondria were re-suspended in mitochondrial assay buffer (MAS; 100 mM KCl, 10 mM KH2PO4, 2 mM MgCl2, 5 mM

HEPES, 1 mM EGTA, 0.1% BSA, 1 mM GDP, pH 7.2) and kept on ice. Two micrograms per well were loaded into Seahorse XF96 microplate in 20 µL volume containing substrates. The loaded plate was centrifuged at 2,000 x g for 5 min at 4°C and an additional 130 µL of MAS buffer + substrate was added to each well. Substrate concentrations in the well were as follow: i) 5 mM pyruvate + 5 mM malate + 4 mM ADP or ii) 2mM malate + 4 mM ADP. For Pyruvate plus malate dependent respiration; oligomycin was injected at port A (3.5 µM), N,N,N',N'-Tetramethyl-p-phenylenediamine (TMPD) + ascorbic acid (0.5mM + 1mM) at port B and azide (50mM) at port C. For palmitoyl-carnitine dependent respiration; 5 mM malate + 4 mM ADP+ 40 µM palmitoyl-carnitine was injected at port A, oligomycin was injected at port B (3.5 µM), N,N,N',N'-Tetramethyl-p-phenylenediamine (TMPD) + ascorbic acid (0.5mM + 1mM) at port C and azide (50 mM) at port D. Mix and measure times were 0.5 min and 4 min, respectively. A 2 minute wait time was included for oligomycin-resistant respiration measurements.

To calculate the effects of Prot K on oxygen consumption rates, we measured state 3 or the capacity of coupled mitochondria to produce ATP in the presence of substrates and ADP, oligomycin resistant leak and ATP-linked respiration, Complex IV-driven respiration and non-mitochondrial oxygen consumption.

Fold changes in respiration were calculated from raw OCR values obtained in each experimental group, where respiration of treated mitochondria isolated in the same day and analyzed on the same plate were normalized to the untreated mitochondria to

establish the effect of PK and PMSF treatment. The individual fold changes over untreated mitochondria obtained from independent experiments were then averaged, represented in bar graphs. For each substrate (pyruvate malate or palmitoyl carnitine) and mitochondrial state (ie State 3, leak, ATP-linked, CoxIV) we calculated the fold change of each individual mitochondrial state between the mitochondria treated with PK and/or PMSF and compared it to the untreated CM or PDM of the group. For example for State 3, we set the CM untreated equal to 1 by dividing by the raw OCR value and then compared the raw OCR values of the 3 other groups to the CM untreated to calculate the fold change. For the comparison between CM Prot K and PDM Prot K as in Figure 2G and Figure 3G, the fold changes were calculated from the raw OCR values of each individual experiment by comparing the OCR values of each state with the CM untreated state 3, which was set to 1.

Peridroplet Mitochondria Quantification

Plate Reader Assay

Fat layer and stripped fat layer were incubated in MAS buffer containing MitoTracker DeepRed from Invitrogen M22426 (MTDR, 500 nM, final) and BODIPY493/503 from Invitrogen D3922 (BD493, 1 μM, final) for 10 minutes at 37^{o}C. Dye was removed by centrifuging the samples at 1000×g for 10 min and removing the infranatant. The stained fat layer or stripped fat layer was resuspended in 100 μl of MAS and fluorescence was measured in clear-bottom black 96-well plate (Corning, NY). MTDR was excited at 625 nm and its emission recorded at 670 nm. BD493 was excited at 488nm

laser and its emission recorded at 500-550nm. MTDR/BD493 was calculated for the fat cake and the stripped fat cake. For PDM quantification, we calculated the difference of the MTDR/BD493 between the fat cake and the stripped fat cake.

ATP Synthesis Assay

10 µg of isolated mitochondria were re-suspended in 10 µl MAS buffer containing 5 mM pyruvate + 5 mM malate + 3.5 mM ADP and plated onto a clear-bottom black 96-well plate (Corning, NY). Luciferin-luciferase mix was added to the mitochondria and luminescence immediately. Luminescent counts were integrated over 0.5 s at 10 s intervals separated by 0.5 s orbital shaking on Spark M10 microplate reader (Tecan, Männedorf, Switzerland). The linear rate of luminescence increase was calculated to determine ATP synthesis rate.

Protein Gel Electrophoresis and Immunoblotting

5-15 mg of isolated mitochondrial protein or fat layer was re-suspended in NuPAGE LDS Sample Buffer containing β-mercaptoethanol (Thermo Fisher Scientific, Waltham, Massachusetts). Samples were then loaded into 4 %–12 % Bis-Tris precast gels (Thermo Fisher Scientific, Waltham, Massachusetts) and electrophoresed, in constant voltage at 60V for 30 min (to clear stacking) and 140V for 60 min. Proteins were transferred to methanol-activated Immuno-Blot PVDF Membrane (Bio-Rad, Hercules, CA) in 30V constant voltage for 1 hr at 4°C. Blots were incubated over-night with primary antibody diluted in PBST (phosphate buffered saline with 1 mL/L Tween-20/PBS) + 5 %

BSA (Thermo Fisher Scientific, Waltham, Massachusetts) at 4°C. The next day, blots were washed in PBST and incubated with fluorescent or HRP secondary antibodies, diluted in PBST+ 5 % BSA for 1 hour at room temperature. Proteins were detected using the following antibodies: MTCO1 antibody [1D6E1A8] (ab14705), Total Rodent OXPHOS Cocktail (ab110413), VDAC (ab15895) all from Abcam, Cambridge, United Kingdom. ATP5A1 Monoclonal Antibody (15H4C4) (43-9800 Thermo), NDUFFB8 monoclonal antibody (20E9DH10C12) (459210, Thermo), SDHA Monoclonal Antibody (2E3GC12FB2AE2) (459200, Thermo) from Thermo Fisher Scientific, Waltham, Massachusetts. UQCRC2 Rabbit Polyclonal Antibody (14742-1-AP) from Proteintech (Rosemont IL), TOMM20 monoclonal antibody clone 4F3 (WH0009804M1-100UG) Sigma (St. Louis, MO) and VDAC (D73D12) Rabbit mAb Cell signaling Technology 4661T (Danvers, MA). Secondary antibodies used were Goat anti-Mouse IgG secondary antibody, Alexa Fluor® 660 conjugate (Thermo Fisher Scientific, Waltham, Massachusetts), Goat anti-Rabbit IgG secondary antibody DyLight 800 (Thermo Fisher Scientific, Waltham, Massachusetts), Donkey anti Mouse IgG (H+L) Highly Cross Adsorbed Secondary Antibody, Alexa Fluor® 488 conjugate (Thermo Fisher Scientific, Waltham, Massachusetts), Anti rabbit IgG, HRP linked Antibody (7074, Cell Signaling Technology, Danvers, MA), Anti mouse IgG, HRP linked Antibody (7076, Cell Signaling Technology, Danvers, MA). Blots were imaged on the ChemiDoc MP imaging system (Bio-Rad Laboratories, Hercules, CA). Band densitometry was quantified using FIJI (ImageJ, NIH).

Fluorescence Microscopy

Imaging Apparatus

All imaging was performed on Zeiss LSM880. Super-resolution imaging was performed with 63x and 40x Apochromat oil-immersion lens and AiryScan super-resolution detector.

Fluorophore Excitation/Emission

All fluorophores were excited on separate tracks to avoid artifacts due to bleed-through emission. BODIPY 493/503 were excited with 488 nm 25 mW Argon-ion laser and their emission captured through 500-550 nm band-pass filter. MitoTracker DeepRed was excited using 633 nm 5 mW Helium-Neon laser and its emission captured through a 645 nm long-pass filter.

Lipid Droplet Imaging

Fractions of large and small lipid droplets were stained with BODIPY493/503 (BD493, 1 μM, final) for 10 minutes at 37^{o}C. 10-20 μl of each sample was mixed in a 1:1 ratio with Matrigel and pipetted into a single compartment of a cellview glass bottom 4 compartment cell culture dish (Griener Bio-One #627975). Imaging was performed using 63x Apochromat oil-immersion lens for lipid droplet layers.

PDM Imaging from Fat Layers

Pre-stripped fat layer and stripped fat layer were incubated in MAS buffer containing MitoTracker DeepRed (MTDR, 500 nM, final) and BODIPY493/503 (BD493, 1 μM, final) for 10 minutes at 37°C. Dye was removed by centrifuging the samples at 1000×g for 10 min and removing the infranatant. The stained fat layer or stripped fat layer was resuspended in 100 μl of MAS. 20 μl of each sample was mixed in a 1:1 ratio with Matrigel and pipetted into a single compartment of a cellview glass bottom 4 compartment cell culture dish (Griener Bio-One #627975). Imaging was performed using 63x for BAT and both 40x and 63x Apochromat oil-immersion lens for WAT.

Image Analysis

Lipid Droplet Size Analysis

Fat layers of large and small LDs stained with BD493 were measured by fluorescence detection using AIVIA image analysis software (Leica Microsystems, version 10.5.0). The LDs were detected and segmented by BD493 fluorescence using pixel classifier machine learning that generated a segmentation mask. LD count and measures of perimeter and surface area occupied by BD493-pixels were extracted by AIVIA software from the segmentation data for each image. The average perimeter and surface area for each image was calculated and graphed as a single point.

Analysis of PDM Content from Fat Layers

Mitochondria-lipid droplet interactions in 2D images of BD493 and MTDR stained fat layers were analyzed with CellProfiler 2.0 (Kamentsky *et al*, 2011). LDs were identified

based on BD493 staining with size cutoffs of 20-100 microns for WAT LDs and 1-50 microns for BAT LDs. Mitochondrial staining was deblurred by subtraction through a 52 pixel median filter. Subsequently, mitochondrial ROIs of 0.5 to 5 microns were recognized through an adaptive Otsu thresholding algorithm. Mitochondrial ROIs within 500 nm distance to the LD border were classified as peridroplet mitochondria, as adopted from Benador et al 2018, and the percentage of interaction was determined as length of perimeter of LD boundary interacting with mitochondria versus the length of total LD perimeter.

Image Presentation

Image contrast and brightness were not altered in any quantitative image analysis protocols. Brightness and contrast were optimized to properly display representative images in figure panels.

Statistical analysis

Statistical analyses were performed using GraphPad Prism 5.03 (GraphPad Software Inc., San Diego, CA, USA). Data were presented as mean ± SEM for all conditions. Normality of data was checked by Kolmogorov-Smirnov test with the Dallal-Wilkinson-Lillie for corrected p value. For data with normal distribution, one-way ANOVA with Šídák multiple comparisons test was employed. Individual means were compared using the parametric two-tail Student's t-test. For non-parametric data, Kruskal-Wallis with Dunn's multiple comparisons test was used. Comparisons between two groups were

assessed by Kolmogorov-Smirnov test, and when appropriate Wilcoxon matched-pairs rank test. Differences of $P < 0.05$ were considered to be significant. All graphs and statistical analyses were performed using GraphPad Prism 9 (GraphPad Software, San Diego, CA).

FIGURES

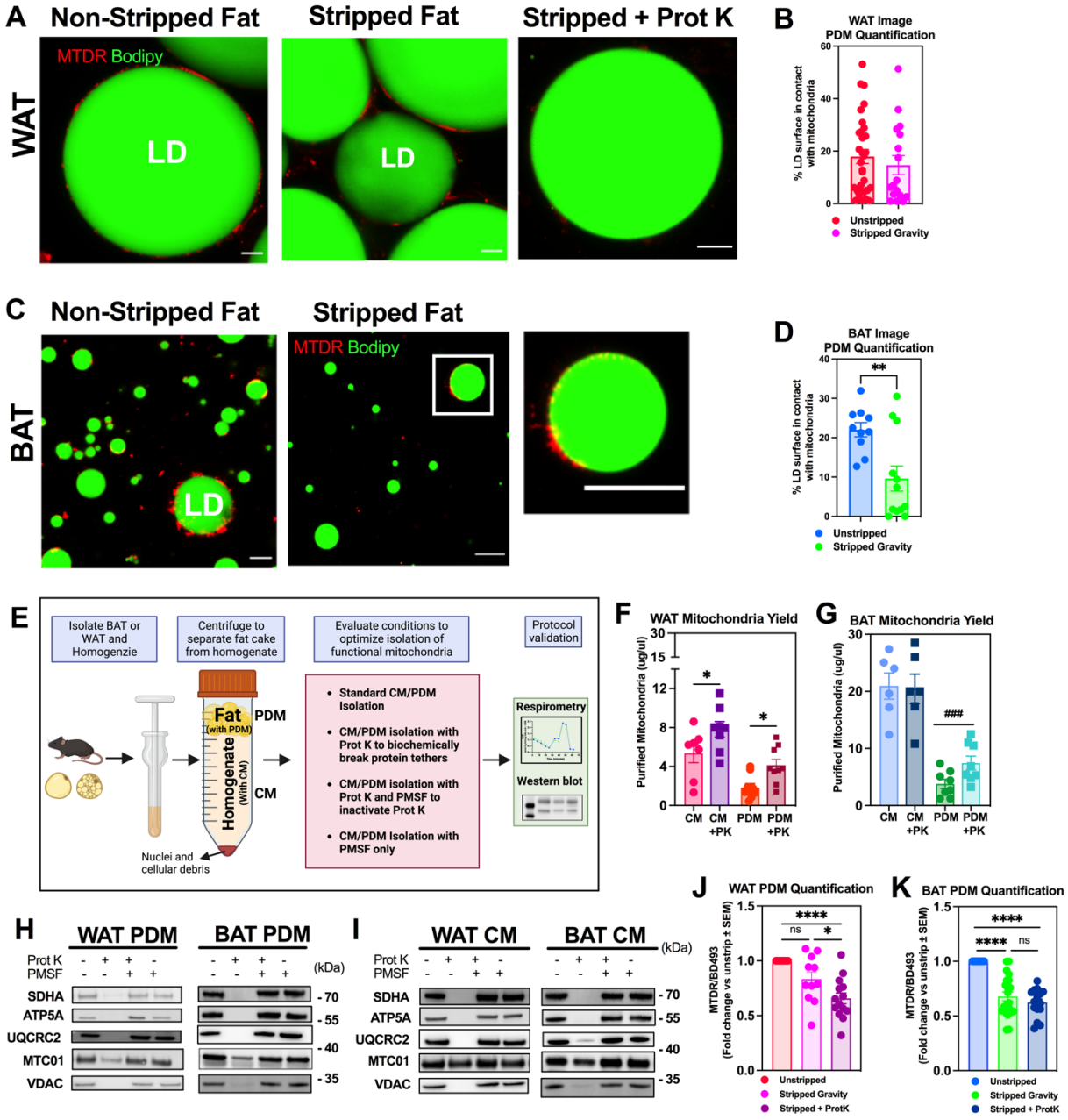

Figure 2-1: Proteinase K treatment enables the isolation of peridroplet mitochondria (PDM) from WAT and increases the yield of PDM isolated from BAT.

(A) Super-resolution confocal microscopy of lipid droplet fractions from white adipose tissue (WAT), visualizing peridroplet mitochondria (PDM, red) attached to lipid droplets (LDs; green) before (Non-stripped Fat) after high-speed centrifugation (Stripped Fat), and after proteinase K (Prot K) treatment and high-speed centrifugation (Stripped + Prot K). Mitochondria were stained with Mitotracker DeepRed (MTDR) and LDs with BODIPY493/503 (BD493). Scale Bar=10 microns. **(B)** PDM quantification of WAT LDs determined by quantifying the % of LD surface covered by mitochondria from images shown in panel **(A)**. 18-32 lipid droplets were analyzed from 4 independent isolations. **(C)** Imaging and staining performed as in **(A)** but using LD fractions from brown adipose tissue (BAT). **(D)** PDM quantification of images from BAT shown in panel **(C).** Dot plot shows quantification of the % of LD surface covered by mitochondria as in panel **(B)**. 10-12 images were analyzed, each with multiple lipid droplets from 5 independent isolations. For each image, the total % of LD surface covered by mitochondria was averaged and represents a single point on the graph. **(E)** Summary of new method enabled by Prot K to isolate PDM and cytoplasmic (CM) mitochondria from WAT and BAT. Fat homogenates were centrifuged at low speed to separate the fat layer containing PDM from supernatant containing the CM. Prot K was added to both the LD fraction and supernatant and incubated for 15 minutes. High-speed centrifugation separated PDM from Prot K treated lipid droplets and CM from the supernatant. **(F and G)** Comparison of protein recovered in PDM and CM fractions in the presence or absence of Prot K treatment from **(F)** WAT and **(G)** BAT. N=6-9 independent isolation experiments, with each individual data point representing one single experiment. **(H and I)** Western blot of PDM **(H)** and CM **(I)**

isolated from WAT and BAT with regular PDM protocol, PDM isolation + Prot K, PDM isolation with Prot K + PMSF and PMSF alone. N=3-4 independent experiments of PDM and CM isolation. **(J and K)** PDM quantification of WAT **(J)** and BAT **(K)** using the fluorescence plate reader assay. Mitochondria were stained with MTDR and LDs with BD493. The ratio of MTDR/BD493 fluorescence was quantified as a measure of PDM mass per LD mass. 5-6 independent isolation experiments. *$P < 0.05$, **$P < 0.01$, ***$P < 0.001$, ****$P < 0.0001$ by one-way ANOVA. ### $P < 0.001$ compared to untreated CM or PDM by Student's *t*-test. All data presented as mean ± SEM. Illustrations were created in Biorender.

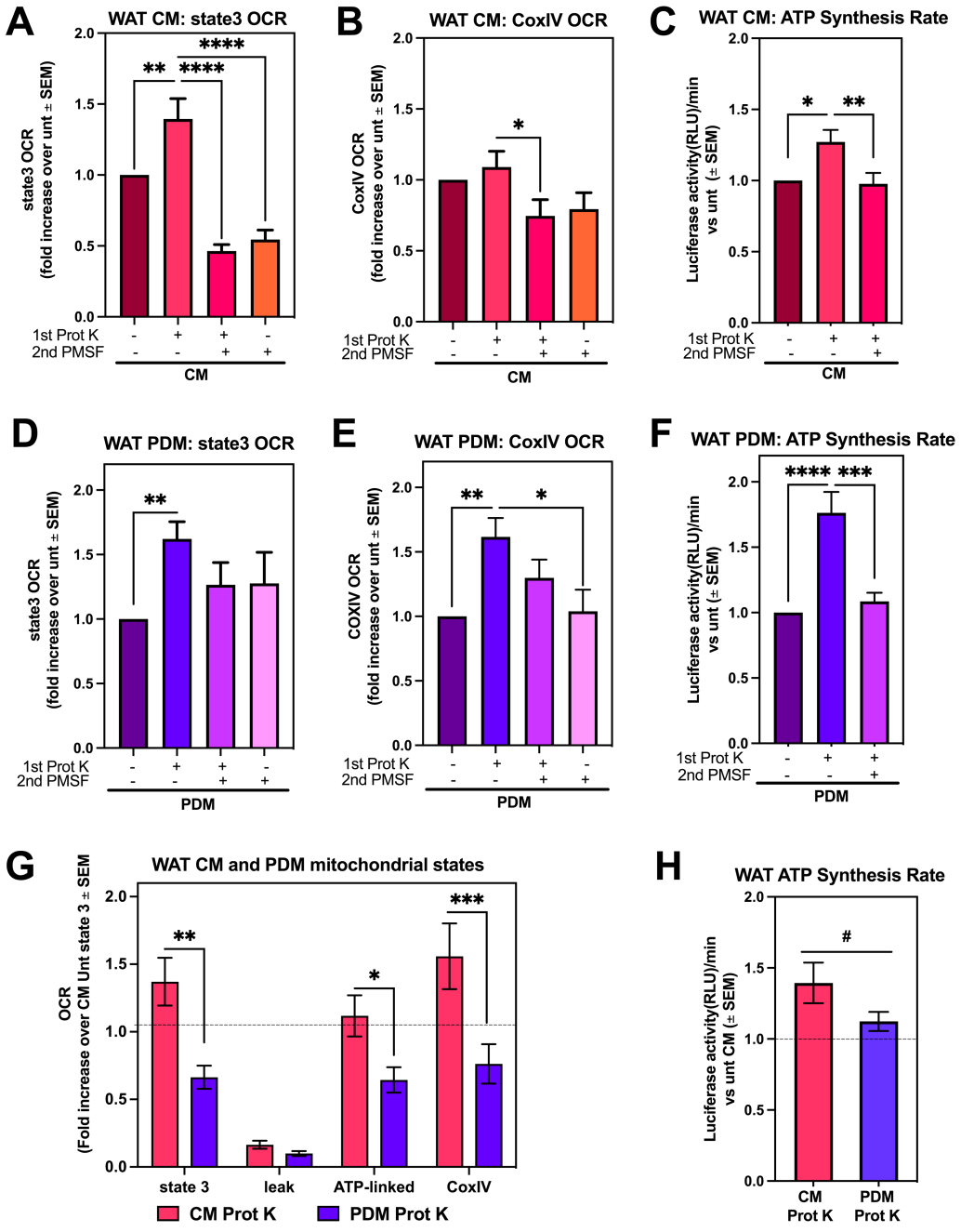

Figure 2-2: Proteinase K treatment enables the isolation of functional PDM from WAT.

Assessing mitochondrial function in WAT after isolation with either centrifugation alone, Prot K, Prot K+PMSF, or PMSF alone. **(A-C)** WAT CM respirometry using pyruvate+malate as the substrate. Data were normalized to untreated CM for each individual experiment. **(A)** State 3 OCR of WAT CM from n=16-20 independent isolation experiments each with 1-2 biological replicates. **(B)** CoxIV OCR after injection of TMPD and ascorbate of WAT CM from 16-20 independent isolations. **(C)** Quantification of ATP synthesis activity in WAT CM from 6 individual isolations. ATP synthesis rates were determined by the rate of luminescence gain. **(D-F)** WAT PDM respirometry using pyruvate+malate as the substrate. Data were normalized to untreated PDM for each individual experiment. **(D)** State 3 OCR of WAT PDM and **(E)** CoxIV OCR of WAT PDM after injection of TMPD and ascorbate from 15-20 independent isolations. **(F)** Quantification of ATP synthase activity in WAT PDM from 6 individual isolations. **(G)** Assessing mitochondrial function in WAT CM and PDM with Prot K from 13-15 independent isolations. Both CM + Prot K and PDM + Prot K were normalized to untreated CM for each individual experiment**. (H)** Quantification of ATP synthesis activity using pyruvate+malate as the substrate from WAT CM and PDM treated with Prot K from 13-15 independent isolations. *$P < 0.05$, **$P < 0.01$, ***$P < 0.001$, ****P < 0.0001 by one-way ANOVA. # $P < 0.05$ by Student's *t*-test. All data presented as mean ± SEM.

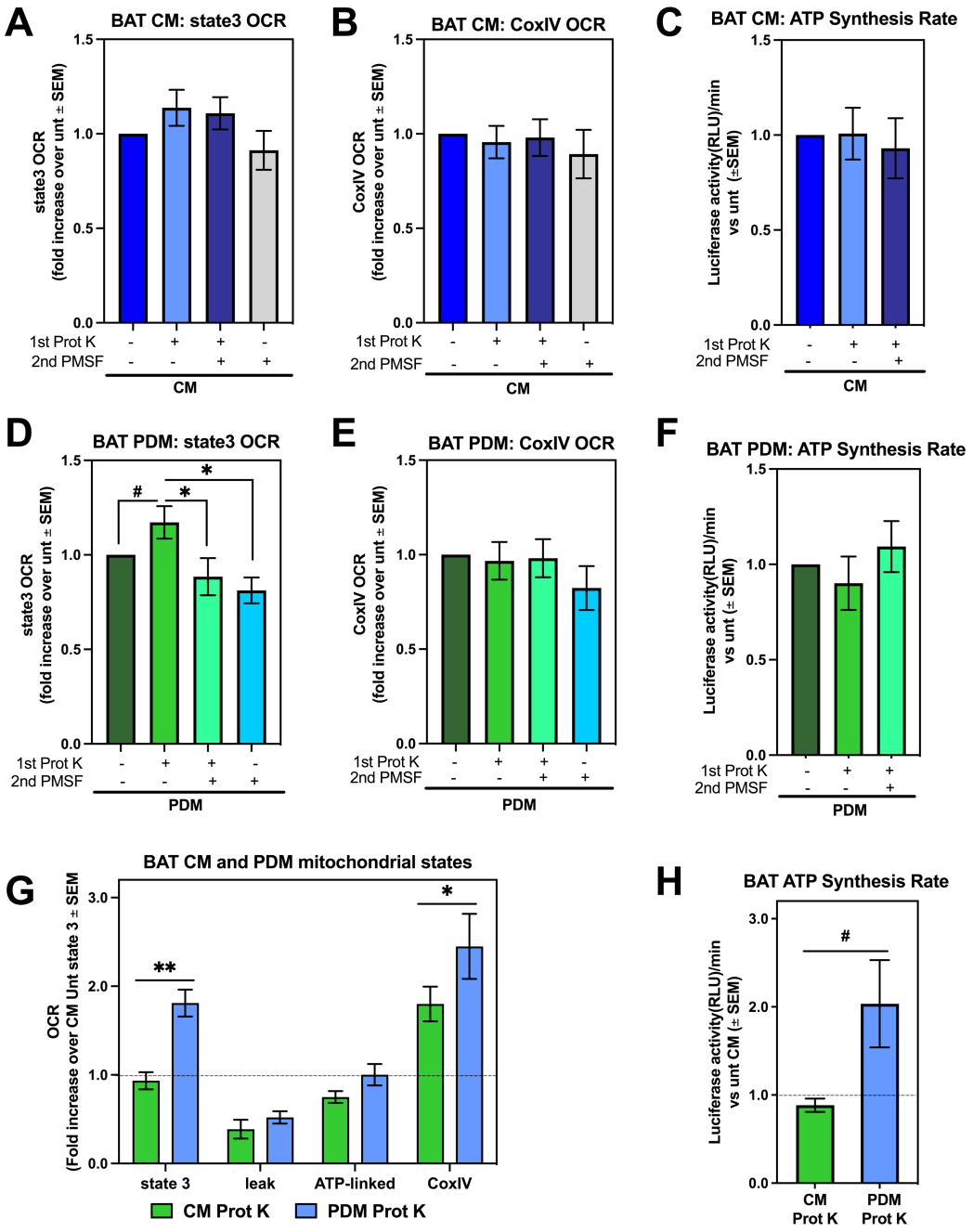

Figure 2-3: Isolation of PDM from BAT with Proteinase K does not decrease mitochondrial respiratory capacity.

Assessing mitochondrial function in BAT after isolation with either regular isolation protocol, Prot K, Prot K+PMSF, or PMSF alone. **(A-C)** BAT CM respirometry using pyruvate+malate as the substrate. Data were normalized to untreated CM for each individual experiment. **(A)** State 3 oxygen consumption rate (OCR) of BAT CM and **(B)** CoxIV OCR after injection of TMPD and ascorbate of BAT CM from 6-13 independent isolation experiments. **(C)** Quantification of ATP synthesis activity in BAT CM from n=5 individual experiments. ATP synthesis rates were determined by the rate of luminescence gain. **(D-F)** BAT PDM respirometry using pyruvate+malate as the substrate. Data were normalized to untreated PDM for each individual experiment. **(D)** State 3 OCR of BAT PDM and **(E)** CoxIV OCR after TMPD and ascorbate injection of BAT PDM from 6-13 independent isolation experiments. **(F)** Quantification of ATP synthase activity in BAT PDM from n=5 individual experiments. **(G)** Assessing mitochondrial function in BAT CM and PDM with Prot K from n=9-12 independent isolations. Both CM + Prot K and PDM + Prot K were normalized to untreated CM for each individual experiment**. (H)** Quantification of ATP synthesis activity using pyruvate+malate as the substrate from BAT CM and PDM treated with Prot K from n=3-4 independent isolations. *$P < 0.05$, **$P < 0.01$ by one-way ANOVA. # $P < 0.05$ by Student's *t*-test. All data presented as mean ± SEM.

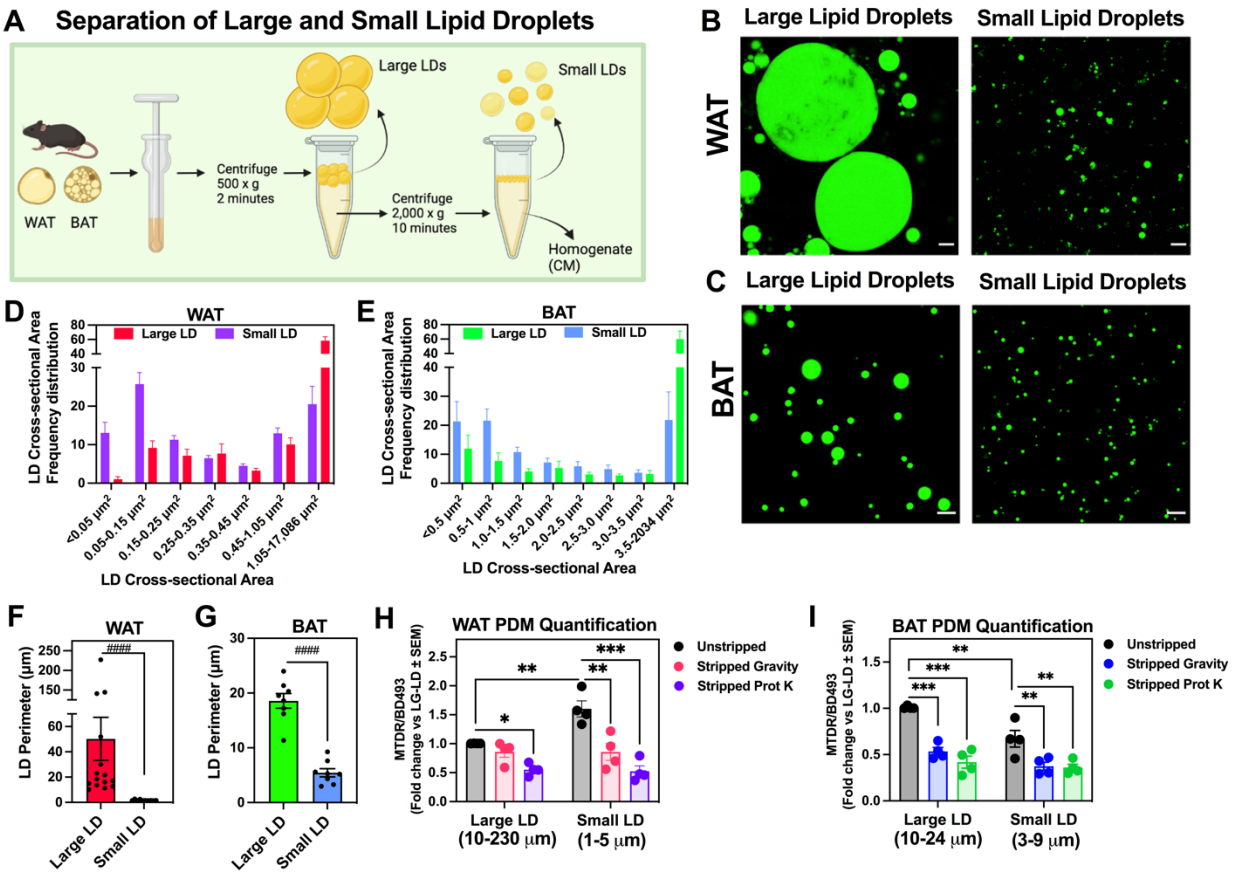

Figure 2-4: Proteinase K treatment enables the isolation of mitochondria attached to small lipid droplets that cannot be detached by centrifugation.

(A) Schematic representation of the isolation protocol for small and large LDs. Tissue was homogenized and first centrifuged at 500 x g to create a fat layer containing large LDs (LG-LDs). After removing the first fat layer, homogenates were centrifuged at 2000 x g to create a second fat layer containing small LDs (SM-LDs). **(B and C)** Super-resolution confocal microscopy of fat layers containing LG-LDs and SM-LDs isolated from WAT **(B)** and BAT **(C).** The fat layers were stained with BD493. Scale bar = 10 microns. **(D and E)**

Examining LD size distribution in fat layers isolated from WAT **(D)** and BAT **(E)** separated by differential centrifugation. N=4-6 individual experiments with n>2 images analyzed per experiment. **(D)** In WAT, the data was grouped into bins with a range of 0.1 starting at 0. The last group contained the frequency of LD area between 1.05 μm^2 and 17,086 μm^2. **(E)** In BAT, the bin range was 0.5 and started at 0. The last group contained the frequency of LD area between 3.5 μm^2 and 2,034 μm^2. **(F and G)** Quantification of the perimeter of lipid droplets found in the large LD and the small LD preparations isolated from WAT **(F)** and BAT **(G)** fat layers. N=4-6 individual experiments with n>2 images analyzed per individual experiment. Each point on the graph represents the average LD perimeter from a single image. **(H and I)** Assessing the amount of PDM associated with large versus small LDs. PDM quantification from WAT **(H)** and BAT **(I)** using the fluorescence plate reader assay in n=4 individual experiments. Mitochondria were stained with MTDR and LDs with BD493. The ratio of MTDR/BD493 was quantified as a measure of PDM abundance. *$P < 0.05$, **$P < 0.01$, ***$P < 0.001$ by one-way ANOVA, #### $P < 0.0001$ by nonparametric Kolomogrov smirnof analysis. All data presented as mean ± SEM. Illustrations were created in Biorender.

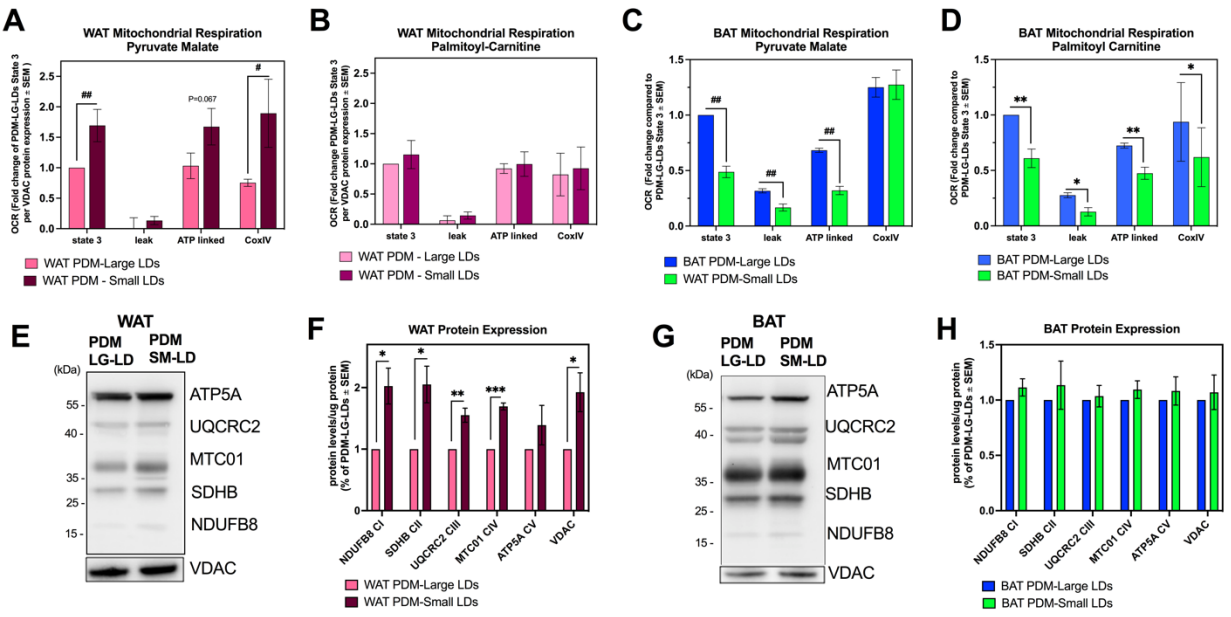

Figure 2-5: PDM isolated from large and small lipid droplets have unique characteristics.

Assessing mitochondrial function in PDM isolated from LG- and SM-LDs from WAT and BAT. All mitochondria were isolated from WAT and BAT using the Prot K protocol. **(A and B)** Quantification of state 3, mitochondrial proton leak, ATP-linked and CoxIV OCR using pyruvate malate **(A)** as substrate or palmitoyl-carnitine+malate **(B)** as substrate in PDM from LG- and SM-LDs in WAT. 4-6 individual isolations were normalized to VDAC protein content for each experiment as a measure of mitochondrial content. **(C and D)** Assessing mitochondrial function in PDM isolated from LG- and SM-LDs in BAT. Quantification of state 3, mitochondrial proton leak, ATP-linked, and CoxIV OCR using pyruvate+malate **(C)** as substrate or palmitoyl-carnitine+malate **(D)** as substrate from 4-6 individual isolations. **(E)** Representative Western blots of mitochondrial proteins from mitochondria isolated from LG- and SM-LDs from WAT and **(F)** quantification of the protein data from

n=3-5 individual isolations. **(G)** Representative Western blots of mitochondrial proteins from mitochondria isolated from LG- and SM-LDs from BAT and **(H)** quantification of the protein data from n=3-5 individual isolations. * $P < 0.05$, ** $P < 0.01$, *** $P < 0.001$ by Student's *t*-test and # $P < 0.05$, ## $P < 0.01$ by nonparametric Kolomogrov smirnof analysis. All data presented as mean ± SEM.

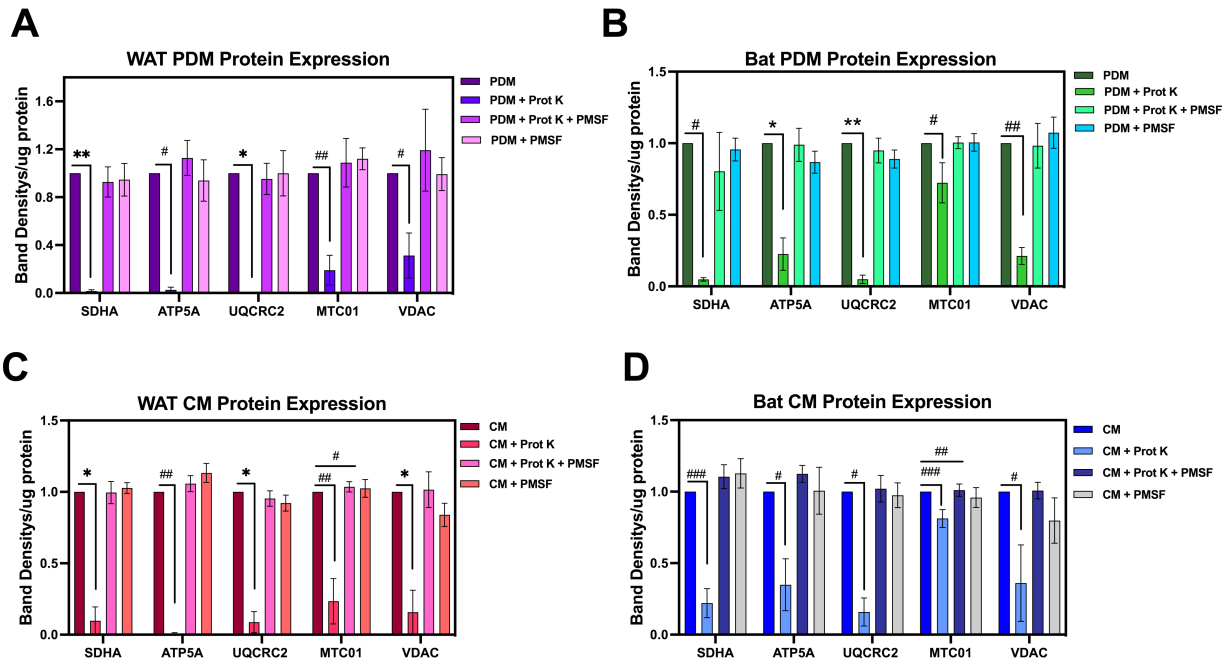

Supplementary Figure 2- 1: Isolation of PDM with Proteinase K requires PMSF inactivation for Western Blot analysis of mitochondrial proteins.

Western Blot analysis of mitochondrial proteins from PDM and CM isolated from WAT and BAT with regular PDM protocol, PDM isolation+ Prot K, PDM isolation with Prot K + PMSF and PMSF alone. All samples were normalized to total protein amount before loading in the gel for comparison. **(A and B)** Western blot analysis of WAT PDM proteins

(A) and BAT PDM proteins **(B)** from Figure 1H. **(C and D)** Western blot analysis of WAT CM proteins **(C)** and BAT CM proteins **(D)** from Figure 1I. Note that Prot K treatment resulted in degradation of mitochondrial proteins when samples were stored at -80ºC. The addition of PMSF after the 15 min Prot K incubation period rescued the degradation of mitochondrial proteins. For all groups n=3-6 individual isolations. **P* < 0.05, ***P* < 0.01, ****P* < 0.001 by non parametric Kruskal-wallis test-for each individual protein. # *P* < 0.05, ## *P* < 0.01, ### *P* < 0.001 compared to untreated CM or PDM by Kolmogorov–Smirnov test. All data presented as mean ± SEM.

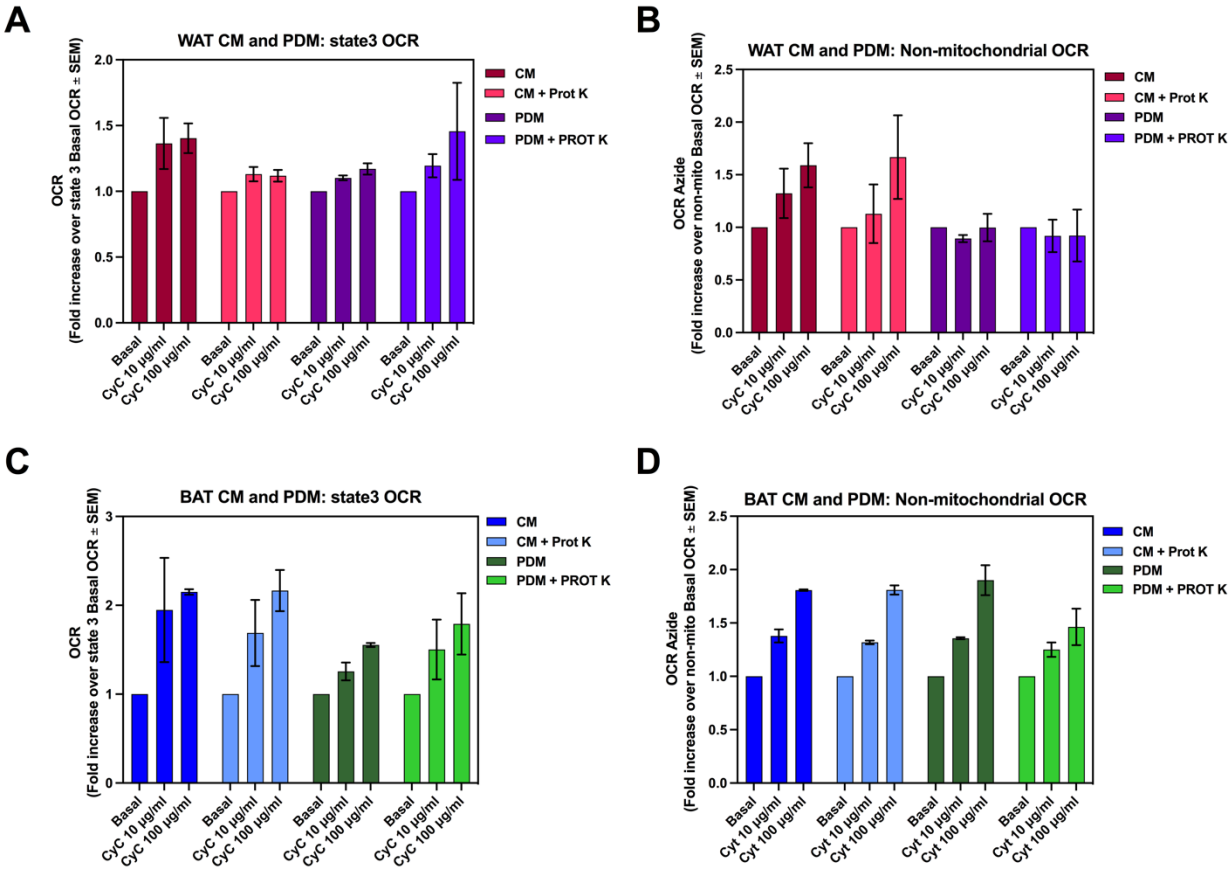

Supplementary Figure 2- 2: Cytochrome c supplementation results in similar increases in oxygen consumption in mitochondria with and without Proteinase K.

Analysis of state 3 oxygen consumption and non-mitochondrial oxygen consumption, determined by the presence of azide in WAT and BAT CM and PDM with or without proteinase K. **(A and B)** State 3 OCR **(A)** and non-mitochondrial oxygen consumption **(B)** of WAT CM and WAT PDM supplemented with cytochrome c, with and without proteinase K. **(C and D)** State 3 OCR **(C)** and non-mitochondrial oxygen consumption **(D)** of BAT CM and BAT PDM supplemented with cytochrome c, with and without proteinase K. No differences were observed between the groups that were treated with proteinase K and those that were not.

Acknowledgments

We would like to thank Dr. Ilan Benador, Dr. Dani Dagan, Dr. Jennifer Ngo, Dr. *Cristiane Beninca,* and Dr. Michael Shum for helpful discussions and advice. Figures created with BioRender.com.

Author contributions

Conceptualization, A.J.B., M.V., R.A-P, M.L. and O.S.S.; Methodology, A.J.B., M.V., R.A-P, F.V., A.P.; Validation, A.J.B., M.V., R.A-P, F.V., A.P.; Writing–Original Draft, A.J.B. and M.V.; Writing–Review & Editing, A.J.B., M.V., R.A-P, M.L. and O.S.S.; Supervision M.L. and O.S.S. All authors read and approved the final version of the manuscript.

Conflict of interest

M.L. and O.S.S. are co-founders and consultants of Enspire Bio LLC..

REFERENCES

Acín-Perez R, Petcherski A, Veliova M, Benador IY, Assali EA, Colleluori G, Cinti S, Brownstein AJ, Baghdasarian S, Livhits MJ *et al* (2021) Recruitment and remodeling of peridroplet mitochondria in human adipose tissue. *Redox Biol* 46: 102087

Badugu R, Garcia M, Bondada V, Joshi A, Geddes JW (2008) N terminus of calpain 1 is a mitochondrial targeting sequence. *J Biol Chem* 283: 3409-3417

Barneda D, Frontini A, Cinti S, Christian M (2013) Dynamic changes in lipid droplet-associated proteins in the "browning" of white adipose tissues. *Biochim Biophys Acta* 1831: 924-933

Benador IY, Veliova M, Mahdaviani K, Petcherski A, Wikstrom JD, Assali EA, Acín-Pérez R, Shum M, Oliveira MF, Cinti S *et al* (2018) Mitochondria Bound to Lipid Droplets Have Unique Bioenergetics, Composition, and Dynamics that Support Lipid Droplet Expansion. *Cell Metab* 27: 869-885.e866

Boudina S, Graham TE (2014) Mitochondrial function/dysfunction in white adipose tissue. *Exp Physiol* 99: 1168-1178

Boutant M, Kulkarni SS, Joffraud M, Ratajczak J, Valera-Alberni M, Combe R, Zorzano A, Cantó C (2017) Mfn2 is critical for brown adipose tissue thermogenic function. *Embo j* 36: 1543-1558

Brasaemle DL, Wolins NE (2016) Isolation of Lipid Droplets from Cells by Density Gradient Centrifugation. *Curr Protoc Cell Biol* 72: 3.15.11-13.15.13

Camara AKS, Zhou Y, Wen PC, Tajkhorshid E, Kwok WM (2017) Mitochondrial VDAC1: A Key Gatekeeper as Potential Therapeutic Target. *Front Physiol* 8: 460

Cannon B, Nedergaard J (2004) Brown adipose tissue: function and physiological significance. *Physiol Rev* 84: 277-359

Cinti S (2000) Anatomy of the adipose organ. *Eat Weight Disord* 5: 132-142

Cinti S (2001) The adipose organ: morphological perspectives of adipose tissues. *Proc Nutr Soc* 60: 319-328

Cinti S (2007) The Adipose Organ. In: *Adipose Tissue and Adipokines in Health and Disease*, pp. 3-19. Humana Press: Totowa, NJ

Cinti S (2018) *Obesity, Type 2 Diabetes and the Adipose Organ*. Springer International Publishing, Switzerland

Cole A, Wang Z, Coyaud E, Voisin V, Gronda M, Jitkova Y, Mattson R, Hurren R, Babovic S, Maclean N *et al* (2015) Inhibition of the Mitochondrial Protease ClpP

as a Therapeutic Strategy for Human Acute Myeloid Leukemia. *Cancer Cell* 27: 864-876

Cui L, Mirza AH, Zhang S, Liang B, Liu P (2019) Lipid droplets and mitochondria are anchored during brown adipocyte differentiation. In: *Protein Cell*, pp. 921-926.

Cushman SW (1970) Structure-function relationships in the adipose cell. I. Ultrastructure of the isolated adipose cell. *J Cell Biol* 46: 326-341

De Pauw A, Tejerina S, Raes M, Keijer J, Arnould T (2009) Mitochondrial (dys)function in adipocyte (de)differentiation and systemic metabolic alterations. *Am J Pathol* 175: 927-939

Denuc A, Núñez E, Calvo E, Loureiro M, Miro-Casas E, Guarás A, Vázquez J, Garcia-Dorado D (2016) New protein-protein interactions of mitochondrial connexin 43 in mouse heart. *J Cell Mol Med* 20: 794-803

Forner F, Kumar C, Luber CA, Fromme T, Klingenspor M, Mann M (2009) Proteome differences between brown and white fat mitochondria reveal specialized metabolic functions. *Cell Metab* 10: 324-335

Freyre CAC, Rauher PC, Ejsing CS, Klemm RW (2019) MIGA2 Links Mitochondria, the ER, and Lipid Droplets and Promotes De Novo Lipogenesis in Adipocytes. *Mol Cell* 76: 811-825.e814

Gold AM (1965) Sulfonyl fluorides as inhibitors of esterases. 3. Identification of serine as the site of sulfonylation in phenylmethanesulfonyl alpha-chymotrypsin. *Biochemistry* 4: 897-901

Gold AM, Fahrney D (1964) Sulfonyl fluorides as inhibitors of esterases. II. Formation and reactions of phenylmethanesulfonyl alpha-chymotrypsin. *Biochemistry* 3: 783-791

Hariri H, Rogers S, Ugrankar R, Liu YL, Feathers JR, Henne WM (2018) Lipid droplet biogenesis is spatially coordinated at ER-vacuole contacts under nutritional stress. *EMBO Rep* 19: 57-72

Hariri H, Speer N, Bowerman J, Rogers S, Fu G, Reetz E, Datta S, Feathers JR, Ugrankar R, Nicastro D *et al* (2019) Mdm1 maintains endoplasmic reticulum homeostasis by spatially regulating lipid droplet biogenesis. *J Cell Biol* 218: 1319-1334

Herms A, Bosch M, Ariotti N, Reddy BJ, Fajardo A, Fernández-Vidal A, Alvarez-Guaita A, Fernández-Rojo MA, Rentero C, Tebar F *et al* (2013) Cell-to-cell heterogeneity in lipid droplets suggests a mechanism to reduce lipotoxicity. *Curr Biol* 23: 1489-1496

Hsieh K, Lee YK, Londos C, Raaka BM, Dalen KT, Kimmel AR (2012) Perilipin family members preferentially sequester to either triacylglycerol-specific or cholesteryl-ester-specific intracellular lipid storage droplets. *J Cell Sci* 125: 4067-4076

Kamentsky L, Jones TR, Fraser A, Bray MA, Logan DJ, Madden KL, Ljosa V, Rueden C, Eliceiri KW, Carpenter AE (2011) Improved structure, function and compatibility for CellProfiler: modular high-throughput image analysis software. *Bioinformatics* 27: 1179-1180

Koncsos G, Varga ZV, Baranyai T, Ferdinandy P, Schulz R, Giricz Z, Boengler K (2018) Nagarse treatment of cardiac subsarcolemmal and interfibrillar mitochondria leads to artefacts in mitochondrial protein quantification. *J Pharmacol Toxicol Methods* 91: 50-58

Kras KA, Willis WT, Barker N, Czyzyk T, Langlais PR, Katsanos CS (2016) Subsarcolemmal mitochondria isolated with the proteolytic enzyme nagarse exhibit greater protein specific activities and functional coupling. *Biochem Biophys Rep* 6: 101-107

Kuramoto K, Okamura T, Yamaguchi T, Nakamura TY, Wakabayashi S, Morinaga H, Nomura M, Yanase T, Otsu K, Usuda N *et al* (2012) Perilipin 5, a lipid droplet-binding protein, protects heart from oxidative burden by sequestering fatty acid from excessive oxidation. *J Biol Chem* 287: 23852-23863

Lai N, M Kummitha C, Rosca MG, Fujioka H, Tandler B, Hoppel CL (2019) Isolation of mitochondrial subpopulations from skeletal muscle: Optimizing recovery and preserving integrity. *Acta Physiol (Oxf)* 225: e13182

Larsson S, Resjö S, Gomez MF, James P, Holm C (2012) Characterization of the lipid droplet proteome of a clonal insulin-producing β-cell line (INS-1 832/13). *J Proteome Res* 11: 1264-1273

Laurens C, Bourlier V, Mairal A, Louche K, Badin PM, Mouisel E, Montagner A, Marette A, Tremblay A, Weisnagel JS *et al* (2016) Perilipin 5 fine-tunes lipid oxidation to metabolic demand and protects against lipotoxicity in skeletal muscle. *Sci Rep* 6: 38310

Lee JH, Park A, Oh KJ, Lee SC, Kim WK, Bae KH (2019) The Role of Adipose Tissue Mitochondria: Regulation of Mitochondrial Function for the Treatment of Metabolic Diseases. *Int J Mol Sci* 20

Listenberger LL, Han X, Lewis SE, Cases S, Farese RV, Jr., Ory DS, Schaffer JE (2003) Triglyceride accumulation protects against fatty acid-induced lipotoxicity. *Proc Natl Acad Sci U S A* 100: 3077-3082

Marcillat O, Zhang Y, Lin SW, Davies KJ (1988) Mitochondria contain a proteolytic system which can recognize and degrade oxidatively-denatured proteins. *Biochem J* 254: 677-683

Martin S, Driessen K, Nixon SJ, Zerial M, Parton RG (2005) Regulated localization of Rab18 to lipid droplets: effects of lipolytic stimulation and inhibition of lipid droplet catabolism. *J Biol Chem* 280: 42325-42335

Mirza AH, Cui L, Zhang S, Liu P (2021) Comparative proteomics reveals that lipid droplet-anchored mitochondria are more sensitive to cold in brown adipocytes. *Biochim Biophys Acta Mol Cell Biol Lipids* 1866: 158992

Najt CP, Adhikari S, Heden TD, Cui W, Gansemer ER, Rauckhorst AJ, Markowski TW, Higgins L, Kerr EW, Boyum MD *et al* (2023) Organelle interactions compartmentalize hepatic fatty acid trafficking and metabolism. *Cell Rep* 42: 112435

Ngo J, Benador IY, Brownstein AJ, Vergnes L, Veliova M, Shum M, Acín-Pérez R, Reue K, Shirihai OS, Liesa M (2021) Isolation and functional analysis of peridroplet mitochondria from murine brown adipose tissue. *STAR Protoc* 2: 100243

Nguyen TB, Louie SM, Daniele JR, Tran Q, Dillin A, Zoncu R, Nomura DK, Olzmann JA (2017) DGAT1-Dependent Lipid Droplet Biogenesis Protects Mitochondrial Function during Starvation-Induced Autophagy. *Dev Cell* 42: 9-21.e25

Nishimoto Y, Tamori Y (2017) CIDE Family-Mediated Unique Lipid Droplet Morphology in White Adipose Tissue and Brown Adipose Tissue Determines the Adipocyte Energy Metabolism. *J Atheroscler Thromb* 24: 989-998

Olzmann JA, Carvalho P (2019) Dynamics and functions of lipid droplets. *Nat Rev Mol Cell Biol* 20: 137-155

Qian K, Tol MJ, Wu J, Uchiyama LF, Xiao X, Cui L, Bedard AH, Weston TA, Rajendran PS, Vergnes L *et al* (2023) CLSTN3β enforces adipocyte multilocularity to facilitate lipid utilization. *Nature* 613: 160-168

Rambold AS, Cohen S, Lippincott-Schwartz J (2015) Fatty acid trafficking in starved cells: regulation by lipid droplet lipolysis, autophagy, and mitochondrial fusion dynamics. *Dev Cell* 32: 678-692

Renne MF, Hariri H (2021) Lipid Droplet-Organelle Contact Sites as Hubs for Fatty Acid Metabolism, Trafficking, and Metabolic Channeling. *Front Cell Dev Biol* 9: 726261

Ruiz-Meana M, Núñez E, Miro-Casas E, Martínez-Acedo P, Barba I, Rodriguez-Sinovas A, Inserte J, Fernandez-Sanz C, Hernando V, Vázquez J *et al* (2014) Ischemic preconditioning protects cardiomyocyte mitochondria through mechanisms independent of cytosol. *J Mol Cell Cardiol* 68: 79-88

Stone SJ, Levin MC, Zhou P, Han J, Walther TC, Farese RV, Jr. (2009) The endoplasmic reticulum enzyme DGAT2 is found in mitochondria-associated membranes and has a mitochondrial targeting signal that promotes its association with mitochondria. *J Biol Chem* 284: 5352-5361

Swift LL, Love JD, Harris CM, Chang BH, Jerome WG (2017) Microsomal triglyceride transfer protein contributes to lipid droplet maturation in adipocytes. *PLoS One* 12: e0181046

Sánchez-González C, Formentini L (2021) An optimized protocol for coupling oxygen consumption rates with β-oxidation in isolated mitochondria from mouse. *STAR Protoc* 2: 100735

Tan Y, Jin Y, Wang Q, Huang J, Wu X, Ren Z (2019) Perilipin 5 Protects against Cellular Oxidative Stress by Enhancing Mitochondrial Function in HepG2 Cells. *Cells* 8

Thiam AR, Beller M (2017) The why, when and how of lipid droplet diversity. *J Cell Sci* 130: 315-324

Veliova M, Petcherski A, Liesa M, Shirihai OS (2020) The biology of lipid droplet-bound mitochondria. *Semin Cell Dev Biol* 108: 55-64

Vernochet C, Damilano F, Mourier A, Bezy O, Mori MA, Smyth G, Rosenzweig A, Larsson NG, Kahn CR (2014) Adipose tissue mitochondrial dysfunction triggers a lipodystrophic syndrome with insulin resistance, hepatosteatosis, and cardiovascular complications. *FASEB J* 28: 4408-4419

Wang C, Zhao Y, Gao X, Li L, Yuan Y, Liu F, Zhang L, Wu J, Hu P, Zhang X *et al* (2015) Perilipin 5 improves hepatic lipotoxicity by inhibiting lipolysis. *Hepatology* 61: 870-882

Wang H, Sreenivasan U, Hu H, Saladino A, Polster BM, Lund LM, Gong DW, Stanley WC, Sztalryd C (2011) Perilipin 5, a lipid droplet-associated protein, provides physical and metabolic linkage to mitochondria. *J Lipid Res* 52: 2159-2168

Wilfling F, Wang H, Haas JT, Krahmer N, Gould TJ, Uchida A, Cheng JX, Graham M, Christiano R, Fröhlich F *et al* (2013) Triacylglycerol synthesis enzymes mediate lipid droplet growth by relocalizing from the ER to lipid droplets. *Dev Cell* 24: 384-399

Wilson-Fritch L, Burkart A, Bell G, Mendelson K, Leszyk J, Nicoloro S, Czech M, Corvera S (2003) Mitochondrial biogenesis and remodeling during adipogenesis and in response to the insulin sensitizer rosiglitazone. *Mol Cell Biol* 23: 1085-1094

Wolins NE, Quaynor BK, Skinner JR, Tzekov A, Croce MA, Gropler MC, Varma V, Yao-Borengasser A, Rasouli N, Kern PA *et al* (2006) OXPAT/PAT-1 is a PPAR-induced lipid droplet protein that promotes fatty acid utilization. *Diabetes* 55: 3418-3428

Yu J, Zhang S, Cui L, Wang W, Na H, Zhu X, Li L, Xu G, Yang F, Christian M *et al* (2015) Lipid droplet remodeling and interaction with mitochondria in mouse brown adipose tissue during cold treatment. *Biochim Biophys Acta* 1853: 918-928

Zhang M, Kenny SJ, Ge L, Xu K, Schekman R (2015) Translocation of interleukin-1β into a vesicle intermediate in autophagy-mediated secretion. *Elife* 4

Zhang S, Wang Y, Cui L, Deng Y, Xu S, Yu J, Cichello S, Serrero G, Ying Y, Liu P (2016) Morphologically and Functionally Distinct Lipid Droplet Subpopulations. *Sci Rep* 6: 29539

Zheng P, Xie Z, Yuan Y, Sui W, Wang C, Gao X, Zhao Y, Zhang F, Gu Y, Hu P *et al* (2017) Plin5 alleviates myocardial ischaemia/reperfusion injury by reducing oxidative stress through inhibiting the lipolysis of lipid droplets. *Sci Rep* 7: 42574

CHAPTER 4: CONCLUSIONS AND FUTURE DIRECTIONS

Intracellular mitochondrial heterogeneity has been observed to play a role in both physiology, as well as pathological states. Heterogeneity in terms of mitochondrial dynamics and morphology, membrane potential, and fuel utilization is correlated with diversity in intracellular needs related to cell specific region and proximity to other organelles within the cell (Kuznetsov & Margreiter, 2009).

In chapter two, I a discuss a novel mechanism to induce lipid cycling in BAT as a mechanism to increase energy expenditure independent of UCP1 activity. Blocking pyruvate entry into the mitochondria is a novel mechanism to increase the proportion of mitochondria that oxidize fatty acid and the MPC may be a novel target to increase energy expenditure. MPC activity adds a new level of regulation controlling and limiting energy expenditure and fuel preference.

Recent identification of a unique population of mitochondria within individual cells that support LD expansion was thought to be a mechanism to induce increased lipid storage and protect from lipotoxicity. Despite the role of PDM in providing ATP for lipid synthesis in brown adipocytes, in chapter three I explore their role in murine white adipose tissue, which seems to be different from BAT PDM. The successful isolation and bioenergetic characterization of PDM vs the cytoplasmic mitochondria in WAT indicate that at least two types of mitochondria with unique bioenergetics that co-exist in WAT. Moreover, we find that WAT PDM have lower-ATP synthesizing capacity and preference for pyruvate when compared to WAT CM. These findings suggest that aspects of mitochondrial heterogeneity including intracellular organization and function can be cell

type and tissue specific. Furthermore, Freyre and colleagues found that MIGA2, and not Plin5 as in BAT, acts as a unique mitochondria-LD tethering protein for PDM in WAT, further supporting tissue-specific regulation of PDM interaction and function (Freyre *et al*, 2019). PDM have been shown to play different roles in several other tissues and be dependent on the nutrient status of the cell. The caveats previously discussed with the current models to induce PDM formation add additional complexity in our pursuit to understand the unique function of PDM.

In support of a tissue-specific role of PDM, recent studies in hepatocytes found that unique subpopulations of hepatic mitochondria support distinct lipid metabolic pathways. In conditions of starvation, fatty acids are selectively trafficked to cytosolic mitochondria (CM) for oxidation, while PDM are the major site of fatty acid trafficking and facilitate esterification under fed conditions or during excess fatty acid exposure. Moreover, Najt et al. found that the proportion of these populations is altered under different metabolic states such as nutrient deprivation, enabling fine tune control of cellular adaptation (Najt *et al*, 2023).

In addition to increasing PDM formation, several studies have suggested that decreasing PDM can be beneficial in different tissues and physiological states. Our finding that PDM in WAT do not have increased ATP-synthesizing capacity or a preference for pyruvate oxidation, suggests these PDM may not support LD build up. In conditions of lipotoxicity, detaching PDM from LDs may represent a promising approach to increase fat oxidation in WAT. Detaching PDM may be a method to induce WAT

browning, by forcing mitochondria to become cytoplasmic and oxidize fat. It is not known if this increase in fat oxidation will require UCP1 expression.

Evidence that detaching PDM from the LD can be beneficial, has also been observed in BAT as BAT PDM detach from the LD upon adrenergic stimulation in order to increase fat oxidation. It has been suggested that PDM detachment may represent a novel mechanism to increase fat oxidation and energy expenditure in BAT. Female mice with BAT-specific knock-out of Mfn2 were resistant to diet induced obesity and had increased capacity to oxidize fatty acid, although they had impaired cold tolerance (Mahdaviani *et al*, 2017). Because Mfn2 KO reduced the interaction of mitochondria and LD, this suggest that PDM detachment promotes resistance to HFD, while also indicating that PDM are required for thermogenesis (Mahdaviani *et al.*, 2017). Of note, a complete lack of PDM might also result in the accumulation of toxic free fatty acids in certain tissues that cannot increase fat oxidation or uncoupling. Mice with DGAT2 KO die shortly after birth due to severe lipopenia (Stone *et al*, 2004). Part of this effect may be due to a lack of PDM, where DGAT2 KO mice lack PDM and therefore cannot esterify fatty acids resulting in severe lipotoxicity, however the mechanism still remains unclear. Although there are caveats associated with PLIN5 and DGAT2 KO studies, we can still infer interesting information on the effect of a lack of PDM.

The potential of PDM as a therapeutic target highlights the overall idea of intracellular mitochondrial heterogeneity and the role of mitochondria in cell function. Changing the subpopulations of mitochondria within individual cells is a potential novel mechanism to fine tune cell and tissue function and whole body metabolic homeostasis.

REFERENCES

Freyre CAC, Rauher PC, Ejsing CS, Klemm RW (2019) MIGA2 Links Mitochondria, the ER, and Lipid Droplets and Promotes De Novo Lipogenesis in Adipocytes. *Mol Cell* 76: 811-825.e814

Kuznetsov AV, Margreiter R (2009) Heterogeneity of mitochondria and mitochondrial function within cells as another level of mitochondrial complexity. *Int J Mol Sci* 10: 1911-1929

Mahdaviani K, Benador IY, Su S, Gharakhanian RA, Stiles L, Trudeau KM, Cardamone M, Enríquez-Zarralanga V, Ritou E, Aprahamian T *et al* (2017) Mfn2 deletion in brown adipose tissue protects from insulin resistance and impairs thermogenesis. *EMBO Rep* 18: 1123-1138

Najt CP, Adhikari S, Heden TD, Cui W, Gansemer ER, Rauckhorst AJ, Markowski TW, Higgins L, Kerr EW, Boyum MD *et al* (2023) Organelle interactions compartmentalize hepatic fatty acid trafficking and metabolism. *Cell Rep* 42: 112435

Stone SJ, Myers HM, Watkins SM, Brown BE, Feingold KR, Elias PM, Farese RV (2004) Lipopenia and skin barrier abnormalities in DGAT2-deficient mice. *J Biol Chem* 279: 11767-11776